SESM 66-4

STRUCTURES AND MATERIALS RESEARCH
DEPARTMENT OF CIVIL ENGINEERING

A BENDING ANALYSIS OF ELASTIC-PLASTIC CIRCULAR PLATES

by
M. KHOJASTEH-BAKHT
S. YAGHMAI
Research Assistants

E. P. POPOV
Faculty Investigator

Report to
National Aeronautics and Space Administration
NASA Research Grant No. NsG 274 S-2

APRIL 1966

STRUCTURAL ENGINEERING LABORATORY
UNIVERSITY OF CALIFORNIA
BERKELEY CALIFORNIA

Structures and Materials Research
Department of Civil Engineering

A BENDING ANALYSIS OF ELASTIC-PLASTIC CIRCULAR PLATES

by

M. Kojasteh Bakht
S. Yaghmai

Research Assistants

E. P. Popov

Faculty Investigator

Report to
National Aeronautics and Space Administration
NASA Research Grant No. NsG 274 S-2

Structural Engineering Laboratory
University of California
Berkeley, California

April 1966

PREFACE

The investigation reported herein is a part of the research carried out under the sponsorship of National Aeronautics and Space Administration, Research Grant No. NsG-274, Supplement No. 2.

The research described in this report was conducted under the supervision and technical responsibility of Egor P. Popov, Professor of Civil Engineering, Division of Structural Engineering and Structural Mechanics, University of California, Berkeley, California.

Mr. M. Khojasteh-Bakht, Graduate Student, Div. of SESM was principally responsible for the work of Chapters 1 and 2. Mr. S. Yaghmai, Graduate Student in the same Division, developed most of the computer programs required in this investigation and was mostly responsible for the preparation of Chapter 3.

In addition to the NASA sponsorship, assistance rendered by the University of California Computer Center (Berkeley) is gratefully acknowledged.

Critical discussions during the progress of the work with John Abel, and H.Y. Chow, Graduate Students, were most helpful.

Mr. B. Kot prepared the drawings and Mrs. M. French typed the final report.

Table of Contents

ABSTRACT

This report is concerned with the problem of elastic-plastic bending of circular plates with axi-symmetric loading and support conditions. Incremental theory of plasticity with von Mises yield condition, and associated flow rule together with the Kirchhoffean small deformation theory of plates have been adopted. Finite element type of approach using direct stiffness method of matrix analysis of structures was employed. An annular plate is taken as the primary element which is subdivided along its depth into a number of layers. The material properties are assigned to each layer, and stiffness matrix of the element has been established. Loadings are applied in increments. Examples of simply supported and clamped circular plates made of elastic-perfectly plastic as well as elastic-plastic with isotropic strain hardening materials are given. Other support conditions and material properties can be treated. The effect of change of material properties within each increment of loading, number of elements, and number of layers have been studied.

INTRODUCTION

The application of the incremental (flow) theory of plasticity in the solution of structural problems, particularly those related to plates and shells, has caused many mathematical difficulties. The closed form solutions have been obtained for a very few simple problems such as thick wall cylinder, wedge, and torsional shaft* made of nonhardening materials with one or at most two parameter loading. Further restrictions, such as incompressibility, have been occasionally imposed to simplify the solution. No general approach to the solution of this class of problems exists so far. Each solution requires a special mathematical treatment and researcher's ingenuity.

A significant amount of literature is devoted to the development of the constitutive laws of plasticity both in micro and macro scales. The foundation of the theory is not as yet firmly established and further research will be needed in the future.

However, due to the great demand in the design of lightweight structures to achieve economical designs and the most realisitic appraisal of the behavior, the best available theories have been employed in the analysis. Several approaches have been pursued.

During the last decade considerable attention has been given to the so-called limit analysis approach. The bounds of the collapse load, in the sense of small deflection theory, have been obtained for a number of problems.

---

* See for example: Prager and Hodge, "Theory of Perfectly Plastic Solids," John Wiley, N.Y., 1951.

Lower and upper bound theorems were employed in attaining the collapse load. In order to apply these theorems, the materials should exhibit considerable deformation under constant load such as in the case of mild steel. Although limit analysis turned out to be fruitful in the analysis of rigidly connected frames where strength is the controlling factor in the design, it generally does not lead to any physically significant results in plates and shells. This is essentially so because of a favorable change in geometrical configuration during loading which brings the membrane forces into action.

A number of solutions are also available for large deformation, for which the elastic deformation is quite negligible compared to the unrecoverable component of deformation. These are particularly applicable in the metal processing.

The attempt to solve the problems, utilizing the total or deformation theory of plasticity has not yet been completely abandoned. In spite of its mathematical inconsistency and physical unsoundness, in general, it can be used satisfactorily if the stress path in the process of loading can be predicted beforehand.

For those problems where the plastic deformation sets in with a small change in geometry a more realistic solution which takes elastic as well as plastic deformation into account should be sought. This will enable a better prediction of deflection and stress distribution than the one using elastic theory.

At the present time, the use of digital computer in the solution of plasticity problems appears to be very fruitful. It is quite feasible to anticipate that in near future many important problems will be solved with the aid of a computer. The improvement of numerical techniques reduces the numerical errors and thus increases the reliability of the results.

This report is concerned with the analysis of circular plates under arbitrary axisymmetric loading. The support conditions are axially symmetric, but, otherwise, they can be specified arbitrarily. The examples are given for clamped and simply supported solid plates. By the proposed approach, the problem of overhanging or annular plates also can be handled without much difficulty. The plate may be connected with other structures such as circular cylinders or rotational shells, and the developed method can be used to determine the redistribution of stresses at junctures due to plastic deformation. The material properties used in the proposed analysis can be completely arbitrary. This can be specified from experimental data or any valid analytical expressions. To illustrate the method, elastic-perfectly plastic and elastic-plastic isotropic strain hardening materials were employed. Any other laws or experimental data can be specified as desired.

The procedures discussed here make use of incremental law which enables one to trace the loading history. The internal forces and deflections can be determined at any stage of loading. The solution is restricted to small deformation so that deflection remains small in comparison to the thickness. In other words, the influence of membrane stresses which may be developed as

the result of deformation is not accounted for. Shear distortion is also neglected in conformity with the conventional Kirchhoff's hypothesis which asserts that a straight fiber perpendicular to the middle plane remains straight, unstretched, and perpendicular to the deflected state of the middle surface after deformation.

The plate is divided into a number of annular elements. Each element is further sub-divided into a number of layers along its depth. The material properties were assigned to each layer at every stage of loading. Direct stiffness method of matrix analysis of structures was used.

The effect of the change of number of elements and layers as well as the influence of variation of material properties within each increment of loading were studied.

All computations were carried out by IBM 7090-7094 digital computer available at the Computer Center of the University of California, Berkeley, using FORTRAN IV language.

I. REVIEW OF PREVIOUS WORK

The problem of behavior of axi-symmetrically loaded and supported circular plates loaded beyond elastic limit has attracted the attention of a number of investigators, because of the apparent simplicity of the problem and the vast number of applications. A brief review of some of the work; utilizing deformation theory of plasticity, limit analysis, and incremental theory of plasticity together with the results of some of the experimental investigations which have been published so far follows.

1.1 Plate Bending Using Deformation Theory of Plasticity

The Heneky type deformation theory of plasticity together with Huber-Mises yield condition was used by Sokolovsky 1944 [1,2] in the solution of bending of circular plates. Kirchhoff's hypothesis and small deflection theory were employed. The problem of simply supported plate under uniform and axisymmetrical partial uniform load which contains as its extreme case concentrated load at the center was solved. The material is considered to be elastic-perfectly plastic and the scheme to solve for material with strain hardening was also indicated.

Bending of circular and annular plates with variable thickness have been discussed by Grigoriev [3]. Dvorak 1959 [4] discussed an annular plate which is subjected to a ring load at outer boundary and has a simply supported inner boundary.

The problem of circular plates clamped around the boundary and subjected to uniform and partial circular uniform load was solved by Ohashi and Murakami [5] 1964. The material is considered to be non-hardening and obeys von Mises' yield condition.

1.2 Limit Analysis

The extension of the theorems of limit analysis* encouraged many authors to apply them to the problems of plates and shells.

The early attempt to apply limit analysis theorems to obtain the collapse load of circular plates was made by Pell and Prager in 1951 [6]. The materials were considered to obey von Mises' yield condition. A simply supported plate subjected to uniformly distributed load was discussed, the bounds of the collapse load were established, and an approximate value for the load-carrying capacity was suggested. Hopkins and Prager in 1953 [7] discussed the problem for materials obeying Tresca's yield condition. Simply supported and clamped plates subjected to certain simple types of axially symmetric loading were treated. The exact collapse loads were obtained. Drucker and Hopkins in 1954 [8] extended the work to the case of large and small overhang. Hopkins and Wang in 1955 [9] compared the collapse loads obtained by utilizing Mises, Tresca, and parabolic yield conditions for both simply and built-in supports. It is interesting to note that the ultimate load derived by Sokolovsky in 1944 [1] using deformation theory of plasticity agrees closely with the collapse

*Drucker, D.C., Prager, W., and Greenberg, H.J., "Extended Limit Design Theorems for Continuous Media." Quart. Applied Math. Vol. 9, No. 4, Jan. 1952, pp. 381-389.

load obtained using limit analysis theorems. Finally, a set of charts for the design of circular plates under axially symmetric loading was compiled by Hu in 1960 [11].

The generalization of the collapse load of circular plate under concentrated load for plates of arbitrary shape was made by Schumann in 1958 [12] and also for variable fixity by Zaid in 1958 [13]. It was found that for materials obeying Tresca's yield condition (regardless of shape and end fixity) the limit load is equal to 2π times the unit yield moment.

The load carrying capacities of annular plates with either fixed or simply supported edge conditions were discussed by Chernina in 1958 [14]. Tresca's yield condition was utilized. The case of simply supported edge conditions was later corrected by Hodge in 1959 [15].

Attention was also directed towards the minimum weight design of circular plates, utilizing limit analysis method. References [16] through [20] can be cited here. In 1964 an analog model was devised by Marcal and Prager [21] and applied to a circular plate problem.

Limit analysis was also employed to obtain the collapse load of circular plates made of initially anisotropic materials. In 1956 Sawczuk [22] discussed a solid plate with either simple or fixed boundary subjected to uniform load. The materials of plates were considered to be cylindrically orthotropic, obeying the modified Tresca's yield condition which has different platic moduli in two perpendicular directions. Non-homogeneity has also been discussed in this paper. Hu 1953 [23] studied the similar problem;

and a series of design charts were constructed for ultimate design of circular plates under axisymmetric loading by Markowitz and Hu in 1964 [24]. Mura et al (1964) [25] extended the work for materials obeying the yield criterion suggested by Hill, which reduces to the Mises yield criterion for isotropic materials.

The problem of interaction of in plane tension and bending in annular plates was discussed in 1960 by Hodge et al [26], and bounds on the interaction curve were established for various inner edge support conditions.

In 1963 Sawczuk et al [27] studied the effect of transverse shear on the plastic bending of simply supported circular plates. Kirchhoff's hypothesis was modified to allow for transverse shear deformation. Both Tresca's and Mises' yield conditions and their associated flow rules were employed. Collapse loads were calculated for plates under uniform load over central area.

Finally, linear programming was also used to obtain the collapse load of plate problems [28]. Examples of simply supported and clamped circular plates under uniform load are given.

Detailed discussions of some of the above solutions can be found in books by Hodge, 1961 [29], and 1963 [30], and Sawczuk and Jaeger, 1963, [31].

1.3 Rigid-Work Hardening Materials

The use of piece-wise linear yield conditions and associated flow rules were suggested by Prager 1955 [34] and Hodge* for the solution of work-

*Hodge, Jr., P.G., "The Theory of Piecewise Linear Isotropic Plasticity," Deformation and Flow of Solids, Colloq. Madrid, Sept. 1955, Edited by R. Grammel, Springer.

hardening problems. It allows total stress-strain laws to be used in the small, at the same time retaining the characteristic features of incremental laws in the large. As indicated by Hodge [35], the plastic flow rules can be explicitly integrated under restrictive conditions, defined as a "regular progression." That is, the stress point may not move from one side to another, from one corner to a side, or back into the elastic zone. This imposes a serious restriction which does not allow it to be used for problems such as clamped plates.

As an example Prager [34] presented the analysis of a simply supported circular plate subjected to a uniformly distributed transverse load. Tresca yield condition together with the linear kinematic hardening was used. The same problem was discussed by Boyce 1956 [32] using a piecewise yield condition which approximates that of Mises'. Later he extended the solution to a partially clamped plate [36]. In 1955 Eason [33] discussed the problem of plates under a concentrated load.

The concept of linear, isotropic strain hardening was employed by Hodge (1957) [35] in the solution of an infinite annular plate. Tresca yield condition was employed and the annulus was assumed to be simply supported at its inner edge and free at infinity. It was subjected to a slowly increasing moment applied to its inner edge. The loading process was divided into four stages, of which the fourth stage deviates from the regular progression.

Perrone and Hodge (1959) [37] derived two sets of strain hardening flow laws based on kinematic hardening for circular plates made of an initially Tresca material. These laws, called complete and direct hardening, differ in the point where the plane stress assumption is introduced. The solutions of finite as well as infinite annular plates and simply supported circular plates, using the derived laws, are reported. The results were compared for complete, direct, and isotropic hardening.

Hwang (1959) [38] treated the problem of simply supported circular plates under uniform load. Mises yield condition and associated flow rule together with the isotropic strain hardening were employed. Numerical integration was used to solve the set of non-linear differential equations.

Finally, in 1963, Chzhu-Khua [39] using Tresca yield condition and linear strain hardening , presented the solution of plate under partially uniform load.

1.4 Elastic-Plastic Analysis Utilizing Incremental Theory of Plasticity

An early attempt to estimate the deflections of circular plates made of elastic-plastic materials using incremental theory of plasticity was made by Haythornthwaite in 1954 [40]. The yield condition of Tresca and associated flow rule were employed. The key assumption was made that at any point on the plate the entire thickness was either fully elastic or fully plastic. An annular plate simply supported at the outer edge and clamped to a centrally loaded rigid disc at the inner edge was analyzed. The results obtained were compared with experiment.

Gaydon et al (1956) [41] discussed the problem of circular plate under a uniform moment around its edge. Mises yield condition and its associated flow rule were assumed to be valid.

Olszak et al (1957) [42], 1958 [44], [45] treated the elastic-plastic bending of non-homogeneous orthotropic circular plates. The material was assumed to exhibit no strain hardening and to obey the generalized Mises' yield condition. The general moment-curvature relations were derived by ordinary plate theory. A restriction that the principal curvatures progress proportionally was later introduced to make the expressions more tractable. Limitation is similar to that of "proportional loading." The authors report that if we require the continuity of stress at the elastic-plastic boundary, it is not possible, in general, to satisfy the normality rule which is a consequence of Drucker's postulate of stability. On the other hand, utilizing the associated flow rule, it is not possible, in general, to attain the continuity of stresses.

The analysis of a clamped circular plate made of incompressible elastic-perfectly plastic materials obeying Tresca's yield condition and the associated flow rule was discussed in 1957 by Tekinalp [43]. An assumption that any plate element is either entirely elastic or entirely plastic was made. This is strictly valid for a sandwich plate.

Eason (1961) [46] discussed the problem of simply supported plate under partial uniform load. The von Mises yield condition and the corresponding flow rule were assumed for the elastic-perfectly plastic material of the plate.

The stress field was obtained, but the velocity field was derived for the limiting case of concentrated load. A comparison has been made with solutions obtained utilizing the Tresca yield condition. It is reported that the stress distribution is relatively insensitive to the change of yield condition, but the plastic zone is expected to be sensitive to the yield condition. Moreover, the behavior of uniformly loaded plate is more sensitive to the variation of yield condition than that subjected to concentrated load.

Analysis of centrally clamped annular sandwich plates under uniform loads was made by French in 1964 [47], utilizing Tresca's yield condition. The plate behavior has been traced from zero to the collapse load, and three phases of loading are considered after initial yield. Collapse pressure is given graphically as a function of the ratio of inner to outer radii.

In 1964, Lackman [48] presented a method for the analysis of axi-symmetrically loaded circular plates. The method makes use of an analogy between plastic strain gradients and transverse loads. The Prandtl-Reuss equations together with the von Mises' yield condition and isotropic hardening were employed. An example is given for a simply supported circular plate under uniform load.

1.5 Experiments on Circular Plates

Experiments other than the ones mentioned earlier to check the theoretical results have also been published. In 1954 Cooper and Shifrin [49] presented the results of nine simply supported mild steel circular plates

under concentric uniformly distributed load. Comparison was made with limit loads obtained by Hopkins and Prager [7]. Similar kinds of tests were performed by Dyrbye et al (1954) [50], Haythornthwaite (1954) [51], and Foulkes et al (1955) [52] on either clamped or simply supported plates.

Correlation of experimental evidence with collapse load using limit analysis turned out to be unsatisfactory.

Haythornthwaite and Onat 1955 [53] reported the test results of steel plates under reversed loading. It was observed that although the limit load is often of little physical significance for a monotonically increasing load, it becomes a measure of the minimum load carrying capacity in reversed loading. This question still needs further investigation.

Lance and Onat 1962 [54] reported additional experiments on mild steel plates under uniform and partial load over a small circular central region. Comparison with collapse load in the sense of limit analysis re-affirmed the previous results. Etching patterns and mill-scale flaking patterns were also studied in this report.

II. ELASTIC-PLASTIC ANALYSIS OF CIRCULAR PLATES

2.1 Foreword

For the purpose of analysis, the plate is divided into a number of annular elements, which are further subdivided into a number of layers along their depths. The primary objective is to establish the stiffness matrix of an annular element for a typical increment of loading. The assemblage of these annuli can be easily accomplished using direct stiffness method of matrix analysis of structures. A modified analysis will also be given for a central circular disc element for solutions of solid plates. Loadings are applied at circular nodes where two consecutive elements meet. Both tributary area approach and consistent equivalent nodal ring load method were employed to convert the transverse load applied within the elements to the nodal ring loads. Possibility of loading as well as unloading is included in the analysis of each load increment.

The following relations were established for a typical loading increment. Notations will be described as they first appear, and they are also collected at the end for reference.

2.2 Equilibrium Equations

By adopting the sign convention for positive quantities as shown in Fig. 1, the equilibrium of the increments of moments and transverse forces for

the case of axisymmetric loading are as follows*

$$\frac{d\,\Delta M_r}{dr} + \frac{1}{r}(\Delta M_r - \Delta M_\theta) + \Delta Q = 0 \tag{2.1}$$

$$\frac{d\,\Delta Q}{dr} + \frac{1}{r}\,\Delta Q = \Delta p(r) \tag{2.2}$$

Eliminating ΔQ between equations (2.1) and (2.2), we get

$$\frac{d^2\,\Delta M_r}{dr^2} + \frac{1}{r}\left(2\,\frac{d\,\Delta M_r}{dr} - \frac{d\,\Delta M_\theta}{dr}\right) + \Delta p(r) = 0 \tag{2.3}$$

Note that the symbol Δ indicates a finite increment.

ΔM_r, and ΔM_θ are increments of radial and tangential moments per unit length.

ΔQ is increment of radial transverse shear per unit length.

2.3 Strain-Displacement Relations

In accordance with small deformation theory and the assumption that plane section normal to reference plane before deformation remains so after, the strain-displacement relations in the absence of in-plane forces are expressed as follows

$$\begin{Bmatrix} \Delta \epsilon_r \\ \Delta \epsilon_\theta \end{Bmatrix} = -z \begin{Bmatrix} \Delta k_r \\ \Delta k_\theta \end{Bmatrix} \quad ; \quad \{\Delta \epsilon\} = -z\,\{\Delta k\} \tag{2.4}$$

* See for example, Timoshenko and Woinowsky-Krieger, "Theory of Plates and Shells," 2nd Edition, pp. 51-53, McGraw-Hill, 1959.

where:

$\Delta\epsilon_r$, $\Delta\epsilon_\theta$ are radial and tangential strain increments, respectively.

Δk_r, Δk_θ are measures of radial and tangential deformations which are only functions of r. z is a coordinate distance measured positive downward from the reference plane.

For axi-symmetric deformation, and neglecting shear distortion, that is assuming plane section normal to the reference plane before deformation remains normal to its deformed state, the following relations hold*

$$\begin{Bmatrix} \Delta k_r \\ \Delta k_\theta \end{Bmatrix} = \begin{Bmatrix} \frac{d^2 \Delta w}{d r^2} \\ \frac{1}{r} \frac{d \Delta w}{dr} \end{Bmatrix} \qquad (2.5)$$

where Δk_r, Δk_θ are now the increments of curvature of the reference surface, and Δw is transverse deflection increment which is taken to be positive in the direction of transverse load application.

2.4 Stress-Strain Relations

A constitutive relation for an elastic-plastic solid should include the state of stress and strain as well as their rates in order to account for the history dependence. As has been mentioned by some authors, an attempt to express the various properties of elastic-plastic solids by means of a single

* Ibid

mathematical model can be hardly achieved. Within the framework of a phenomenological approach, the attempt has been made both to construct the general theories to be adequate for describing the phenomena occurring beyond the elastic limit, and to formulate it in a manner suitable for practical applications. Because of non-linearity and irreversibility of the deformation processes, even the simplest model is generally too complicated to apply.

In order to establish constitutive relations for plastic solids three ingredients -- yield condition, flow law, and hardening rule -- must be defined. A number of surveys regarding the constitutive laws of plasticity have been published. The discussion here will be limited to those which are closely related to the laws chosen to demonstrate the proposed method of plate analysis. The general theories will not be discussed. The reader, however, is referred to references [55] through [62] for details of recent progress in this area.

Prandtl-Reuss theory is most widely used to describe elastic-plastic deformation. The materials, here, are considered to be time independent and initially free from residual stresses. In addition, the process is considered to be isothermal and the deformation small. Following Prandtl-Reuss theory, strain tensor is assumed to consist of two components: elastic or recoverable and plastic or permanent.

$$\epsilon_{ij} = \epsilon_{ij}^{E} + \epsilon_{ij}^{P} \qquad i,j = 1,2,3 \tag{2.6}$$

or

$$d\,\epsilon_{ij} = d\,\epsilon_{ij}^{E} + d\,\epsilon_{ij}^{P} \tag{2.7}$$

where superscripts E and P designate elastic and plastic components, respectively. Some authors, instead, have preferred to use the rate of strain $\dot{\epsilon}_{ij} = \frac{d\,\epsilon_{ij}}{dt}$, and similarly rates of stress and displacement. Since, however, it has been already assumed that the material behavior, and consequently its constitutive relations, are time independent, the latter notation seems to be unnecessary. This avoids a possible confusion with viscosity, and its use is abandoned here.

The elastic component of strain is related to stress through the generalized Hooke's law

$$d\,\epsilon_{ij}^{E} = C_{ijk\ell}\, d\,\tau_{k\ell} \qquad i,j,k,\ell = 1,2,3 \tag{2.8}$$

which in the case of isotropic materials becomes

$$d\,\epsilon_{ij}^{E} = \frac{1+\nu}{E}\, d\,\tau_{ij} - \frac{\nu}{E}\, d\tau_{kk}\, \delta_{ij} \tag{2.8b}$$

Here, the repeated indices imply summation.

In order to establish relations between the plastic component of strain, and the state of stress; the existence of the plastic potential, and the validity of normality rule at a regular point on the yield surface are generally assumed, that is

$$d\,e_{ij}^{p} = d\,\epsilon_{ij}^{p} = d\Phi\, \frac{\partial f}{\partial \tau_{ij}} \qquad ; \epsilon_{ii}^{p} = 0 \tag{2.9}$$

where,

$$f\ (\tau_{k\ell},\ \epsilon^{p}_{k\ell},\ \kappa) = 0$$

is the yield condition, and

$$e_{ij} = \epsilon_{ij} - \frac{1}{3}\ \epsilon_{kk}\ \delta_{ij}$$

is the deviatoric strain tensor.

Φ is a non-negative function which may depend on stress, stress rate, strain, and history of loading.

κ is a work-hardening parameter.

The condition of loading, neutral loading, or unloading is distinguished by whether, $\frac{\partial f}{\partial \tau_{ij}}\ d\ \tau_{ij}$ is greater, equal, or smaller than zero, respectively. Drucker* suggested

$$d\Phi = G\ \frac{\partial f}{\partial \tau_{k\ell}}\ d\ \tau_{k\ell} \qquad (2.10)$$

where G is independent of the stress rate.

2.4.1 Elastic-Perfectly Plastic Solids

Since the plastic deformation can be assumed to occur without a change of volume, i.e., $\epsilon^{p}_{ii} = 0$, expression (2.7) can be re-written as follows

$$d\ e_{ij} = d\ e^{E}_{ij} + d\ e^{P}_{ij} = d\ e^{E}_{ij} + d\Phi\ \frac{\partial f}{\partial \tau_{ij}}\ .$$

*Drucker, D.C., "A Definition of Stable Inelastic Material," J. Appl. Mech., Vol. 26, pp. 101-161, 1959.

Assuming the materials obey the Mises yield condition

$$f = J_2 - k^2 = 0 \tag{2.12}$$

where

$$J_2 = \frac{1}{2} \; s_{ij} \; s_{ij}$$

is the second invariant of stress deviator, and

$$s_{ij} = \tau_{ij} - \frac{1}{3} \; \tau_{kk} \; \delta_{ij}$$

where k, the yield stress in simple shear is $k = \frac{1}{\sqrt{3}} \sigma y$, where σy is yield stress in uniaxial tension. Using these definitions,

$$\frac{\partial f}{\partial \tau_{ij}} = s_{ij} \tag{2.13}$$

For isotropic elastic material the Hooke's law in terms of stress and strain deviators is expressed as

$$e_{ij}^{E} = \frac{1}{2\mu} \; s_{ij} \tag{2.14}$$

or

$$d \; e_{ij}^{E} = \frac{1}{2\mu} \; d \; s_{ij} \tag{2.15}$$

Where, μ is the shear modulus.

Substitutions of (2.13) and (2.15) into (2.11) yields

$$d \; e_{ij} = \frac{1}{2\mu} \; d \; s_{ij} + s_{ij} \; d\Phi \tag{2.16}$$

Considering that

$$df = s_{ij}\, d\, s_{ij} = 0 \tag{2.17}$$

multiplying (2.16) by s_{ij}, and summing, we obtain

$$s_{ij}\, d\, e_{ij} = \frac{1}{2\mu}\, \cancel{s_{ij}\, d\, s_{ij}}^{\,0} + s_{ij}\, s_{ij}\, d\Phi = 2\, k^2\, d\Phi$$

$$d\Phi = \frac{s_{ij}\, d\, e_{ij}}{2\, k^2} \tag{2.18}$$

Substituting (2.18) into (2.16) and transposing, we get

$$d\, s_{ij} = 2\mu\, \left(d\, e_{ij} - \frac{1}{2\, k^2}\, s_{k\ell}\, s_{ij}\, de_{k\ell} \right) \tag{2.19}$$

The hydrostatic state of stress, of the order of yield stress, does not produce yielding; and it is related to volumetric strain through elastic law

$$\tau_{kk} = (3\lambda + 2\mu)\, \epsilon_{kk} \tag{2.20}$$

or

$$d\, \tau_{kk} = (3\, \lambda + 2\mu)\, d\, \epsilon_{kk} \tag{2.21}$$

where λ and μ are Lamé constants.

Multiplying (2.21) by $\frac{1}{3}\, \delta_{ij}$ and adding it to (2.19), and by considering the relations between stress or strain tensor with its deviatoric components, we obtain

$$d\, \tau_{ij} = 2\mu d\epsilon_{ij} + \lambda\, d\tau_{kk}\, \delta_{ij} - \frac{2\mu}{2k^2}\, s_{k\ell}\, s_{ij}\, d\epsilon_{k\ell} \tag{2.22}$$

Note that:

$$s_{k\ell}\ d\ e_{k\ell} = s_{k\ell}\ (d\epsilon_{k\ell} - \frac{1}{3}\ d\epsilon_{mm}\ \delta_{k\ell}) = s_{k\ell}\ d\epsilon_{k\ell} \tag{2.23}$$

Finally,

$$d\ \tau_{ij} = E_{ijk\ell} d\epsilon_{k\ell} \quad ; \quad \underset{9x1}{\{d\tau\}} = \underset{9x9}{[E]}\ \underset{9x1}{\{d\epsilon\}} \tag{2.24}$$

where

$$E_{ijk\ell} = 2\mu\ \ \delta_{ik}\ \delta_{j\ell} + \lambda\ \delta_{ij}\ \delta_{k\ell} - \frac{2\mu}{2k^2}\ \ s_{ij}\ \ s_{k\ell} \tag{2.25}$$

λ and μ can be expressed in terms of Young's modulus E and Poisson's ratio as

$$\lambda = \frac{\nu E}{(1+\nu)\ (1-2\nu)}\ ,\ \mu = \frac{E}{2(1+\nu)} \tag{2.26}$$

Substitution of (2.26) into (2.25), gives

$$E_{ijk\ell} = \frac{E}{1+\nu}\ \ (\delta_{ik}\ \delta_{j\ell} + \frac{\nu}{1-2\nu}\ \ \delta_{ij}\ \delta_{k\ell} - \frac{1}{2k^2}\ \ s_{ij}\ s_{k\ell}) \tag{2.27}$$

Generalized Plane Stress

The general expression (2.24) can be specialized for the state of plane stress. For this purpose assume that $\tau_{i3}=0$, $d\tau_{i3}=0$, where i = 1,2,3 and further that $d\epsilon_{13} = d\epsilon_{23}=0$, and

$$d\tau_{33} = E_{33\gamma\delta}\ d\epsilon_{\gamma\delta} + E_{3333}\ d\epsilon_{33}=0. \qquad \gamma,\delta = 1,2.$$

Then

$$d\,\epsilon_{33} = -\frac{E_{33\gamma\delta}}{E_{3333}}\, d\epsilon_{\gamma\delta} \tag{2.28}$$

$$d\,\tau_{\alpha\beta} = E_{\alpha\beta\gamma\delta}\, d\,\epsilon_{\gamma\delta} + E_{\alpha\beta 33}\, d\,\epsilon_{33} \quad \text{where} \quad \alpha,\beta = 1,2 \tag{2.29}$$

Substitution of (2.28) into (2.29) gives

$$d\,\tau_{\alpha\beta} = \bar{E}_{\alpha\beta\gamma\delta}\, d\,\epsilon_{\gamma\delta} \qquad \alpha,\beta,\gamma,\delta = 1,2 \tag{2.30}$$

and

$$\bar{E}_{\alpha\beta\gamma\delta} = \frac{E_{\alpha\beta\gamma\delta}\, E_{3333} - E_{\alpha\beta 33}\, E_{33\gamma\delta}}{E_{3333}} \tag{2.31}$$

For the principal directions of stress increment, where the principal directions of stresses do not change during loading, the basic relation for the generalized plane stress can be written down as

$$\begin{Bmatrix} d\,\tau_{11} \\ d\,\tau_{22} \end{Bmatrix} = \begin{bmatrix} \bar{E}_{1111} & \bar{E}_{1122} \\ \bar{E}_{2211} & \bar{E}_{2222} \end{bmatrix} \begin{Bmatrix} d\,\epsilon_{11} \\ d\,\epsilon_{22} \end{Bmatrix} \tag{2.32}$$

or symbolically as $\underset{2x1}{\{d\tau\}} = \underset{2x2}{[E]}\ \underset{2x1}{\{d\,\epsilon\}}$

Where

$$\bar{E}_{1111} = E \frac{s_{22}^2}{s_{11}^2 + s_{22}^2 + 2\nu\, s_{11}\, s_{22}}$$

$$\bar{E}_{1122} = \bar{E}_{2211} = -E \frac{s_{11}\, s_{22}}{s_{11}^2 + s_{22}^2 + 2\nu\, s_{11}\, s_{22}} \qquad (2.33)$$

$$\bar{E}_{2222} = E \frac{s_{11}^2}{s_{11}^2 + s_{22}^2 + 2\nu\, s_{11}\, s_{22}}$$

In this case,

$$s_{11} = \frac{2}{3}\left(\tau_{11} - \frac{1}{2}\,\tau_{22}\right) \; ; \quad s_{22} = \frac{2}{3}\left(\tau_{22} - \frac{1}{2}\,\tau_{11}\right) \qquad (2.34)$$

Note that the [E] matrix in (2.32) is singular. This is also true in the general case of (2.24). This follows from the fact that the stress increments $d\,\tau_{ij}$ are linearly dependent as can be seen from (2.17), since

$$s_{ij}\, d\, s_{ij} = s_{ij}\, d\, \tau_{ij} = 0 \qquad (2.35)$$

Therefore, we can only specify strain increments and solve for the stress increments; however, the reverse is not possible. This is obvious for a uniaxial stress condition for a perfectly plastic solid by noting its stress-strain diagram.

The expression (2.24) is valid for loading when

$$\frac{\partial f}{\partial \tau_{ij}} \, d\,\tau_{ij} = s_{ij}\, d\,\tau_{ij} = 0 \tag{2.36}$$

That is when the point in the stress space moves on the yield surface or stays on it. Stated otherwise,

$$f^{(1)} = f^{(2)} = 0 \tag{2.37}$$

But, if

$$\frac{\partial f}{\partial \tau_{ij}} \, d\,\tau_{ij} < 0$$

unloading takes place, and instead of (2.24) the Hooke's law must be used, i.e.,

$$\begin{Bmatrix} d\,\tau_{11} \\ d\,\tau_{22} \end{Bmatrix} = \frac{E}{1-\nu^2} \begin{bmatrix} 1 & \nu \\ \nu & 1 \end{bmatrix} \begin{Bmatrix} d\,\epsilon_{11} \\ d\,\epsilon_{22} \end{Bmatrix} \tag{2.38}$$

It is interesting to note, that for a strain increment vector, which is in the direction of normal to the yield surface, the stress increment vector vanishes. Therefore, if for a stress point located on the yield surface, we resolve the strain increment vector into two components -- tangent and perpendicular to the yield surface, see Fig. 2 -- it is only necessary to retain the tangential component in the computation of stress increment. Hence,

$$\{d\tau\} = [E]\ \{d\epsilon\} = [E]\ \{d\epsilon^T\} + [E]\ \{d\epsilon^N\}$$

$$\{d\tau\} = [E]\ \{d\epsilon^T\} \tag{2.39}$$

This property is preserved for the generalized plane stress case discussed earlier. In this case both $\{d\tau\}$ and $\{d\epsilon^T\}$ are tangent to the yield curve. This indicates that the transformation [E] only stretches $\{d\epsilon^T\}$ with a proper scale.

The stress-strain relations (2.32) are strictly true for infinitesimal increments. Here it is necessary to establish relations for finite increments. Thus, the infinitesimal increments are to be integrated within a small interval. Prager [34] and Hodge* suggested the concept of piecewise linear yield condition. It enables one to integrate stress-strain relations locally while preserving the incremental characteristics in the total. Another approach has been employed here.

The equations (2.32) essentially specify an initial value problem. For a finite increment of strain, the stress increment should move along the yield curve as from A to C shown in Fig. 3. By following a tangent at A, one reaches an incorrect point B. However, by projecting point B back to the yield curve point C is located. This point C is taken as the new state of stress from which the next step in calculations is made. In Fig. 3 the locations of points B and C are greatly exaggerated and the result of example I, Fig. 14 indicates that for a relatively small increment of stress the distance between such

*See footnote on pp. 9.

points are small. Therefore the error committed in this process is not very significant. As the first approximation the initial state of stress in each increment can be used to determine the [E] matrix. Iteration procedures or the techniques of numerical integration such as the Runge-Kutta or Euler's modified method* was employed to compare the results found with the first approximation.

A difficulty arises in the transition zone, when the point initially located inside the yield surface reaches the surface during the increment of loading. In this process the associated deformation contains a purely elastic part. During deformation the point moves elastically within the yield surface until it just touches the surface. When the point reaches the yield surface the plastic part of the deformation occurs. If the total deformation produced during an increment of loading is given, equation (2.38) can be used to determine the corresponding stress increment. Depending on the relative distance of the initial and final state of stress with respect to the yield curve, point D and E, of Fig. 3, the point closer to the yield surface, point E in this figure, is chosen for a radial approximation. The intersection of the radius vector with the yield surface, F in Fig. 3 is taken as the point of the initiation of yielding. Strain increment associated with DF is obtained using (2.38). It is subtracted from the given strain increment to find the strain associated with the elastic-plastic deformation. The remainder of the procedure follows as before.

---

* See for example Collatz, L., "The Numerical Treatment of Differential Equations." pp. 53-61, Springer-Verlag, 1960.

2.4.2 Elastic-Plastic Strain Hardening Solids

From the observations of the behavior of hardening materials in uniaxial and biaxial tests, it is known that during plastic deformation the yield surface is continuously changing in size and shape.

Isotropic hardening (see Fig. 4a), which at higher stresses exhibits uniform expansion of the initial yield surface, is the most widely used law to describe hardening. Thus, the yield surface for initially isotropic materials depends on a single parameter κ and may be written as

$$f = g\ (J_2,\ J_3) - \kappa = 0 \tag{2.40}$$

where J_2, J_3 are the second and third invariants of stress deviator, and κ is the hardening parameter which describes the strain history. Two measures of hardening for κ are frequently used. The first approach suggests that the degree of hardening is a function only of the total plastic work, and is otherwise independent of the strain path.*

$$\kappa = \kappa\ (W_p)\ ,\quad W_p = \int \tau_{ij}\ d\ \epsilon_{ij}^{p} \tag{2.41}$$

where W_p is positive definite, since plastic deformation is an irreversible process. The second approach states that the so-called equivalent plastic strain increment

$$d\ \bar{\epsilon}^{\,p} = \sqrt{\frac{2}{3}}\quad [\ d\ \epsilon_{ij}^{p}\ \ d\ \epsilon_{ij}^{p}\ ]^{1/2} \tag{2.42}$$

---

* Hill, R., "The Mathematical Theory of Plasticity," pp. 23-33, Oxford, Clarendon Press, 1950.

integrated over the strain path provides a measure of the plastic deformation*. That is

$$\kappa = \kappa \left(\int d \bar{\epsilon}^{p} \right).$$

As pointed out by Hill*, the above two concepts are equivalent for the materials obeying von Mises yield condition. Hill's remark was later generalized by Bland**, showing that for any g to be a homogeneous polynomial of degree n, and have regular regimes of yield surface, the above property holds true, if, and only if, g is linear or quadratic function in the principal components of stress. Certain restrictions on the coefficients are imposed in the quadratic case.

For proportional loading, if the strain ratios remain constant, (2.43) can be integrated

$$\bar{\epsilon}^{p} = \int d \bar{\epsilon}^{p} = \sqrt{\frac{2}{3}} \left[\epsilon_{ij}^{p} \epsilon_{ij}^{p} \right]^{1/2} \qquad (2.44a)$$

$$\kappa = \kappa (\bar{\epsilon}^{p}) \qquad (2.44b)$$

Expression (2.44b) was checked by some investigators***, with the experimental results, where the stress ratios were not constant. In the tests on mild steel and annealed copper, agreements to within 5 percent are reported.

---

* ibid

**Bland, D.R., "The Two Measures of Work-Hardening," Proc. 9th Int. Congr. Appl. Mech. (Brussels, 1956), Vol. 8, pp. 45-50, 1957.

***See Hill, R., footnote on pp. 29.

The concept of isotropic hardening does not account for Bauschinger effect. Actually, it predicts a negative Bauschinger effect. Therefore, isotropic hardening would predict erroneous results in problems involving unloading followed by reloading along some new path. To include the Bauschinger effect, a hardening rule was suggested by Prager*, which assumes a rigid translation of the initial yield surface (see Fig. 4b). Prager employed a kinematical model to describe this hardening rule. For this reason it is termed "kinematic hardening." This hardening rule can be represented mathematically by

$$f(\tau_{ij} - \alpha_{ij}) = F(\tau_{ij} - \alpha_{ij}) - k^2 = 0 \tag{2.45}$$

where $f(\tau_{ij}) = 0$ is the initial yield surface, and α_{ij} is a tensor representing the total translation of the center of the initial yield surface. Prager suggested that the yield surface be translated in the direction of the normal to the yield surface for any increment of strain.

$$d\,\alpha_{ij} = c\; d\,\epsilon^{p}_{ij} \tag{2.46}$$

where c is generally assumed to be constant. In such a case the process is called linear hardening. Shortly after Prager's proposal it was recognized that the properties of preserving the shape, and of pure translation of the

---

*Prager, W., "The Theory of Plasticity: A Survey of Recent Achievements," (Jame Clayton Lecture) Proc. Inst. Mech. Eng. Vol. 169, pp. 41-57, 1955.

yield surface along a normal, do not generally remain invariant if the nine dimensional stress space is degenerated into subspaces. To resolve this inconsistency Ziegler* suggested to replace (2.46) by

$$d\alpha_{ij} = (\tau_{ij} - \alpha_{ij})\ d\eta \tag{2.47}$$

Further suggestions such as piecewise linear yield conditions, which accomodate both translation and expansion of the yield surface (see Fig. 4d), and the concept of yield corner stating that the yield surface changes only locally (see Fig. 4c), have also been advanced. Numerous tests have been conducted to check these theories, but no definite conclusions have been reached so far.

After considering the several possibilities of a constitutive law, isotropic hardening was adopted in this report. The material is assumed to obey von Mises' yield condition. Then, in equation (2.40) the function g becomes

$$g = J_2 \tag{2.48}$$

Assuming the validity of (2.44b) for non-radial loading; and substituting (2.44b) and (2.48) into (2.40), we obtain

$$f = J_2 - \kappa(\bar{\epsilon}^p) = 0 \tag{2.49}$$

---

*Ziegler, H., "A Modification of Prager's Hardening Rule," Quant. Appl. Math. Vol. 17, pp. 55-65, 1959.

The unknown function κ can be determined from a simple experiment; namely, uniaxial tension or simple shear. The expression (2.49) has been sometimes called the J_2 - theory and is frequency expressed as

$$\bar{\sigma} = H\ (\bar{\epsilon}^{\,p}) \tag{2.50}$$

where,

$$\bar{\sigma} = \sqrt{\frac{3}{2}}\ \left[\ s_{ij}\ s_{ij}\ \right]^{1/2} = \sqrt{3J_2} \tag{2.51}$$

is the so-called effective stress.

Now, recall (2.9) and (2.13) which gives

$$d\ \epsilon_{ij}^{p} = d\ \Phi\ s_{ij} \tag{2.52}$$

To determine $d\Phi$ multiply (2.52) by $\frac{2}{3}\ d\ \epsilon_{ij}^{p}$ and sum, then note (2.42) and (2.51) to obtain

$$(d\ \bar{\epsilon}^{\,p})^2 = \frac{2}{3}\ (d\ \epsilon_{ij}^{p}\ \ d\ \epsilon_{ij}^{p}\ ) = \frac{2}{3}\ \ (d\Phi)^2\ \ s_{ij}\ s_{ij} = (\frac{2}{3}\ \bar{\sigma}\ d\ \Phi)^2$$

$$d\ \Phi = \frac{3}{2}\ \ \frac{d\ \bar{\epsilon}^{p}}{\bar{\sigma}} \tag{2.53}$$

If the curve of $\bar{\sigma}$ - $\bar{\epsilon}^{\,p}$ is given as in (2.50), then

$$d\ \bar{\epsilon}^{\,p} = \frac{d\bar{\sigma}}{H'} \tag{2.54}$$

where $H' = \dfrac{d\bar{\sigma}}{d\ \bar{\epsilon}^{\,p}}$ is the slope of J_2 curve. Whence upon substituting (2.54) into (2.53), we obtain

$$d\,\Phi = \frac{3}{2}\,\frac{1}{H'}\,\frac{d\bar{\sigma}}{\bar{\sigma}} = \frac{3}{2}\,\frac{1}{H'}\,\frac{1}{\bar{\sigma}}\,\frac{\partial\bar{\sigma}}{\partial\tau_{k\ell}}\,d\,\tau_{k\ell} \tag{2.55}$$

Also note that

$$s_{ij} = \frac{\partial J_2}{\partial\tau_{ij}} = \frac{2}{3}\,\bar{\sigma}\,\frac{\partial\bar{\sigma}}{\partial\tau_{ij}} \tag{2.56}$$

Substitute (2.55) and (2.56) into (2.52) to obtain

$$d\,\epsilon^{p}_{ij} = \frac{1}{H'}\,\frac{\partial\bar{\sigma}}{\partial\tau_{ij}}\,\frac{\partial\bar{\sigma}}{\partial\tau_{k\ell}}\,d\,\tau_{k\ell} \tag{2.57}$$

This relation is similar to expression (2.10) proposed by Drucker. It can be re-cast into another form:

$$d\,\epsilon^{p}_{ij} = \frac{3}{2}\,\frac{1}{H'}\,\frac{s_{ij}\,s_{k\ell}}{s_{mn}\,s_{mn}}\,d\,\tau_{k\ell} \tag{2.58}$$

If the data for uniaxial tension test are used to define H', it is easily seen that

$$\frac{1}{H'} = \frac{1}{E_t} - \frac{1}{E} \tag{2.59}$$

where E_t is the tangent modulus, and E the Young's modulus. If the data from pure shear test are used, then to define H' we have

$$\frac{1}{H'} = \frac{1}{3}\left(\frac{1}{\mu_t} - \frac{1}{\mu}\right) \tag{2.60}$$

where μ_t is the tangent modulus in shear for $\tau - \gamma$ diagram, and μ is the elastic shear modulus.

For H' to be invariant, the comparison of (2.59) and (2.60) leads to the following requirement:

$$\frac{3}{E_t} - \frac{1}{\mu_t} = \frac{1-2\nu}{E} \tag{2.61}$$

Expression (2.61) imposes a restriction on E_t and μ_t, which generally does not hold true for all materials.

Now, returning to Prandtl-Reuss equation (2.7) and substituting for $d\epsilon_{ij}^{p}$ from (2.58), and considering the uniaxial tension test as the basis, we obtain

$$d\,\epsilon_{ij} = \frac{1+\nu}{E}\, d\,\tau_{ij} - \frac{\nu}{E}\, d\,\tau_{kk}\,\delta_{ij} + \frac{3}{2}\left(\frac{1}{E_t} - \frac{1}{E}\right)\frac{s_{ij}\, s_{k\ell}}{s_{mn}\, s_{mn}}\, d\,\tau_{k\ell} \tag{2.62}$$

or

$$d\,\epsilon_{ij} = S_{ijk\ell}\, d\,\tau_{k\ell} \tag{2.63}$$

where

$$S_{ijk\ell} = \frac{1+\nu}{E}\,\delta_{ik}\,\delta_{j\ell} - \frac{\nu}{E}\,\delta_{ij}\,\delta_{k\ell} + \frac{3}{2}\left(\frac{1}{E_t} - \frac{1}{E}\right)\frac{s_{ij}\, s_{k\ell}}{s_{mn}\, s_{mn}} \tag{2.64}$$

Symbolically we can express (2.63) in matrix form as

$$\underset{9x1}{\{d\epsilon\}} = \underset{9x9}{[S]}\ \underset{9x1}{\{d\tau\}} \tag{2.65}$$

Specializing (2.63) for the case of plane stress in principal stresses and following the similar procedures for elastic-perfectly plastic solids, we obtain

$$\begin{Bmatrix} d\,\epsilon_{11} \\ d\,\epsilon_{22} \end{Bmatrix} = \begin{bmatrix} \bar{S}_{1111} & \bar{S}_{1122} \\ \bar{S}_{2211} & \bar{S}_{2222} \end{bmatrix} \begin{Bmatrix} d\,\tau_{11} \\ d\,\tau_{22} \end{Bmatrix} \tag{2.66}$$

Where,

$$\bar{S}_{1111} = \frac{1}{E} + \left(\frac{1}{E_t} - \frac{1}{E} \right) \frac{\left(\tau_{11} - \frac{1}{2}\tau_{22}\right)^2}{\bar{\sigma}^2}$$

$$\bar{S}_{1122} = \bar{S}_{2211} = -\frac{\nu}{E} + \left(\frac{1}{E_t} - \frac{1}{E} \right) \frac{\left(\tau_{11} - \frac{1}{2}\tau_{22}\right)\left(\tau_{22} - \frac{1}{2}\tau_{11}\right)}{\bar{\sigma}^2} \tag{2.67}$$

$$\bar{S}_{2222} = \frac{1}{E} + \left(\frac{1}{E_t} - \frac{1}{E} \right) \frac{\left(\tau_{22} - \frac{1}{2}\tau_{11}\right)^2}{\bar{\sigma}^2}$$

Inversion of (2.66) gives

$$\begin{Bmatrix} d\,\tau_{11} \\ d\,\tau_{22} \end{Bmatrix} = \begin{bmatrix} \bar{E}_{1111} & \bar{E}_{1122} \\ \bar{E}_{2211} & \bar{E}_{2222} \end{bmatrix} \begin{Bmatrix} d\,\epsilon_{11} \\ d\,\epsilon_{22} \end{Bmatrix} \tag{2.68}$$

Where

$$\bar{E}_{1111} = E \frac{\xi + \frac{3}{4} \frac{s_2^2}{s_1^2 - s_1 s_2 + s_2^2}}{(1-\nu^2)\ \xi + \frac{3}{4} \frac{s_1^2 + 2\nu\, s_1 s_2 + s_2^2}{s_1^2 - s_1 s_2 + s_2^2}}$$

$$\bar{E}_{1122} = \bar{E}_{2211} = E \frac{\nu\ \xi - \frac{3}{4} \frac{s_1 s_2}{s_1^2 - s_1 s_2 + s_2^2}}{(1-\nu^2)\ \xi + \frac{3}{4} \frac{s_1^2 + 2\nu\, s_1 s_2 + s_2^2}{s_1^2 - s_1 s_2 + s_2^2}} \qquad (2.69)$$

$$\bar{E}_{2222} = E \frac{\xi + \frac{3}{4} \frac{s_1^2}{s_1^2 - s_1 s_2 + s_2^2}}{(1-\nu^2)\ \xi + \frac{3}{4} \frac{s_1^2 + 2\nu\, s_1 s_2 + s_2^2}{s_1^2 - s_1 s_2 + s_2^2}}$$

where

$$\xi = \frac{E_t}{E-E_t}\ , \quad s_1 = \frac{2}{3}\ (\tau_{11} - \frac{1}{2}\ \tau_{22}),\ \ s_2 = \frac{2}{3}\ (\tau_{22} - \frac{1}{2}\ \tau_{11})$$

$$\bar{\sigma}^2 = \tau_{11}^2 - \tau_{11}\ \tau_{22} + \tau_{22}^2 \qquad (2.70)$$

It is easily seen that if E_t tends to zero expressions (2.69) will be reduced to (2.33).

Stress-strain relations (2.32) and (2.68) will be employed to describe the material properties of any annular layer during loading. During unloading,

apply relations (2.38). Since in the computation processes we are dealing with finite increment of loading, (2.32) and (2.68) are not strictly valid. As mentioned earlier, however, the errors introduced are not very significant for small increments.

Although the examples which are given in this report have been based on (2.32) and (2.68) the developed procedures are perfectly general and any other constitutive relations can be employed by properly defining the [E] matrix. Should necessity arise, experimental data may be used directly.

2.5 Stress Resultants

To determine stress-resultant increments, we proceed as follows:

Take the middle plane as the plane of reference, and divide the plate into a number of layers symmetrically arranged with respect to the middle plane (Fig. 5). Then upon assigning the material properties to each layer, we can formulate the expression for $\{\Delta M\}$ as

$$\{\Delta M\} = 2 \sum_{k=1}^{n} \int_{h_{k-1}}^{h_k} \{\Delta \tau\} \, z dz = 2 \sum_{k=1}^{n} \int_{h_{k-1}}^{h_k} [E^{(k)}] \{\Delta \epsilon\} \, z dz \qquad (2.71)$$

where $\{\Delta M\}$ contains both the radial and the tangential moments, i.e.,

$$\{\Delta M\} = \begin{Bmatrix} \Delta M_1 \\ \Delta M_2 \end{Bmatrix} = \begin{Bmatrix} \Delta M_r \\ \Delta M_\theta \end{Bmatrix}$$

Upon substituting from (2.4), and integrating, we obtain

$$\{\Delta M\} = - [D] \{\Delta K\} \tag{2.72}$$

where, with $h_o = o$,

$$[D] = \frac{2}{3} \sum_{k=1}^{n} [E^{(k)}] (h_k^3 - h_{k-1}^3) \tag{2.73}$$

If the layers are taken of equal thickness

$$h_k = k\, h \; ; \quad h_1 = \frac{h}{2n} \tag{2.74}$$

and

$$[D]_{2x2} = \frac{h^3}{12} \sum_{k=1}^{n} [E^{(k)}] (3\, k^2 - 3\, k+1) \tag{2.75}$$

here,

$$[D] = \begin{bmatrix} D_{11} & D_{12} \\ D_{21} & D_{22} \end{bmatrix} \quad , \text{ where } D_{12} = D_{21} \tag{2.76}$$

This equation together with (2.72) yields the following results:

$$\begin{aligned} \Delta M_r = \Delta M_1 &= - D_{11} \Delta K_r - D_{12} \Delta K_\theta \\ \Delta M_\theta = \Delta M_2 &= - D_{21} \Delta K_r - D_{22} \Delta K_\theta \end{aligned} \tag{2.77}$$

2.6 Governing Differential Equation

Substitute (2.77) into the differential equation of equilibrium (2.3), and define curvatures as given by (2.5). Then the governing differential equation becomes

$$D_{11}\,\Delta w^{IV} + \frac{2}{r}\,D_{11}\,w^{III} - \frac{1}{r^2}\,D_{22}\,\Delta w'' + \frac{1}{r^3}\,D_{22}\,\Delta w' = \Delta\, p(r) \tag{2.78}$$

Dividing by D_{11}, and letting

$$\Lambda^2 = \frac{D_{22}}{D_{11}} \tag{2.79}$$

$$\Delta w^{IV} + \frac{2}{r}\,\Delta w^{III} - \left(\frac{\Lambda}{r}\right)^2 \left(\Delta w'' - \frac{1}{r}\,\Delta w'\right) = \frac{\Delta p(r)}{D_{11}} \tag{2.80}$$

where primes denote differentiation with respect to r.

The solution of part of homogeneous (2.80) has three different forms depending on the value of Λ .

(a) For $\Lambda = 1$

$$\Delta w = a_1 + a_2\, r^2 + a_3\, \ell n\, r + a_4\, r^2\, \ell n\, r \tag{2.81}$$

(b) $\Lambda = 0$

$$\Delta w = a_1 + a_2\, r^2 + a_3\, r + a_4\, r\, \ell n\, r \tag{2.82}$$

(c) $\Lambda \neq 1,\ \Lambda \neq 0$

$$\Delta w = a_1\, r^{1+\Lambda} + a_2\, r^{1-\Lambda} + a_3\, r^2 + a_4 \tag{2.83}$$

Case (b) is not frequently encountered.

2.7 Stiffness Matrix For an Annular Element

In this section the relations between nodal ring forces applied at the edges of an annular element, and their corresponding nodal ring displacement are established. Here the term "nodal ring force" includes both transverse force and moment. Similarly, the "nodal ring displacement" implies both displacement and rotation.

In order to set up the element stiffness matrix, two frequencly encountered cases $\Lambda = 1$ and $\Lambda \neq 1$, $\Lambda \neq 0$ will be considered.

Case I $\Lambda = 1$

From expression (2.81) we can obtain all nodal forces and displacements in terms of a_i , i = 1,2,3,4.

Thus,

Increment of rotation:

$$\Delta \omega = \Delta w' = 2 a_2 r + a_3 r^{-1} + a_4 r \ (2 \ell n \ r + 1) \tag{2.84}$$

Increment of radial curvature:

$$\Delta K_r = \Delta w'' = 2a_2 - a_3 r^{-2} + a_4 \ (2 \ell n \ r + 3) \tag{2.85}$$

Increment of tangential curvature:

$$\Delta K_\theta = \frac{1}{r} \Delta w' = 2 a_2 + a_3 r^{-2} + a_4 \ (2 \ell n \ r + 1) \tag{2.86}$$

Substitution of (2.85) and (2.86) into (2.77) yields moments

$$\Delta M_r = -2 a_2 (D_{11} + D_{12}) - a_3 (-D_{11} + D_{12}) r^{-2} - a_4 (D_{11} (3 + 2 \ell n\, r) + D_{12} (1 + 2 \ell n\, r) \tag{2.87}$$

$$\Delta M_\theta = -2 a_2 (D_{11} + D_{12}) + a_3 (-D_{11} + D_{12}) r^{-2} - a_4 [D_{11} (1+2 \ell n\, r) + D_{12} (3 + 2 \ell n\, r)] \tag{2.88}$$

Finally, substitution of (2.87) and (2.88) into (2.1) gives

$$\Delta Q = 4 a_4 D_{11} r^{-1} \tag{2.89}$$

Next, consider the annular element shown in Fig. 6 with all quantities having positive sense. Nodal ring forces ΔS can be defined in terms of a_i, $i = 1,2,3,4$, as

$$\underset{4x1}{\{\Delta S\}} = \underset{4x4}{[B_s]} \quad \underset{4x1}{\{a\}} \tag{2.90}$$

where

$$\{\Delta S\} = \begin{Bmatrix} \Delta Q^i \\ \Delta M_r^{\,i} \\ \Delta Q^j \\ \Delta M_r^{\,j} \end{Bmatrix}, \quad \{a\} = \begin{Bmatrix} a_1 \\ a_2 \\ a_3 \\ a_4 \end{Bmatrix} \tag{2.91}$$

The elements of $[B_s]$ are given in Appendix A. Note that because of the change of sign convention from that of strength of material shown in Fig. 1, to the one shown in Fig. 6, the following modification should be made:

$$\Delta M_r(r_j) = -\Delta M_r^j$$
$$\Delta Q(r_j) = -\Delta Q^j \tag{2.92}$$

Similarly, nodal ring displacements can be expressed in terms of a_i, i = 1,2,3,4, as

$$\underset{4x1}{\{\Delta v\}} = \underset{4x4}{[B_v]}\ \underset{4x1}{\{a\}} \tag{2.93}$$

where, $\{a\}$ is defined as before in (2.91), and

$$\{\Delta v\} = \begin{Bmatrix} \Delta w^i \\ \Delta \omega^i \\ \Delta w^j \\ \Delta \omega^j \end{Bmatrix}, \quad \Delta \omega^{i,j} = (\Delta w')^{i,j} \tag{2.94}$$

The matrix $[B_v]$ is given in Appendix A. To evaluate the stiffness matrix, solve (2.93) for $\{a\}$, and substitute in (2.90). Thus

$$\underset{4x1}{\{a\}} = \underset{4x4}{[B_v]^{-1}}\ \underset{4x1}{\{\Delta v\}} \tag{2.95}$$

$$\underset{4x1}{\{\Delta S\}} = \underset{4x4}{[B_s]} \quad \underset{4x4}{[B_v]^{-1}} \quad \underset{4x1}{\{\Delta v\}} = [k] \quad \{\Delta v\} \tag{2.96}$$

where $[k]$ is the element stiffness matrix, and

$$\underset{4x4}{[k]} = \underset{4x4}{[B_s]} \quad \underset{4x4}{[B_v]^{-1}} \tag{2.97}$$

Case II, $\Lambda \neq 0, 1$

In this case nodal forces and displacements can be derived from expression (2.83), similar to that of Case I:

Increment of rotation:

$$\Delta \omega = \Delta w' = a_1 (1+\Lambda) \; r^{\Lambda} + a_2 (1-\Lambda) \; r^{-\Lambda} + 2 a_3 r \tag{2.98}$$

Increments of curvatures

$$\Delta K_r = \Delta w'' = a_1 \; (1+\Lambda) \; r^{\Lambda-1} - a_2 \Lambda (1-\Lambda) \; r^{-\Lambda-1} + 2a_3$$

$$\Delta K_\theta = \frac{1}{r} \; \Delta w' = a_1 (1+\Lambda) \; r^{\Lambda-1} + a_2 (1-\Lambda) \; r^{-\Lambda-1} + 2a_3 \tag{2.99}$$

Moments -- Substitute (2.99) into (2.77) to get

$$\Delta M_r = -a_1 (1+\Lambda) (\Lambda D_{11}+D_{12}) \; r^{\Lambda-1} - a_2 (1-\Lambda) (-\Lambda D_{11}+D_{12}) \; r^{-\Lambda-1}$$

$$-2a_3 (D_{11}+D_{12}) \tag{2.100}$$

and

$$\Delta M_\theta = -a_1 (1+\lambda) (D_{22}+\lambda D_{12}) r^{\lambda-1} + a_2 (1-\lambda) (-D_{22}+\lambda D_{12}) r^{-\lambda-1}$$

$$-2a_3 (D_{12}+D_{22}) \qquad (2.101)$$

Utilizing the equilibrium equation (2.1), upon substitution into it of (2.100) and (2.101), we obtain

$$\Delta Q = 2 a_3 (D_{11}-D_{22}) r^{-1} \qquad (2.102)$$

Following the same steps as shown in (2.90) through (2.96), we obtain the stiffness matrix for Case II. Formally, the equations are the same as before,

$$\underset{4x1}{\{\Delta S\}} = \underset{4x4}{[k]} \underset{4x1}{\{\Delta v\}} \qquad (2.96)$$

and

$$\underset{4x4}{[k]} = \underset{4x4}{[B_s]} \underset{4x4}{[B_v]}^{-1} \qquad (2.97)$$

However, the matrices $[B_s]$ and $[B_v]$ for this case are different as can be seen in Appendix B.

2.8 Stiffness Matrix for a Disc Element

The condition of axial symmetry, and the requirement that the load is applied only at nodal rings require that ΔQ for a disc element should vanish

throughout (see Fig. 7). For such an element two cases of different Λ's must again be recognized.

Case I $\Lambda = 1$

(1) Since Δw must be finite, $a_3 = 0$

(2) Since $\Delta Q \equiv 0$, $a_4 = 0$

Therefore, as before,

$$\Delta w = a_1 + a_2 r^2 \tag{2.103}$$

$$\Delta \omega = \Delta w' = 2 a_2 r \tag{2.104}$$

$$\begin{Bmatrix} \Delta w^j \\ \Delta \omega^j \end{Bmatrix} = \begin{bmatrix} 1 & r_j^2 \\ 0 & 2r_j \end{bmatrix} \begin{Bmatrix} a_1 \\ a_2 \end{Bmatrix} \quad ; \underset{2x1}{\{\Delta v\}} = \underset{2x2}{[B_\upsilon]} \underset{2x1}{\{a\}} \tag{2.105}$$

$$[B_v] = \begin{bmatrix} 1 & r_j^2 \\ 0 & 2r_j \end{bmatrix} \tag{2.106}$$

$$[B_\upsilon]^{-1} = \begin{bmatrix} 1 & -\frac{1}{2} r_j \\ 0 & \frac{1}{2} r_j^{-1} \end{bmatrix} \tag{2.107}$$

Also

$$\Delta M_r = -2 a_2 (D_{11}+D_{12}) = \Delta M_\theta \tag{2.108}$$

$$\Delta Q = 0 \tag{2.109}$$

Hence,

$$\begin{Bmatrix} \Delta Q^j \\ \Delta M_r{}^j \end{Bmatrix} = \begin{bmatrix} 0 & 0 \\ 0 & 2\,(D_{11}+D_{12}) \end{bmatrix} \begin{Bmatrix} a_1 \\ a_2 \end{Bmatrix} \tag{2.110}$$

That is

$$[B_s]_{2x2} = \begin{bmatrix} 0 & 0 \\ 0 & 2(D_{11}+D_{12}) \end{bmatrix} \tag{2.111}$$

Therefore

$$[k]_{2x2} = [B_s]_{2x2} \; [B_v]_{2x2}^{-1} = \begin{bmatrix} 0 & 0 \\ 0 & (D_{11}+D_{12})\; r_j^{-1} \end{bmatrix} \tag{2.112}$$

The Case II, $\Lambda \neq 1, \Lambda \neq 0$ is not encountered in this problem since the ratio of radial to tangential moment increment remains constant (i.e., unity). Therefore, this case will not be discussed here.

Note that stiffness matrices developed for annular and disc elements are singular. This condition is due to the fact that the elements of vector $\{\Delta S\}$ must satisfy the condition of equilibrium, and are therefore not linearly independent.

2.9 Plate Stiffness Matrix

The element stiffness matrices developed in Articles 2.7 and 2.8 can be easily assembled to obtain the plate stiffness matrix, by considering the conditions of equilibrium, and compatibility at nodal rings.

Consider the n-th element, and partition its stiffness matrix as shown

$$\underset{4x1}{\left\{\begin{array}{c} \Delta S_n^i \\ \hline \Delta S_n^j \end{array}\right\}} = \underset{4x4}{\left[\begin{array}{c|c} k_{ii}^n & k_{iy}^n \\ \hline k_{ji}^n & k_{jj}^n \end{array}\right]} \underset{4x1}{\left\{\begin{array}{c} \Delta v_n^i \\ \hline \Delta v_n^j \end{array}\right\}} \tag{2.111}$$

At a nodal ring, where the n-th and the (n+1)-th elements meet, the equilibrium equations are

$$\underset{2x1}{\left\{\Delta R_n\right\}} = \underset{2x1}{\left\{\Delta S_n^j\right\}} + \underset{2x1}{\left\{\Delta S_{n+1}^i\right\}} \tag{2.112}$$

Compatibility of deflection and slope at the same nodal ring require that

$$\underset{2x1}{\left\{\Delta r_n\right\}} = \underset{2x1}{\left\{\Delta v_n^j\right\}} = \underset{2x1}{\left\{\Delta v_{n+1}^j\right\}} \tag{2.113}$$

where

$\{\Delta R_n\}$ is plate (external) nodal ring force.

$\{\Delta r_n\}$ is plate nodal ring displacement

From (2.111) it is seen that

$$\{\Delta S_n^j\} = [k_{ji}^n] \{\Delta v_n^i\} + [k_{jj}^n] \{\Delta v_n^j\} \tag{2.114}$$

Similarly, for (n+1)-th element

$$\{\Delta S_{n+1}^i\} = [k_{ii}^{n+1}] \{\Delta v_{n+1}^i\} + [k_{ij}^{n+1}] \{\Delta v_{n+1}^j\} \tag{2.115}$$

Substitution of (2.114) and (2.115) into (2.112), and consideration of (2.113), yields

$$\underset{2x1}{\{\Delta R_n\}} = \underset{2x2}{[k_{ji}^n]} \underset{2x1}{\{\Delta r_{n-1}\}} + \underset{2x2}{[k_{jj}^n + k_{ii}^{n+1}]} \underset{2x1}{\{\Delta r_n\}} + \underset{2x2}{[k_{ij}^{n+1}]} \underset{2x1}{\{\Delta r_{n+1}\}} \tag{2.116}$$

repeating the above procedure for all the elements, we obtain stiffness matrix for the entire plate, which is a tri-diagonalized matrix of the assemblage. This matrix can be schematically represented as follows:

(a) $\underset{2Nx2N}{[K]} =$

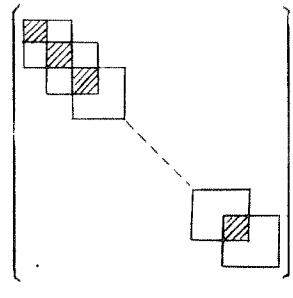

(b) $\underset{2Nx1}{\{\Delta R\}} = \underset{2Nx2N}{[K]} \underset{2Nx1}{\{\Delta r\}}$ (2.117)

where N is the number of elements. Note that the stiffness matrix [K] established here is singular. It is necessary, at this point, to impose the boundary conditions, and to make the proper deletions in [K] in order to make this matrix non-singular. Then, the remaining set of equations (2.117 b) can be solved for $\{\Delta r\}$. Having obtained $\{\Delta r\}$, moments, curvatures, and stresses can be found using appropriate expressions established before.

Since, in this report, nodal ring forces per unit length were taken, the stiffness matrices developed here are not symmetric. It is easy to show, however, that they satisfy Betti's law.

2.10 Transformation of Distributed Transverse Loads on the Element to Nodal Ring Forces

Both tributary area and consistent equivalent nodal ring forces were used in the solution of problems.

The tributary area approach simply concentrates the distributed loads at nodal ring junctures. The distributed loads extending half-way between the neighboring elements are included in the nodal load.

Consistent equivalent nodal ring forces* are derived by equating the virtual work of transverse loads on the element through the given displacement pattern to virtual work of their corresponding nodal ring forces. This is briefly explained below.

Expressions (2.81) or (2.83) can be written as follows:

$$\Delta \bar{w} = \underset{1x4}{\left\{\bar{a}\right\}^T} \underset{4x1}{\left\{\phi_m(r)\right\}} \quad , m = 1,2,3,4 \qquad (2.118)$$

*Archer, J.S., "Consistent Matrix Formulations for Structural Analysis Using Finite-Element Techniques." AIAA Jour. Vol. 3, No. 10, pp. 1910-1918, Oct., 1965.

Recalling (2.93), we also have

$$\left\{\Delta \bar{v}\right\} = [B_v] \left\{\bar{a}\right\} \tag{2.93}$$

Note that a bar over the symbols in the above equations is used to designate the quantities associated with the virtual displacements.

The work of a distributed transverse load $\Delta p(r)$ on the element through the virtual displacement $\Delta \bar{w}$ is

$$\Delta \bar{W}_p = \int_{r_i}^{r_j} \Delta p(r)\, \Delta \bar{w}(r)\, 2\pi r dr = 2\pi \left\{\bar{a}\right\}^T \left\{\Delta p^*_m\right\} \tag{2.119}$$

where

$$\left\{\Delta p^*_m\right\} = \int_{r_i}^{r_j} \Delta p(r)\, \phi_m(r)\, r dr \qquad m = 1,2,3,4 \tag{2.120}$$

On the other hand, the work of equivalent (consistent) nodal ring forces $\left\{\Delta P\right\}$ through the virtual displacement $\left\{\Delta \bar{v}\right\}$ is given as

$$\Delta \bar{w}_p = \left\{\Delta \bar{v}\right\}^T \left\{\begin{matrix} 2\pi r_i \Delta P_i \\ \hline 2\pi r_j \Delta P_j \end{matrix}\right\} = 2\pi \left\{\bar{a}\right\}^T [B_v]^T \left\{\begin{matrix} r_i\, \Delta P_i \\ \hline r_j\, \Delta P_j \end{matrix}\right\} \tag{2.121}$$

Equating (2.119) and (2.121), and considering that the generalized coordinates $\left\{\bar{a}\right\}$ are linearly independent, we get

$$\underset{4x1}{\left\{\begin{matrix} r_i\, \Delta P_i \\ \hline r_j\, \Delta P_j \end{matrix}\right\}} = \underset{4x4}{[B_v^T]^{-1}} \underset{4x1}{\left\{\Delta p^*_m\right\}} \tag{2.122}$$

where $\{\Delta P\}$ are the forces per unit length.

Having established (2.122), the nodal ring forces are obtained from the following relation

$$\underset{2x1}{\{\Delta R_n\}} = \frac{\{r_j^n \ \Delta P_j^n\} + \{r_i^{n+1} \ \Delta P_i^{n+1}\}}{r_n} = \underset{2x1}{\{\Delta P_j^n\}} + \underset{2x1}{\{\Delta P_i^{n+1}\}} \qquad (2.123)$$

where,

$$r_n = r_j^n = r_i^{n+1}$$

In (2.120) any distribution of $\Delta p(r)$ over the element can be specified. It is also possible to develop expressions for linear or parabolic distribution of transverse load acting on the element, and any distribution can then be approximated by a linear or a parabolic curve. The linear approximation was used in this investigation, and the appropriate expressions for $\{\Delta p^*\}$ are given in Appendix C.

The above procedure can be used to transform transverse ring load on an element to nodal ring force as well. Perhaps, however, it is preferrable in such cases to take the applied ring load as the nodal ring load.

A comparison of the results using the two approaches discussed above of transforming the transverse distributed forces to nodal ring forces shows that the difference is not very significant for the small size element.

2.11 General Remarks

The procedure employed in the analysis of plates described in this report can be outlined as follows: The plate is assumed to be initially free from residual stresses. The first increment of loading is applied and the magnitude of the load increased so that yielding just begins at some points within the plate. The loadings is then continued in small load increments. For each increment, after the Eqns. (2.117b) have been solved for $\{\Delta r\}$, curvatures, strain increments, and stress increments are determined successively. The new state of stress is found, and $[E]^o$ matrices are computed. For the first approximation $[E]^o$ are taken to be the material properties for the next increment. In a more refined procedure, Euler's modified method is utilized. That is, the $[E]^o$ is utilized to calculate $\{\Delta r\}$ for the same increment. The new $[E]'$ matrices are established, and the average of these two is taken to be representative of the material properties for the increment in questions.

Depending on the magnitude of the load increment, this modification was relatively of more significance for perfectly plastic materials than those exhibiting hardening. It was observed that the first approximation was satisfactory for a relatively small loading increment and hardening materials. The influence of the magnitude of the loading increments was studied, and some results are shown in the next chapter.

A computational difficulty arises at the instant of initiation of the plastification of an element. If the radial and tangential stress increments differ slightly, the material exhibits a slight anisotropy after exceeding the

elastic limit. The corresponding Λ changes from unity to a value very close to unity. Therefore, the matrices $[B_v]^{-1}$ and [k] become ill-conditioned. To overcome this difficulty two approaches have been used. The first makes use of double precision computation procedure, which retains 16 significant digits in the analysis. The second consisted of expanding the elements of $[B_v]^{-1}$ and [k] matrices in terms of $(1-\Lambda)$, clearing fractions, and treating the ill-conditioning factors separately. The expanded forms of elements of these matrices are given in Appendix D.

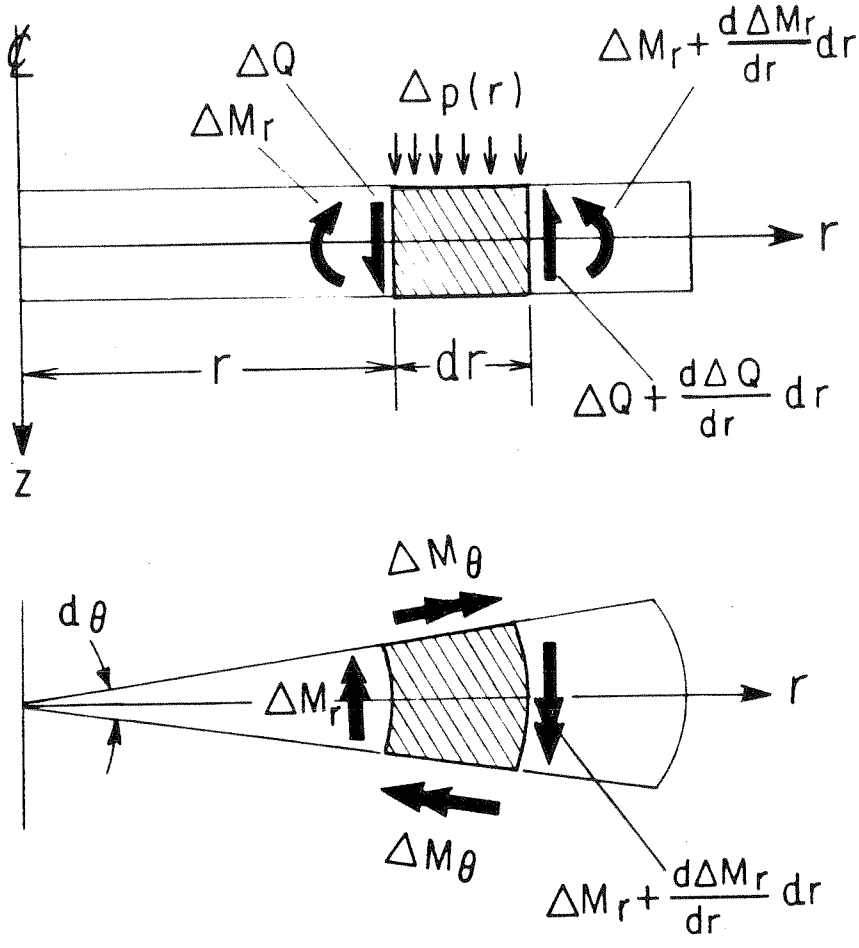

FIG.1 AXI-SYMMETRIC LOADING

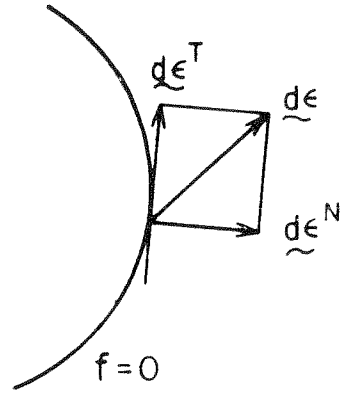
$d\underset{\sim}{\epsilon}^T$
$d\underset{\sim}{\epsilon}$
$d\underset{\sim}{\epsilon}^N$
f=0

FIG. 2

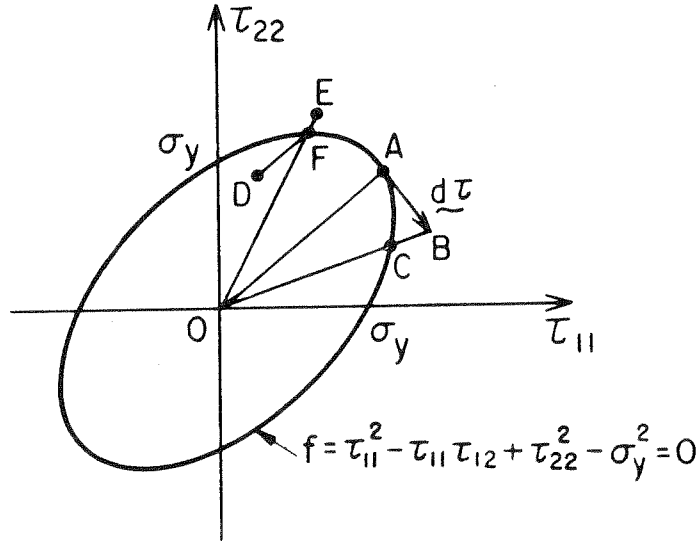
τ_{22}
E
σ_y
F
A
D
$d\underset{\sim}{\tau}$
B
C
0
σ_y
τ_{11}
$f=\tau_{11}^2-\tau_{11}\tau_{12}+\tau_{22}^2-\sigma_y^2=0$

FIG. 3

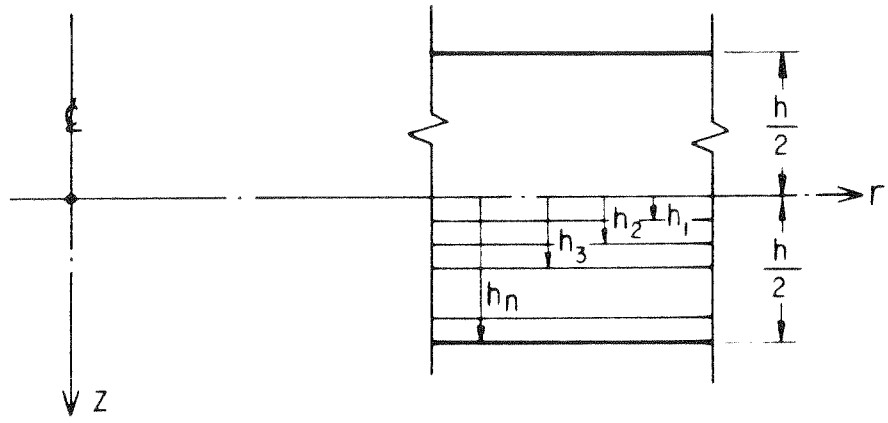

FIG. 5

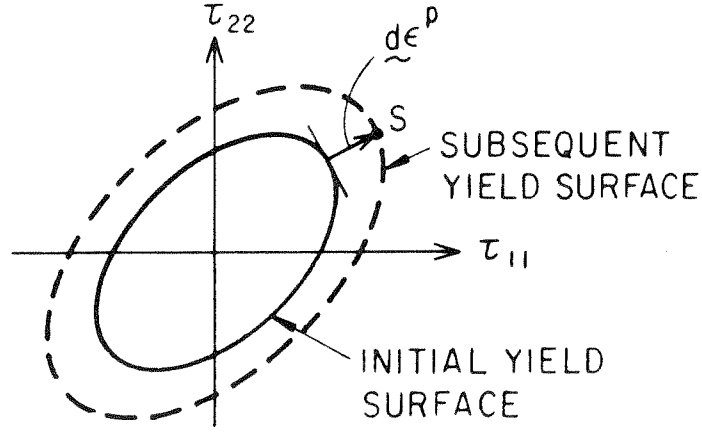

(a) ISOTROPIC HARDENING

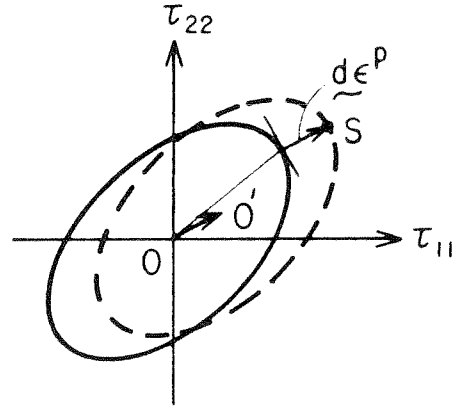

(b) KINEMATIC HARDENING

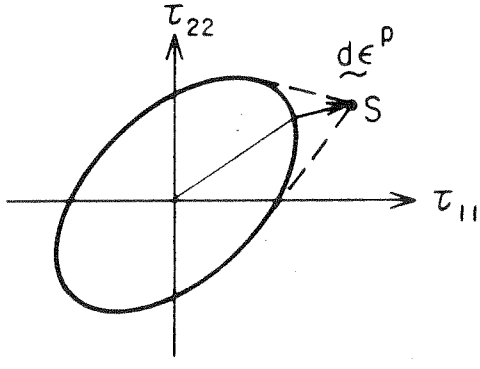

(c) YIELD CORNER

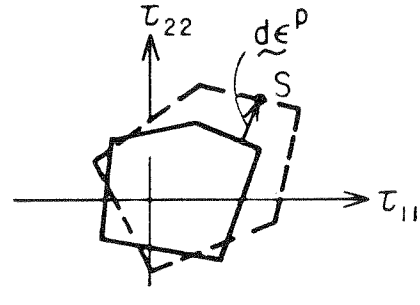

(d) PIECEWISE LINEAR
YIELD CONDITION

FIG. 4 HARDENING RULES

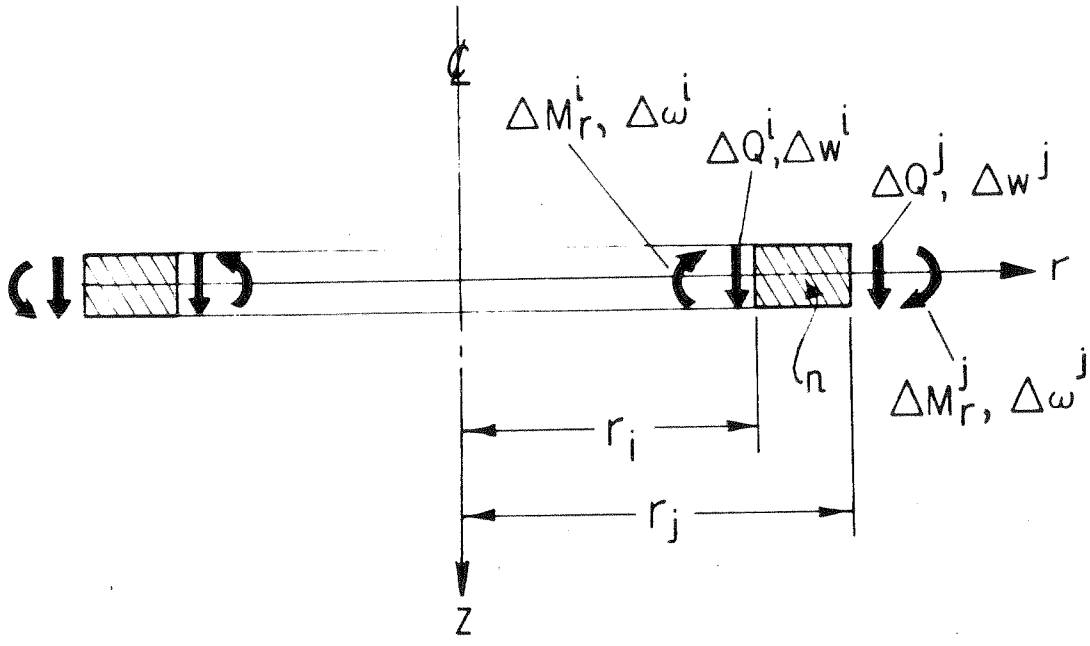
$\Delta M_r^i, \Delta\omega^i$
$\Delta Q^i, \Delta w^i$
$\Delta Q^j, \Delta w^j$
r
n
$\Delta M_r^j, \Delta\omega^j$
r_i
r_j
Z

FIG. 6

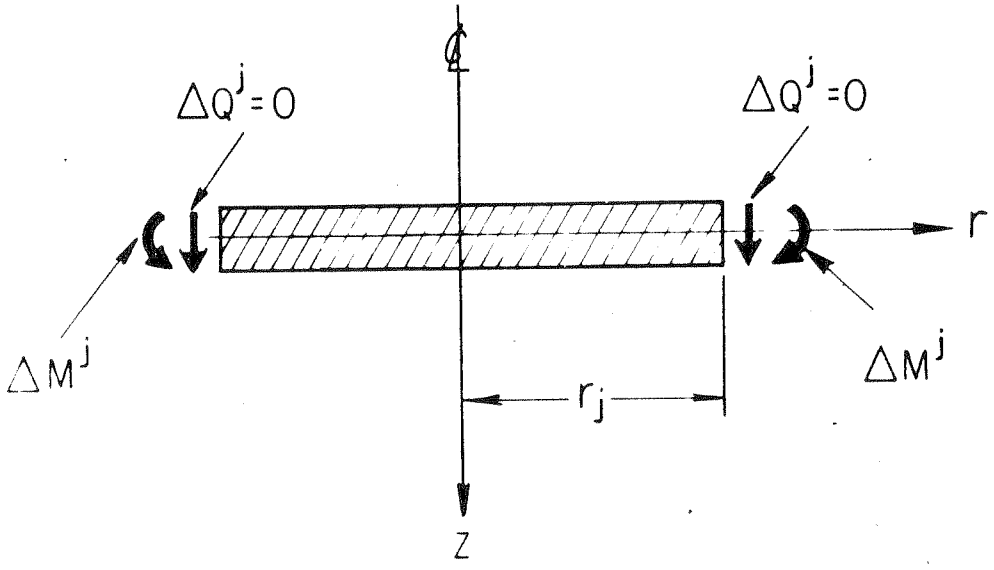
$\Delta Q^j = 0$
$\Delta Q^j = 0$
r
ΔM^j
ΔM^j
r_j
Z

FIG. 7

III. APPLICATIONS

This chapter consists of two parts. In the first part several examples are presented; in the second, a description of computer programs is given.

3.1 Examples

Eleven examples have been prepared to illustrate the main features, and to test the accuracy of the method of solution developed for circular plates in Chapter II.

Except for Example 11, the same size plate is used throughout to facilitate comparisons for different boundary conditions and also for different material properties. The total magnitude of load applied to the plate was controlled by the deflection of the plate. It is believed that in using the small deformation theory of plates a total central deflection of up to 0.3 the plate thickness does not induce appreciable membrane action. The developed solution is applicable to relatively thick circular plates.

Example 1

The behavior of the simply supported plate shown in Fig. 8 under uniformly distributed load is analyzed.

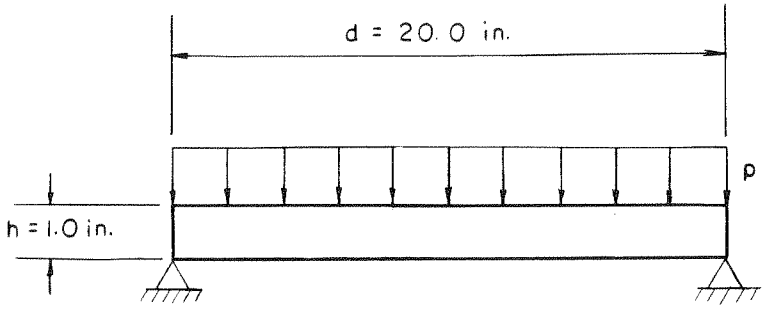

Fig. 8

The material properties are: $E = 10^7$ psi, $\nu = 0.24$. The yield stress in uniaxial tension $\sigma_y = 16$ ksi. The material is elastic perfectly plastic.

The number of elements and layers is 20 and 40, respectively. Load increments of 5 and 4 psi are used.

The results are plotted in Fig. 9 to 14. Comparison with a solution due to V.V. Sokolovskii who used the deformation law of plasticity is given in Fig. 15.

Example 2

The same plate as in example 1 but with clamped outer support is studied.

The numbers of elements and layers are 20 and 40, respectively. Load increments of 10 psi are used.

Results are plotted in Fig. 16 to 19.

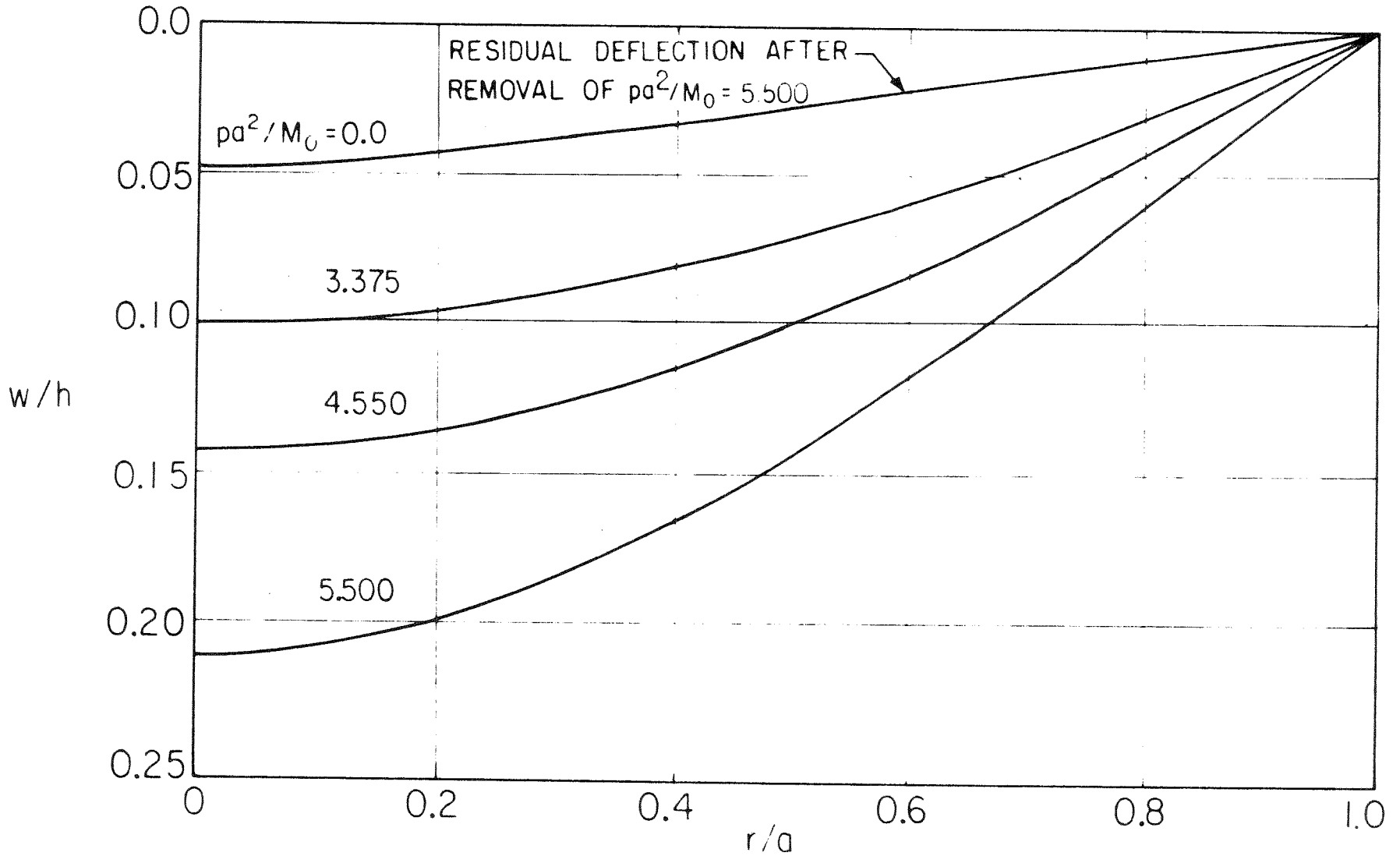

FIG. 9 DISTRIBUTIONS OF DEFLECTION

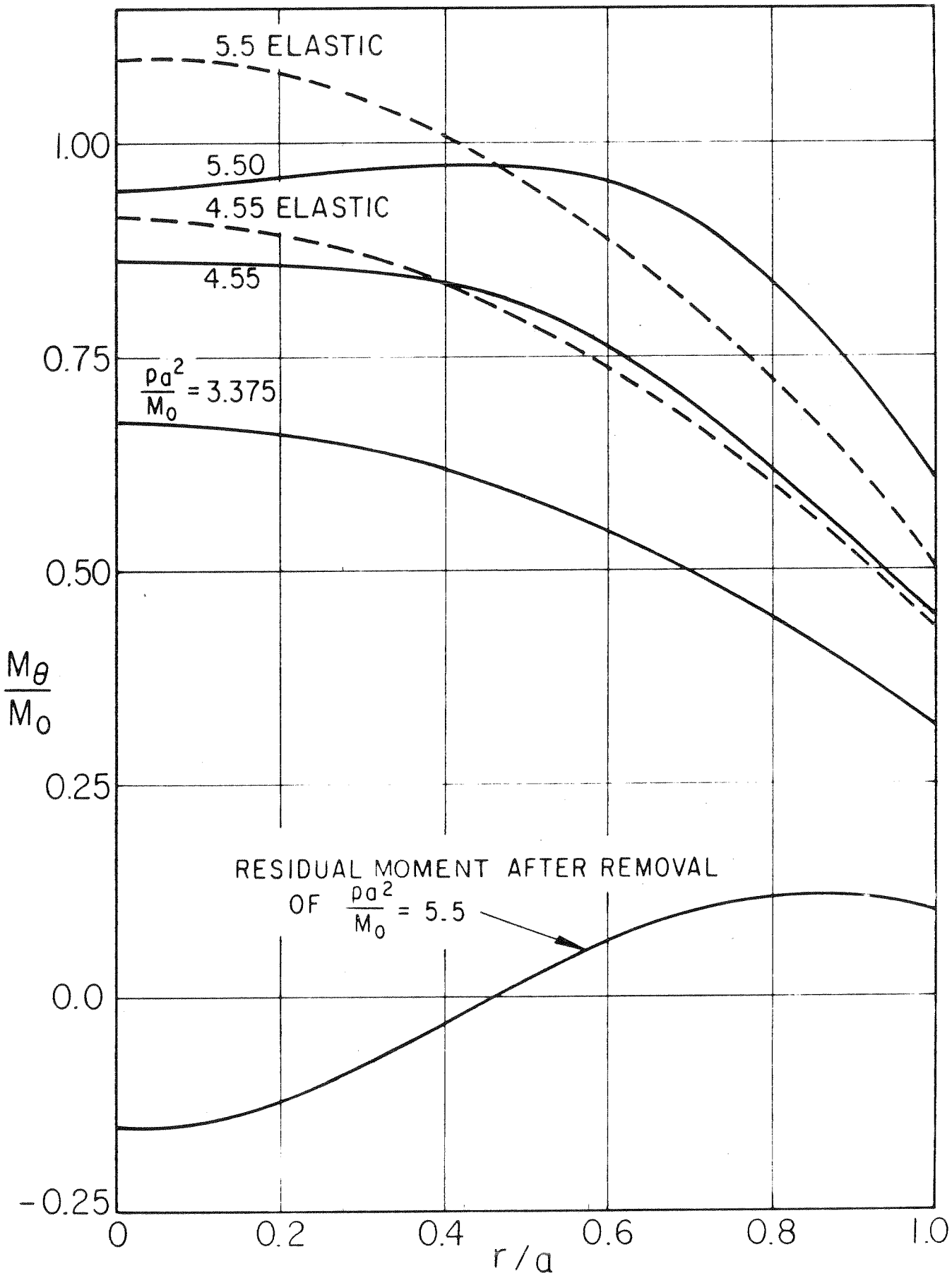

FIG.10 DISTRIBUTIONS OF TANGENTIAL MOMENT

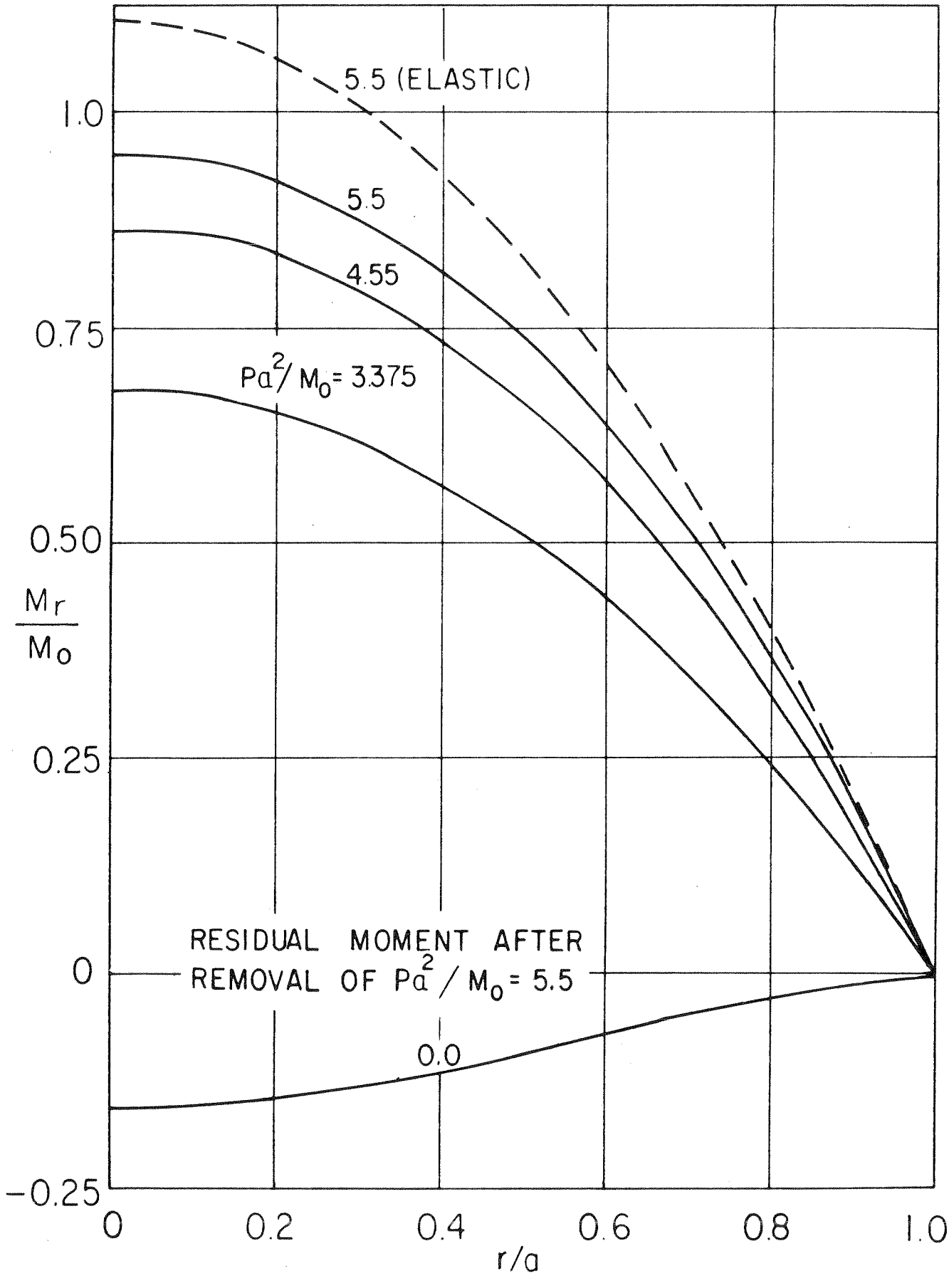

FIG. 11 DISTRIBUTION OF RADICAL MOMENT

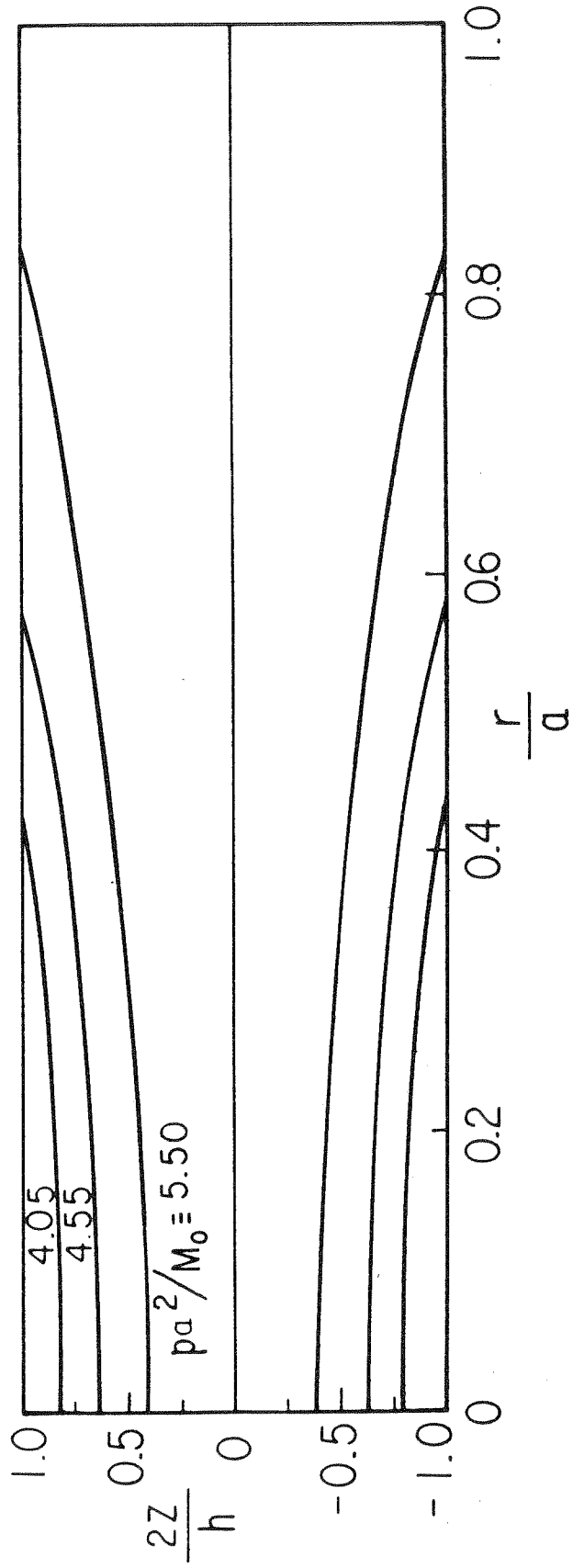

FIG. 12 ELASTIC-PLASTIC BOUNDARIES

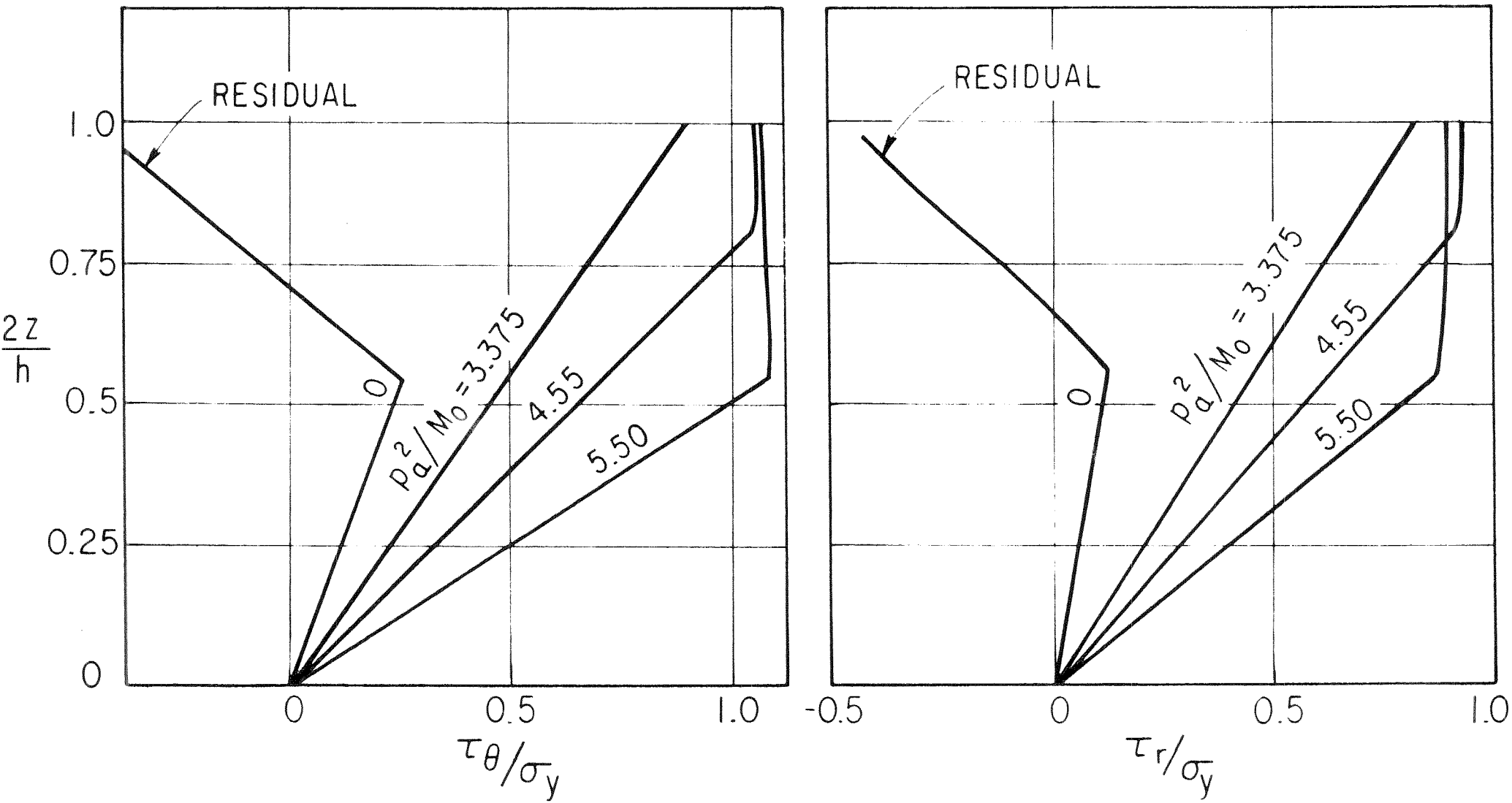

FIG. 13 VARIATIONS OF STRESSES AT $\frac{r}{a} = 0.425$

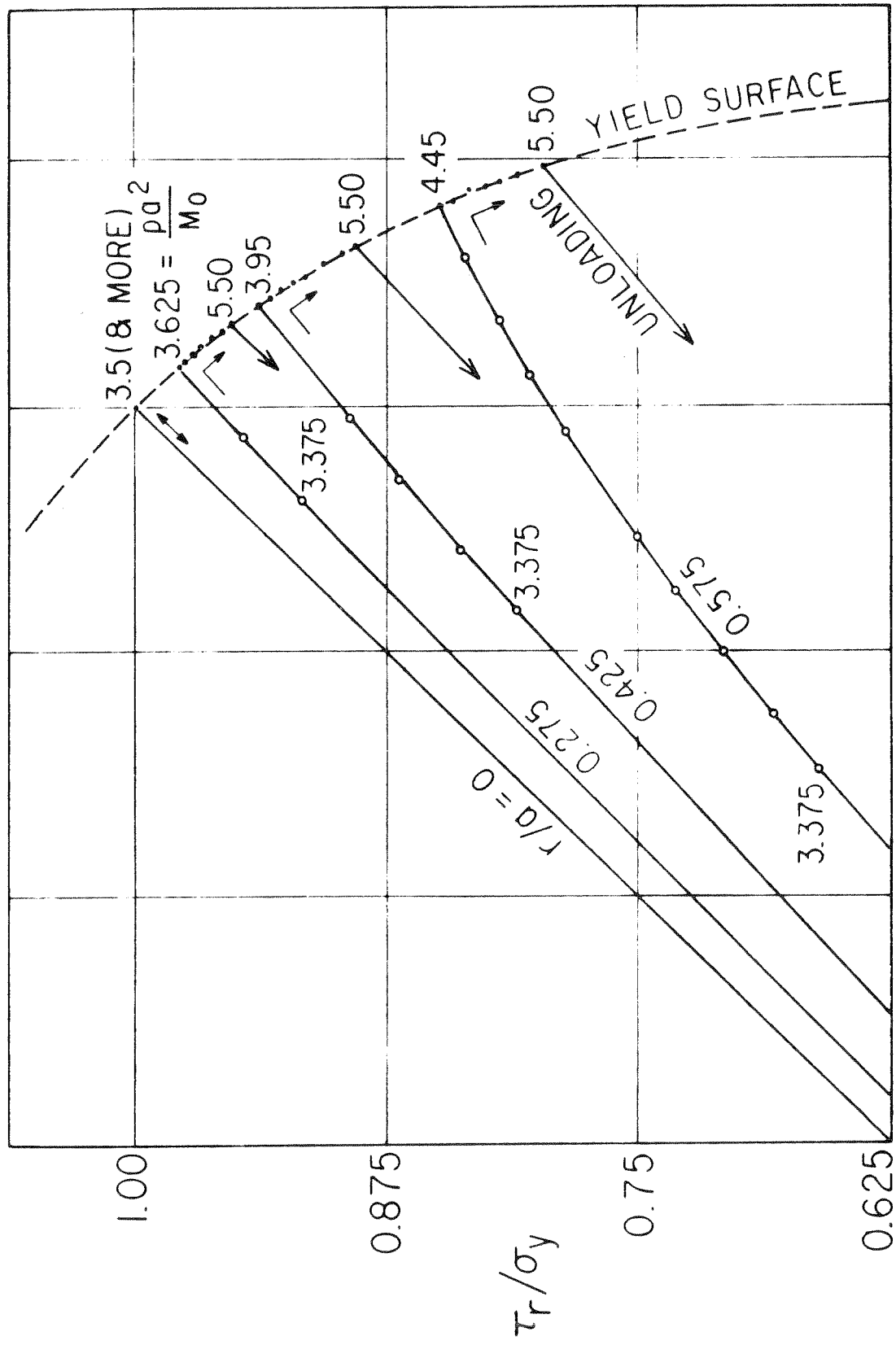

FIG.14 STRESS PATHS

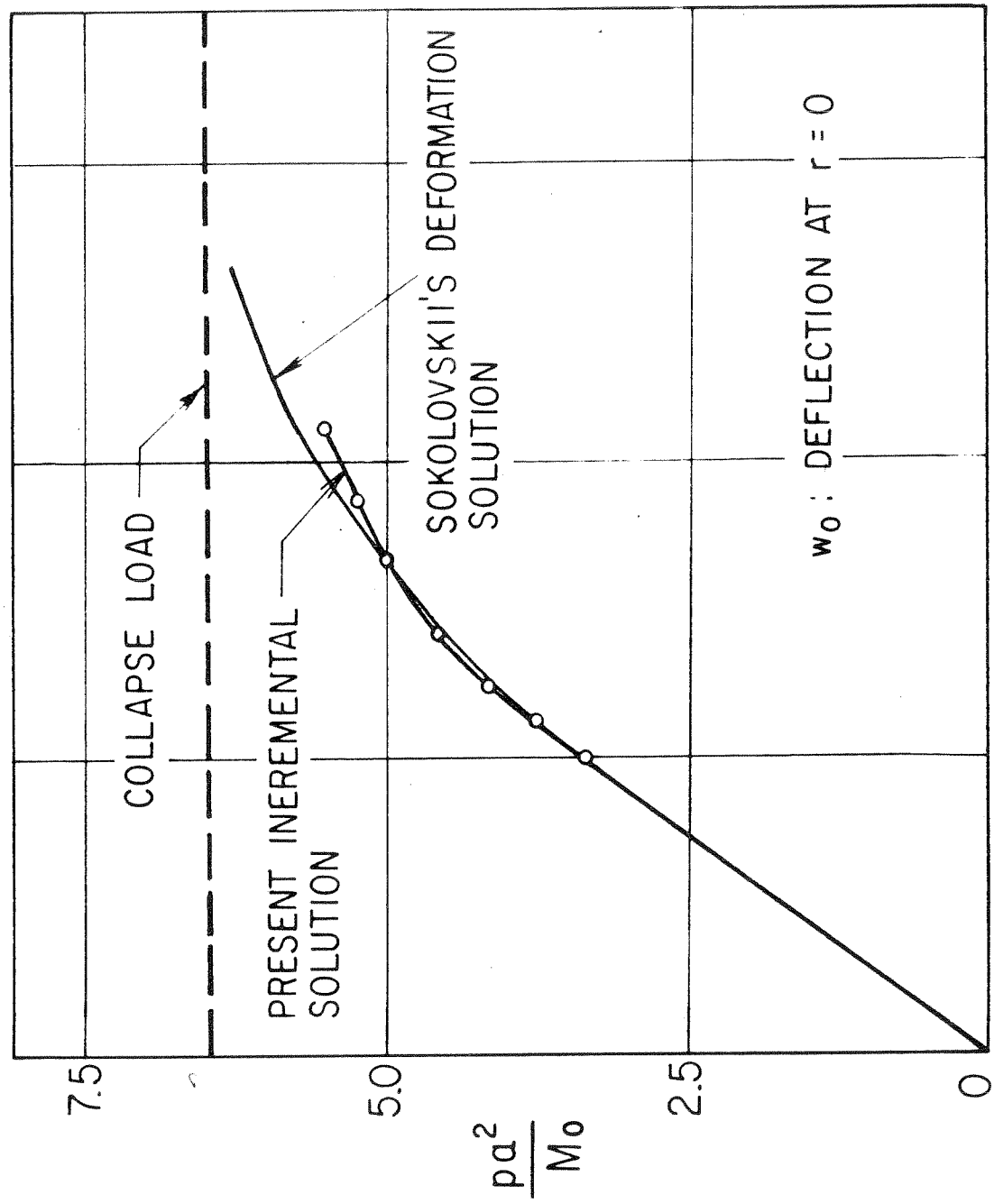

FIG.15 COMPARISON WITH SOKOLOVSKII'S DEFORMATION SOLUTION

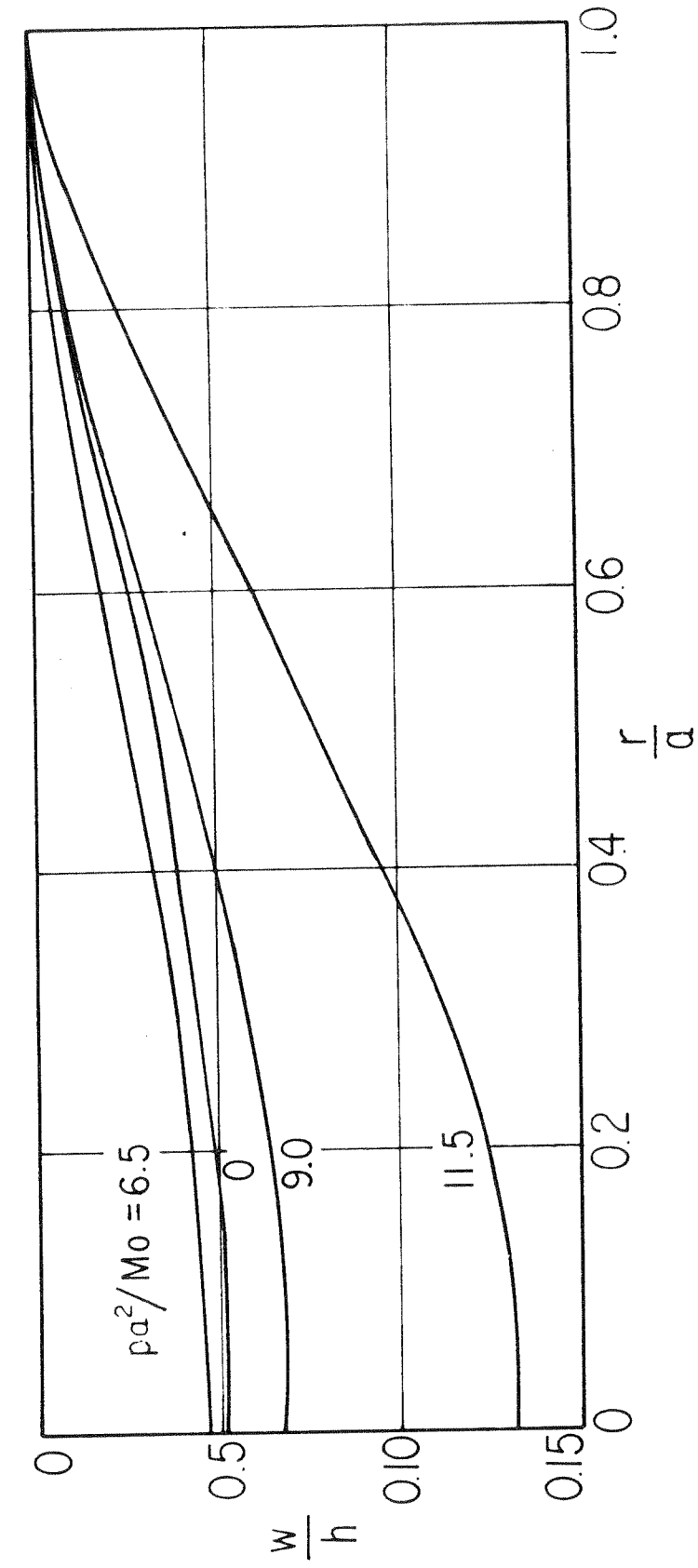

FIG.16 DISTRIBUTIONS OF DEFLECTION

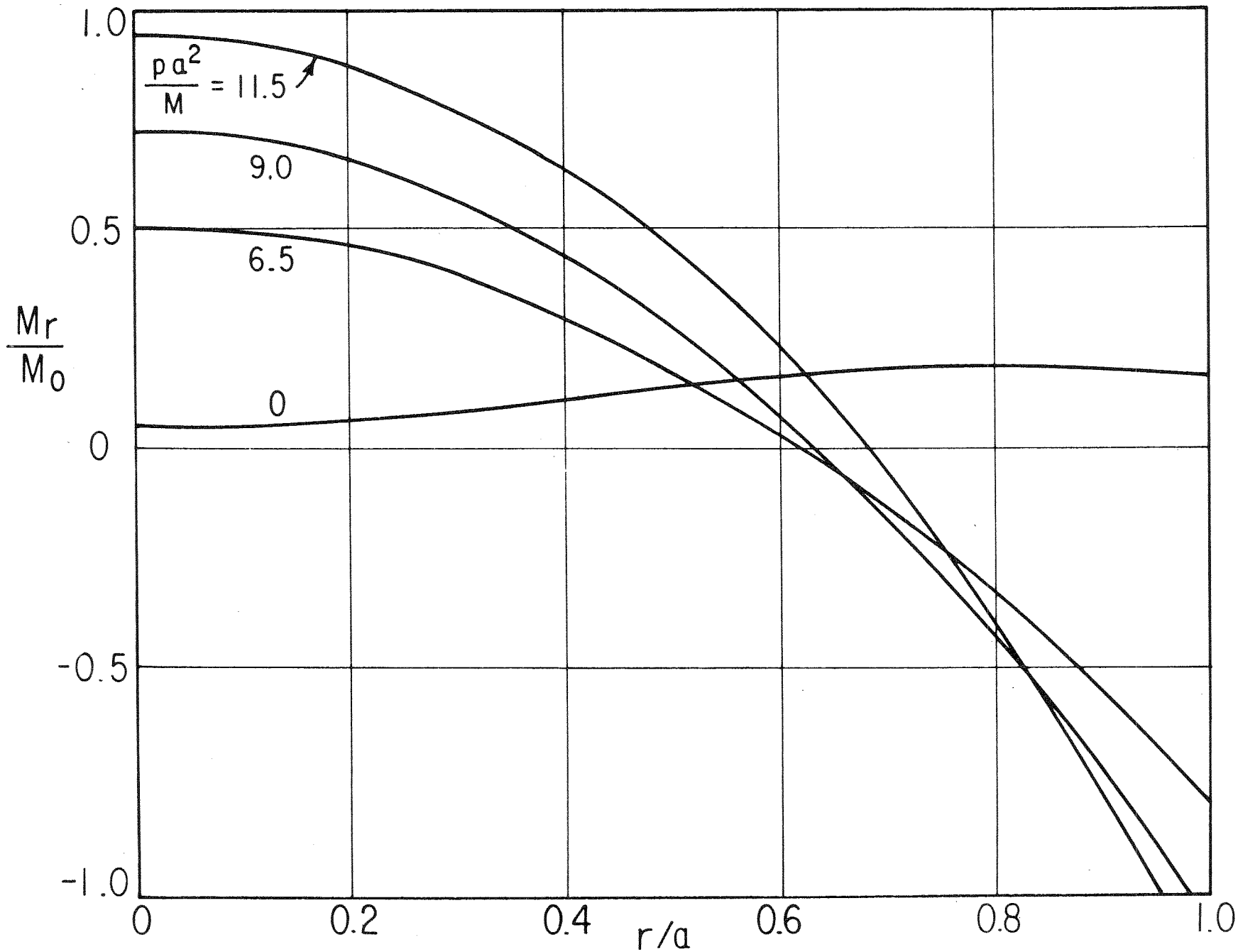

FIG 17 DISTRIBUTION OF RADIAL BENDING MOMENT

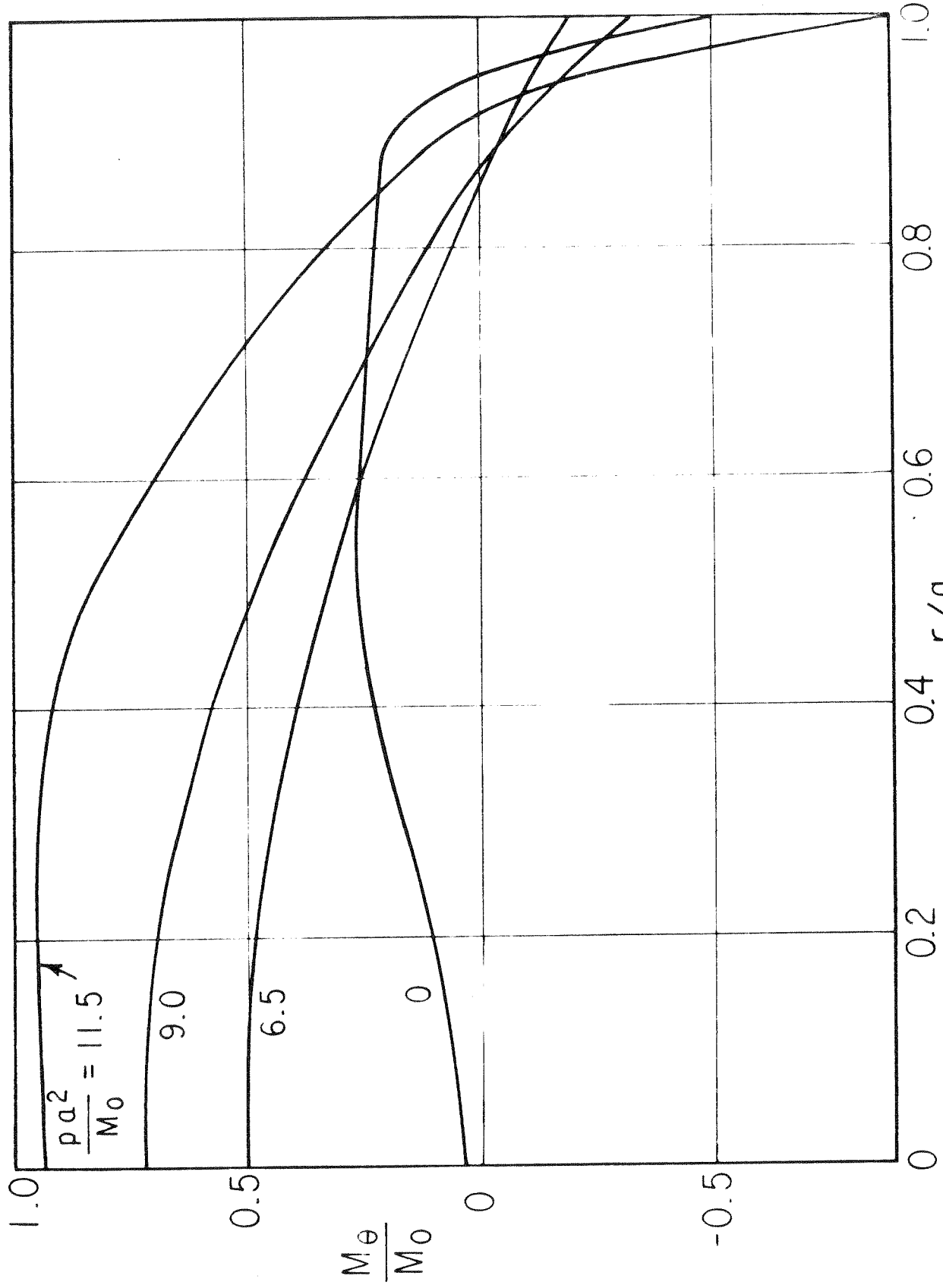

FIG 18 DISTRIBUTIONS OF TANGENTIAL BENDING MOMENT

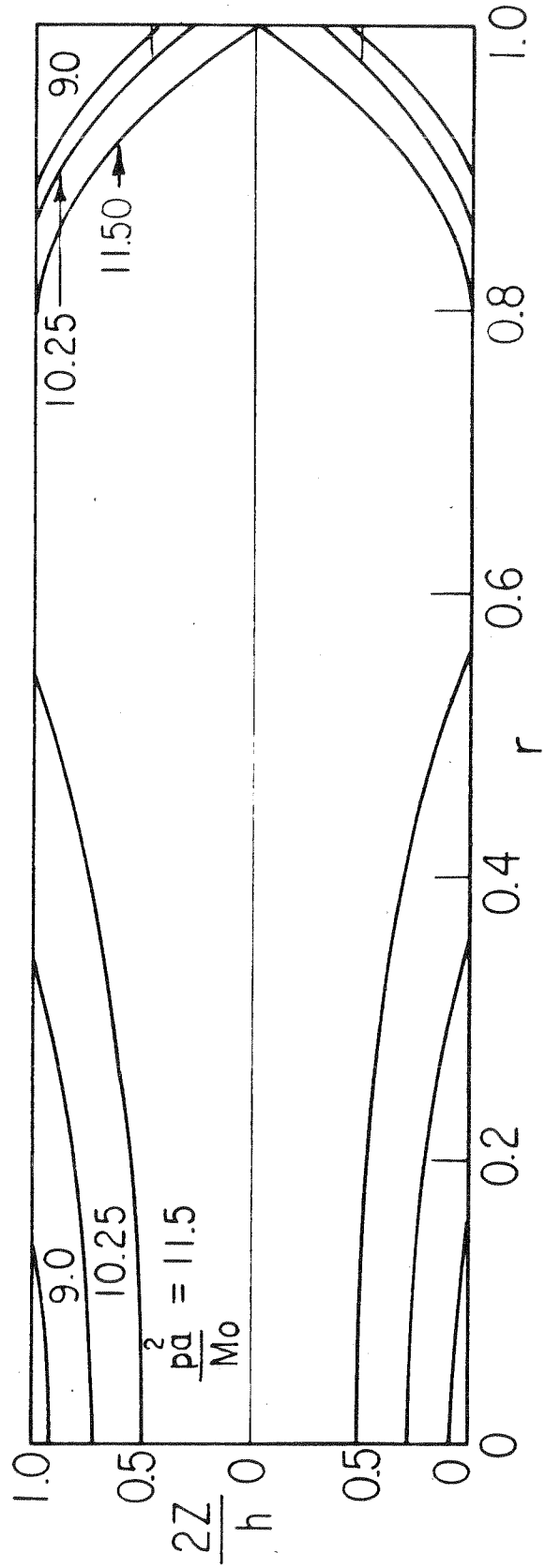

FIG 19 ELASTIC-PLASTIC BOUNDARIES

Example 3

The purpose of this example is to study the effect of history of external loading on the behavior of the simply supported elastic-perfectly plastic plate.

The plate is exactly the same as in Example 1 except that $\nu = 0.3$.

First the plate is loaded as shown in Fig. 20-a to obtain the maximum possible elastic deformation. Thereafter, two different schemes of loading are used: In the loading sequence 1, triangular increments of load are added to reach the final load of Fig. 20-d. In the loading sequence 2, load increments are added from r = 3.75 in. to the outer edge of the plate until the final load of Fig. 20-d is achieved.

Results are plotted in Figs. 21 and 22.

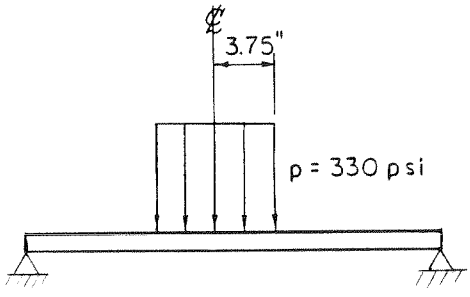

Fig. 20-a
First Loading Step for
both schemes of loading

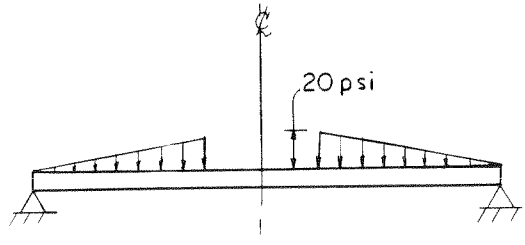

Fig. 20-b
Increments of load in Loading
Sequence 1

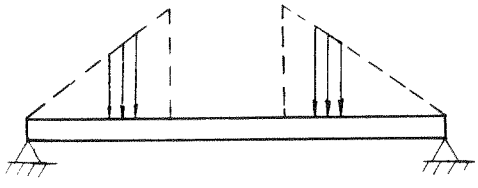

Fig. 20-c
Typical Load Increment in
Loading Sequence 2

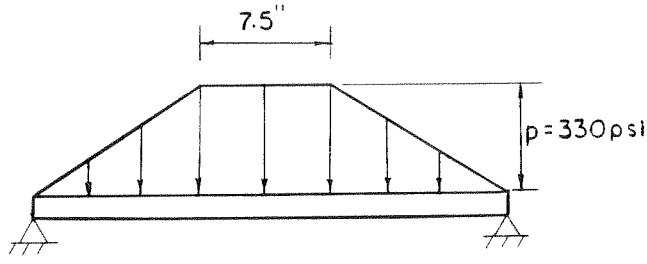

Fig. 20-d
Final Load

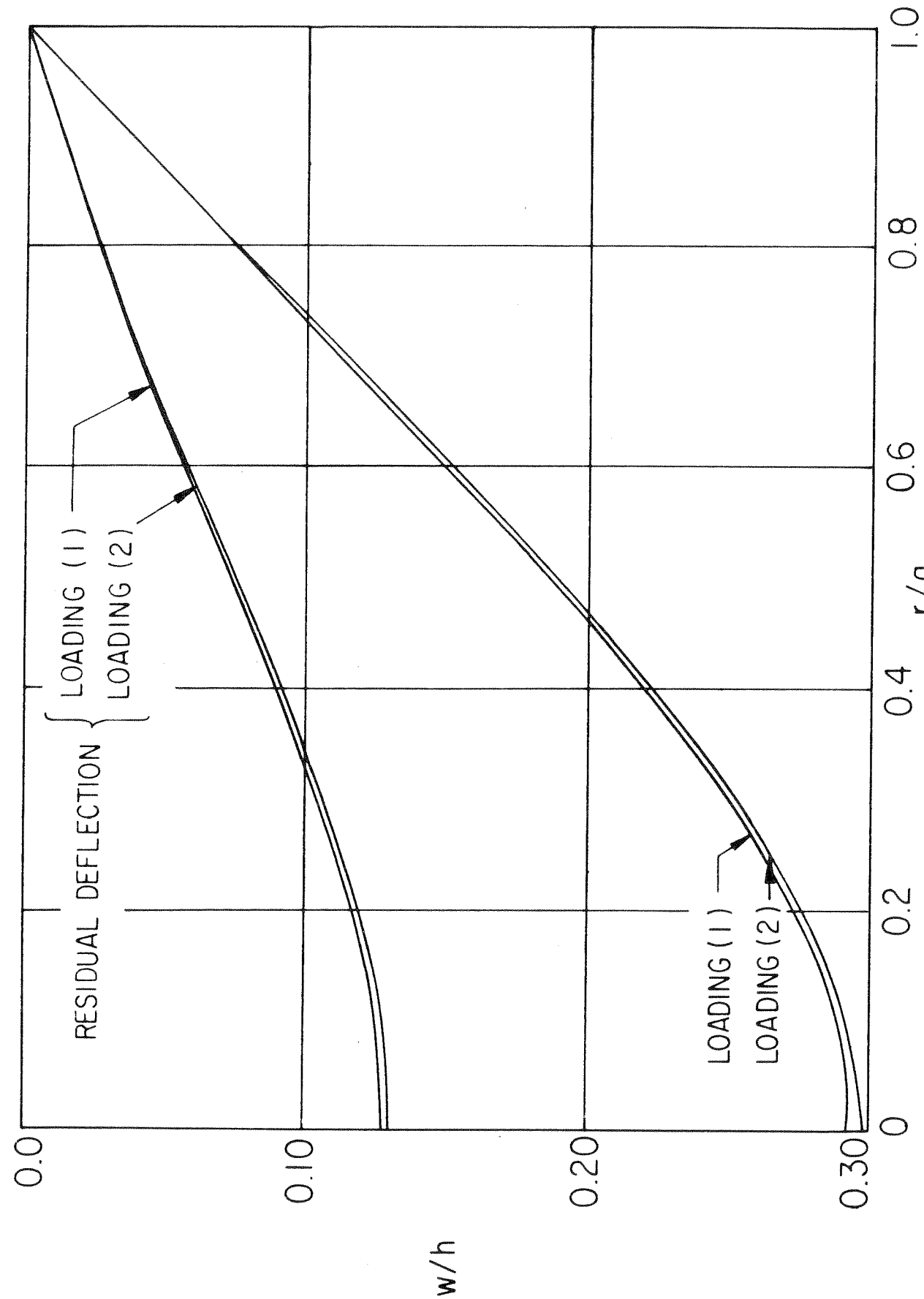

FIG. 21 FINAL DISTRIBUTION OF DEFLECTION DUE TO DIFFERENT LOADING SEQUENCES

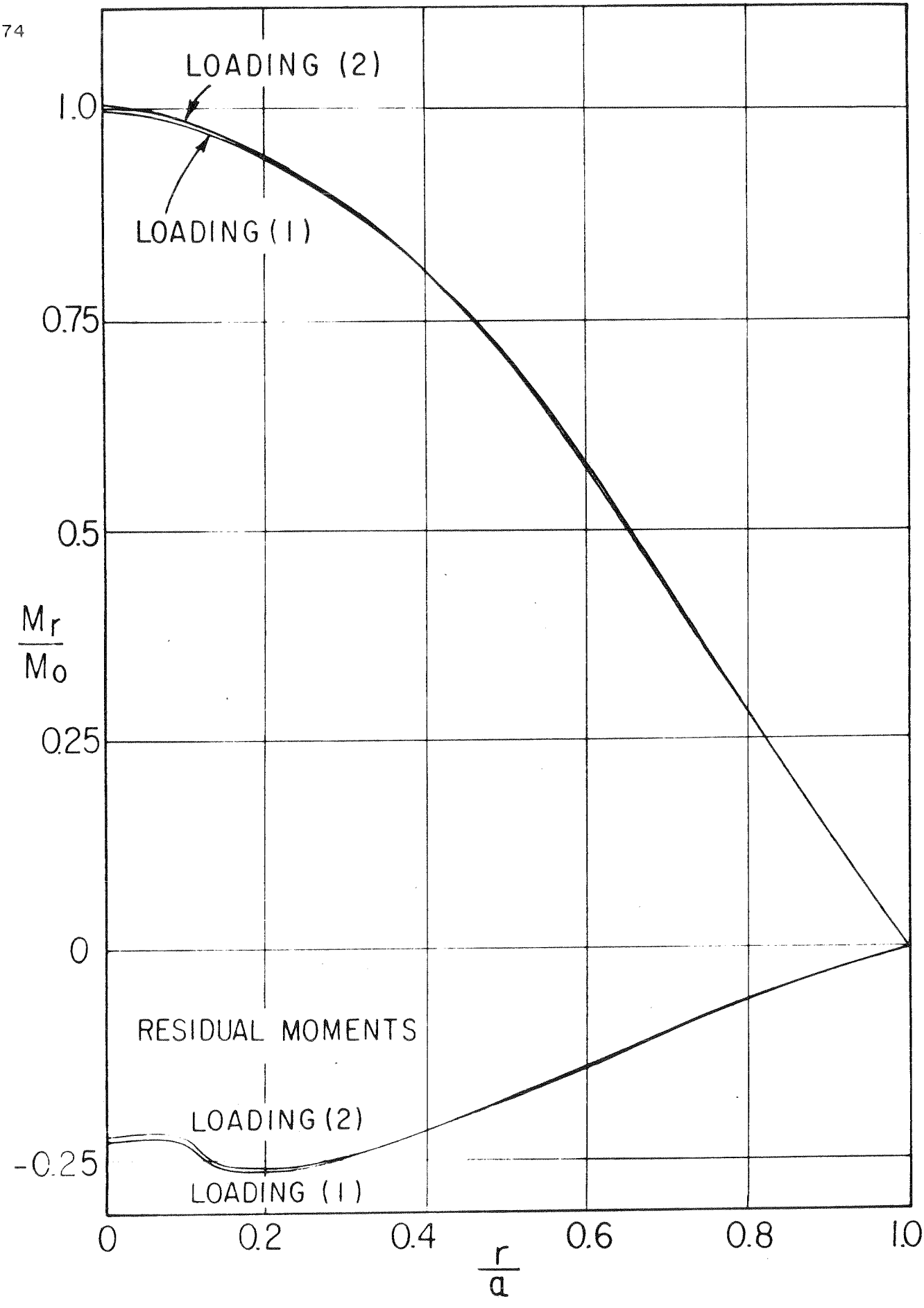

FIG 22 FINAL DISTRIBUTIONS OF RADIAL MOMENT DUE TO DIFFERENT LOADING SEQUENCES

Example 4

The purpose of this example is to study the effect of load history on the behavior of clamped elastic-perfectly plastic plate.

The plate is exactly the same as in Example 1 except that $\nu = 0.3$

After the first step of loading (Fig. 23-a) two different loading schemes are used to reach finally the load in Fig. 23-d. In loading sequence 1, typical load increments are as in Fig. 23-b. In the loading sequence 2 load increments are added from r = 4.75 in. to the boundary of the plate (Fig. 23-c).

The results are plotted in Fig. 24 to 26.

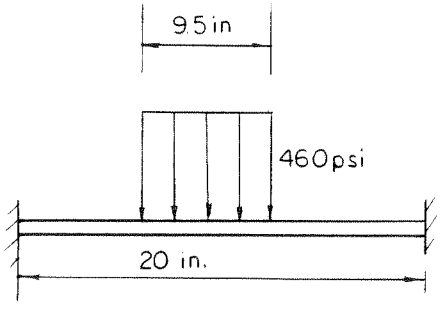

Fig. 23-a
First Loading Step

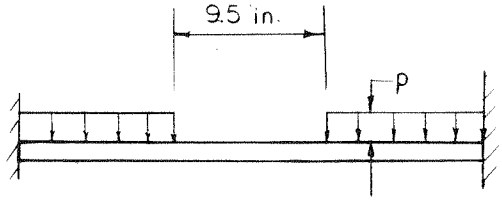

Fig. 23-b
Increment of Load in
Loading Sequence 1

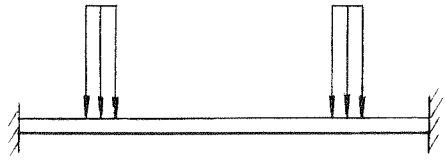

Fig. 23-c
Increment of Load in
Loading Sequence 2

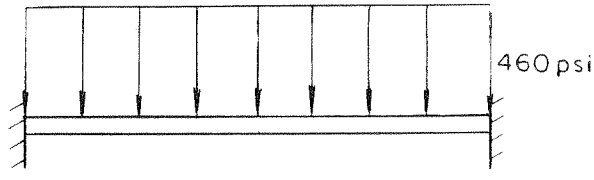

Fig. 23-d
Final Load

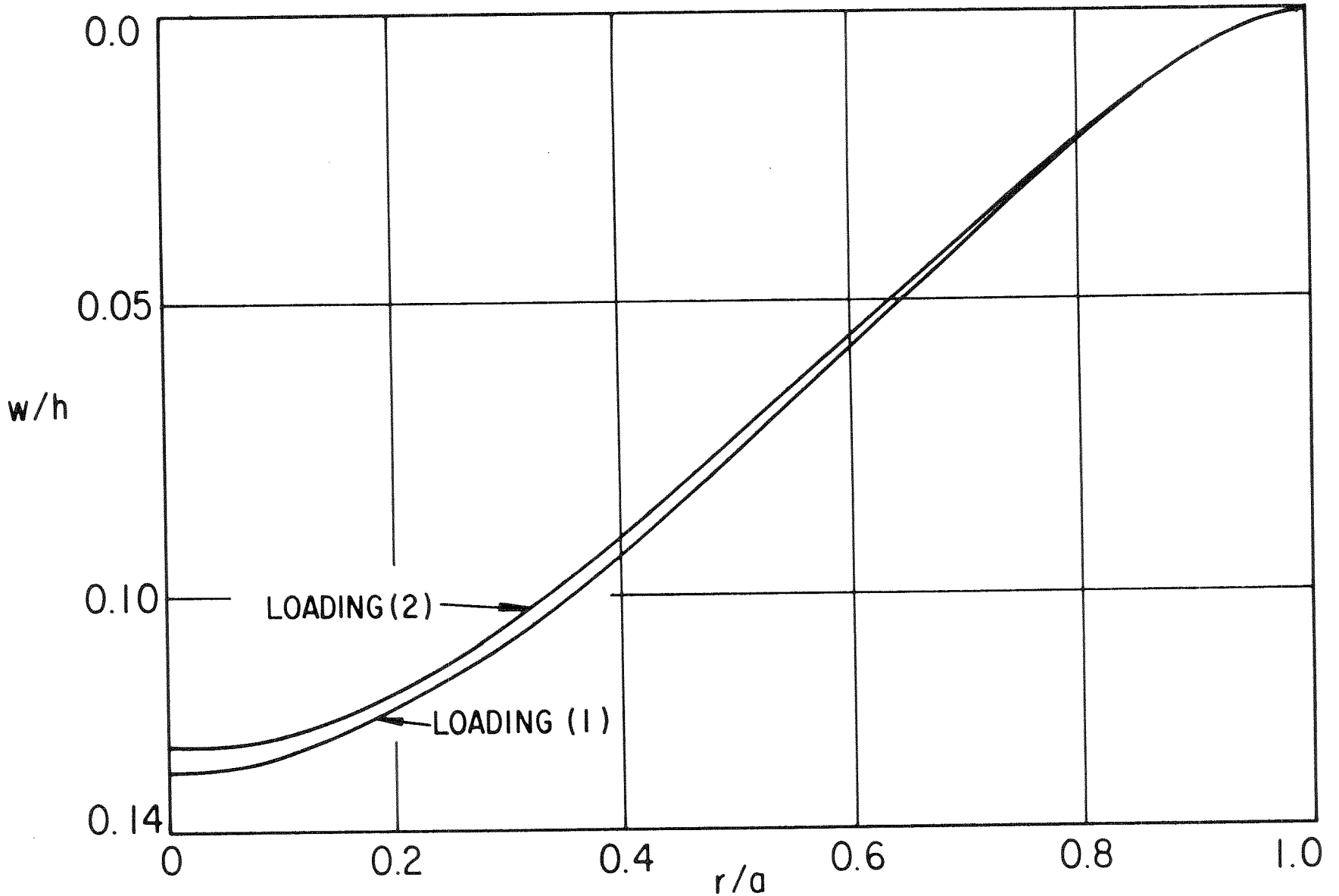

FIG. 24 FINAL DISTRIBUTION OF DEFLECTION DUE TO DIFFERENT LOADING SEQENCES

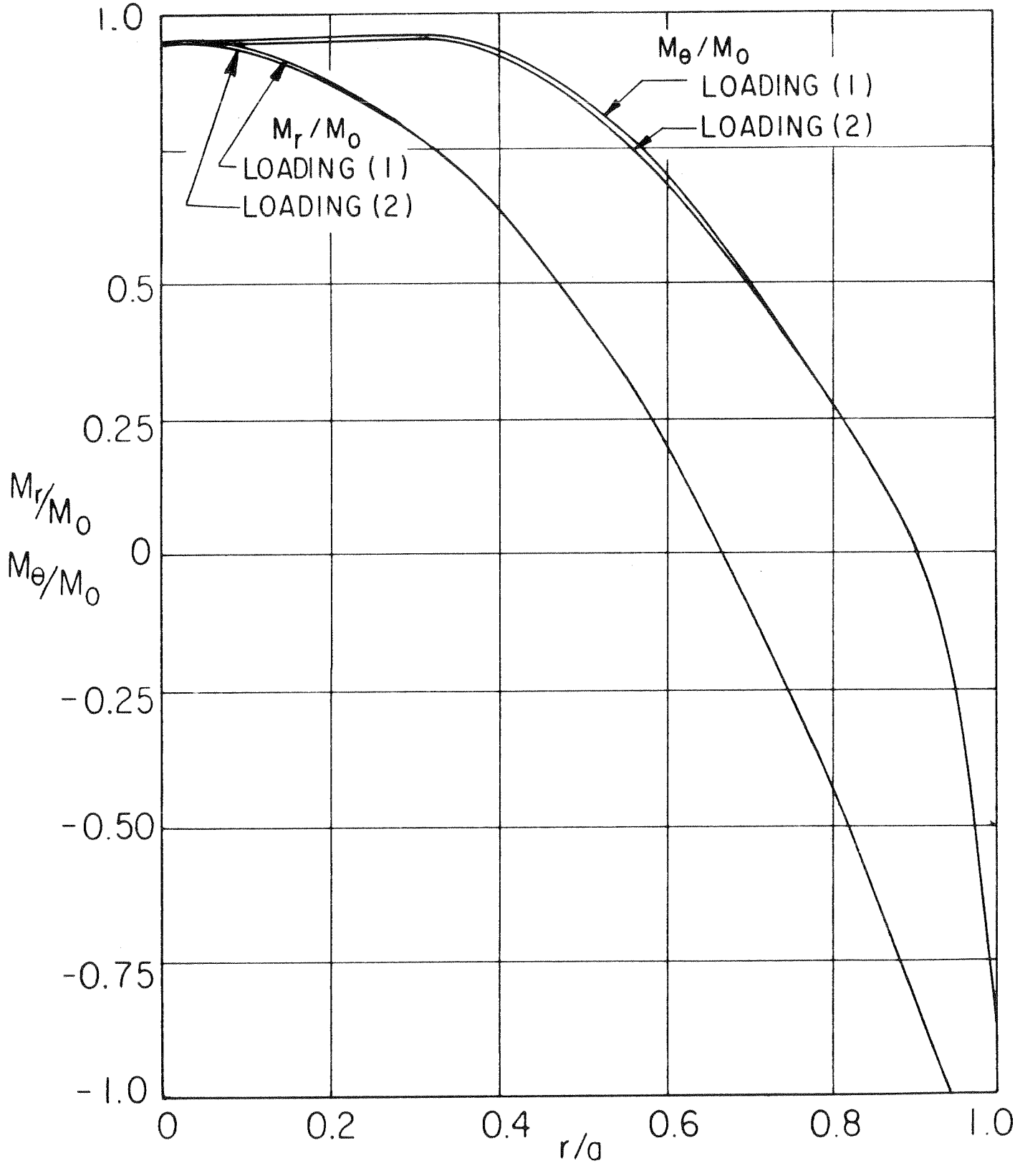

FIG. 25 DISTRIBUTION OF MOMENTS DUE TO DIFFERENT LOADING SEQUENCES

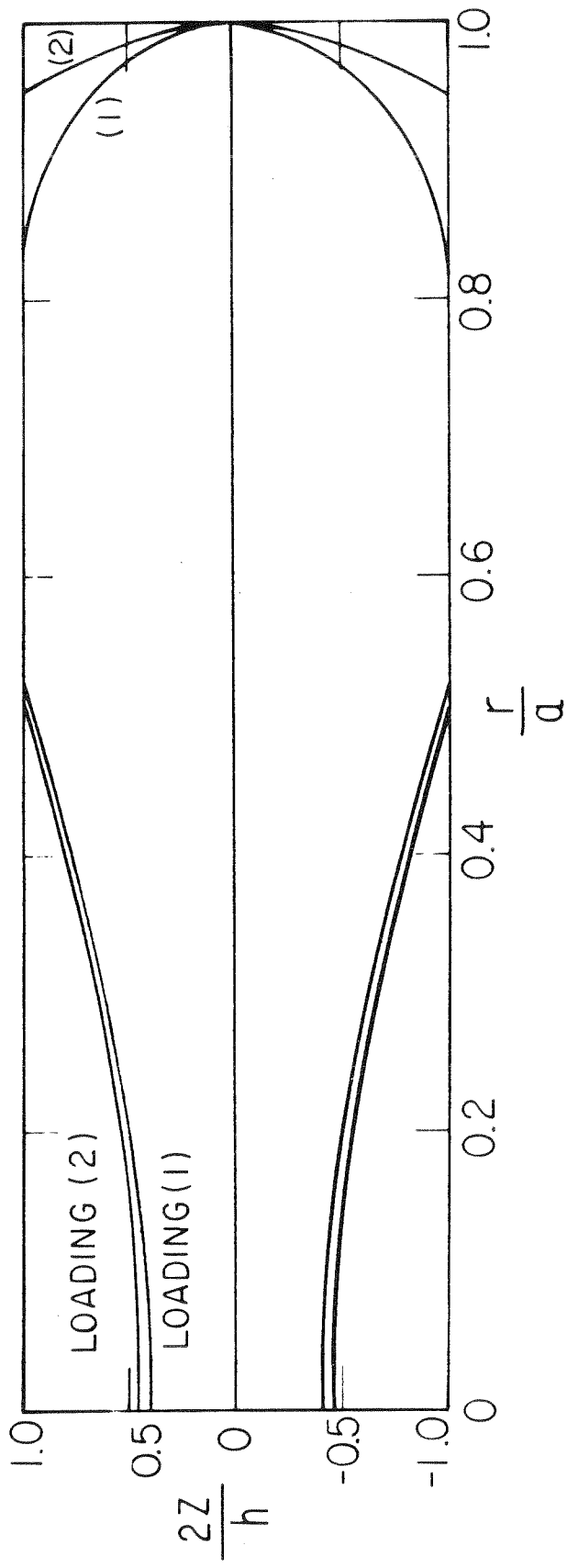

FIG.26 ELASTIC PLASTIC BOUNDARIES

Example 5

The purpose of this example is to show the effect of the magnitude of load increments on the moments and deflections. The numerical experiments are on 0.75 x 16 in. Simply supported elastic-perfectly plastic plates with E = 10.6 psi and σ_y = 16,000 psi. The numbers of elements and layers are 20 and 40, respectively. It should be noted that these results were obtained before including the Euler modification to take into account the variation of material properties within a loading step.

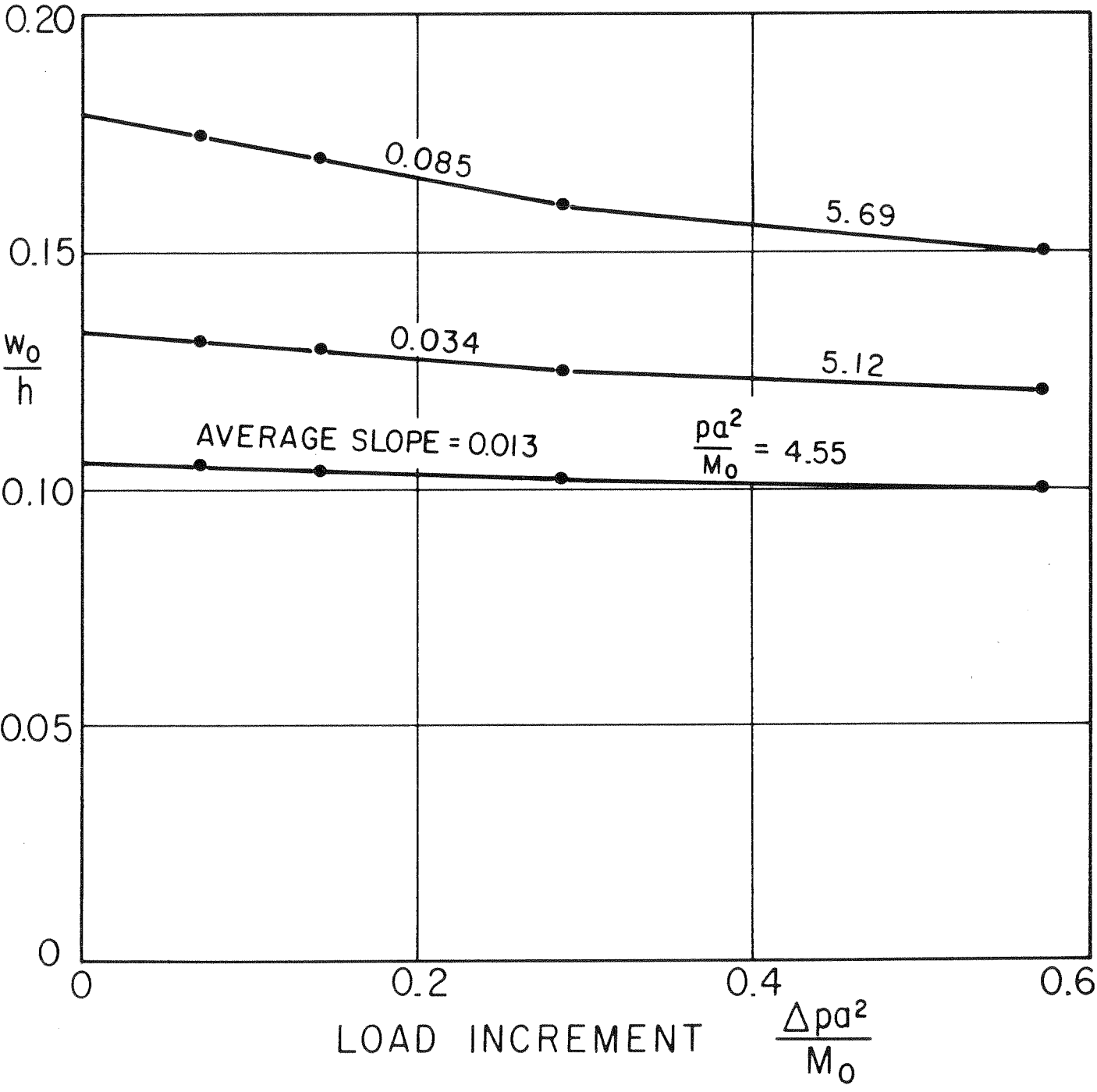

FIG. 27 VARIATION OF DEFLECTION AT r = 0 USING DIFFERENT LOAD INCREMENTS

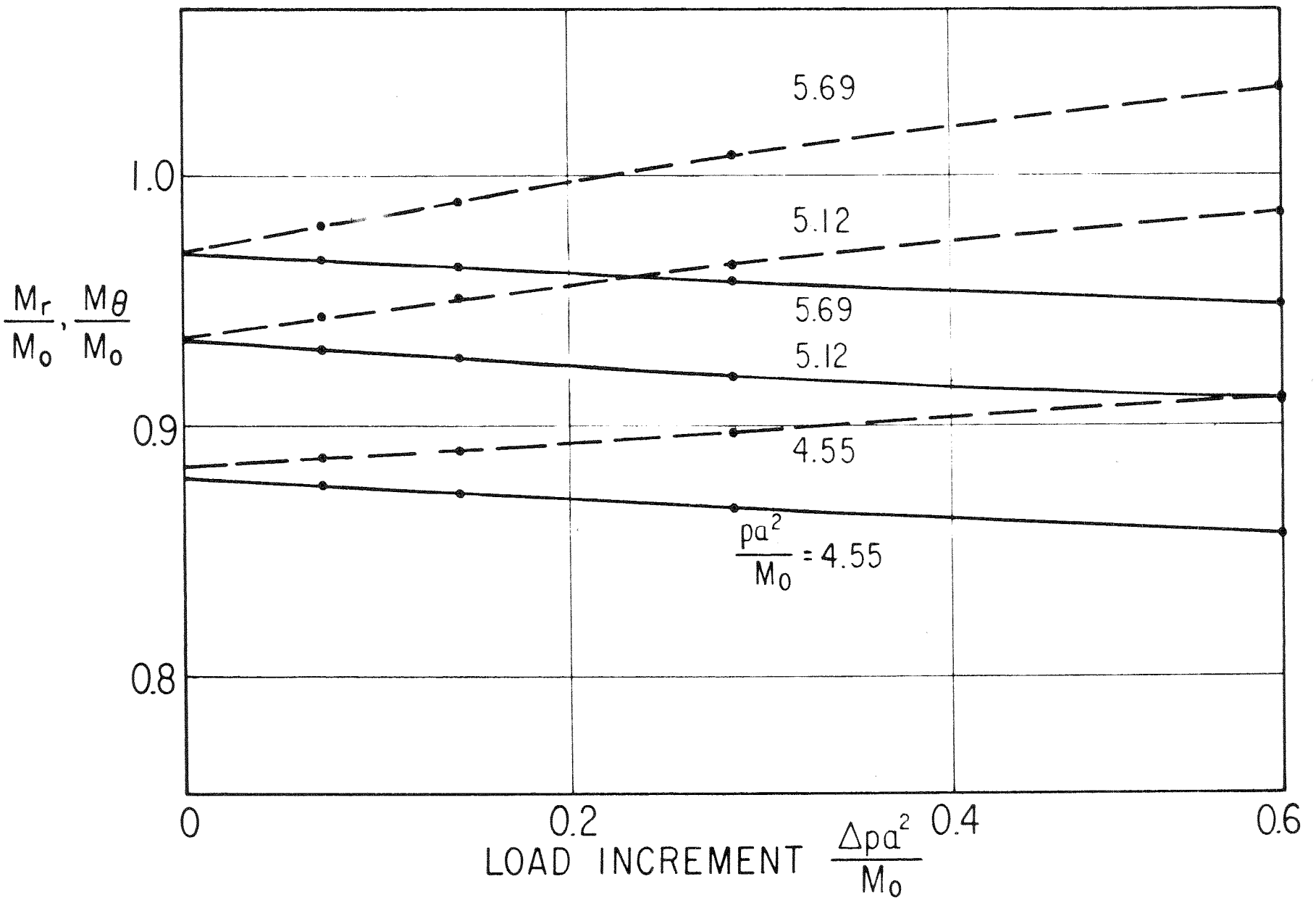

FIG. 28 VARIATION OF MOMENT AT r = 0 USING DIFFERENT LOAD INCREMENTS

Example 6

A 1x20 in. simply supported plate is subjected to uniformly distributed load. The material property of the plate is shown in Fig. 30. $\nu = 0.33$.

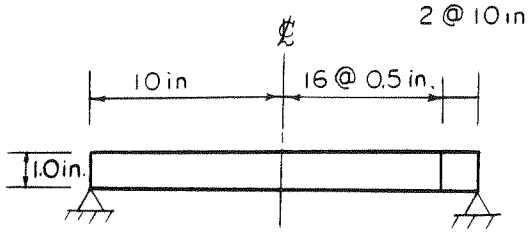

Fig. 29

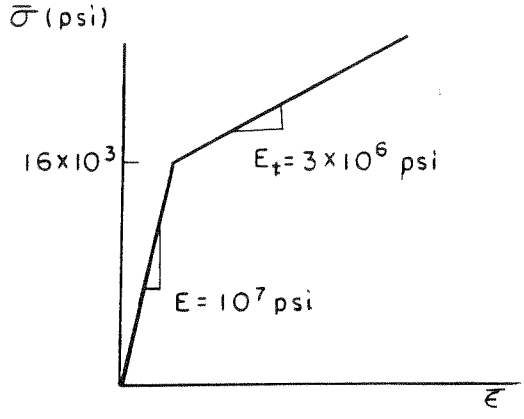

Fig. 30
Uniaxial Stress-Strain diagram

18 elements are used as indicated in Fig. 29. The thickness is divided into 40 layers. Load increments of 15 and 10 psi are used.

The results are plotted in Figs. 31 to 35.

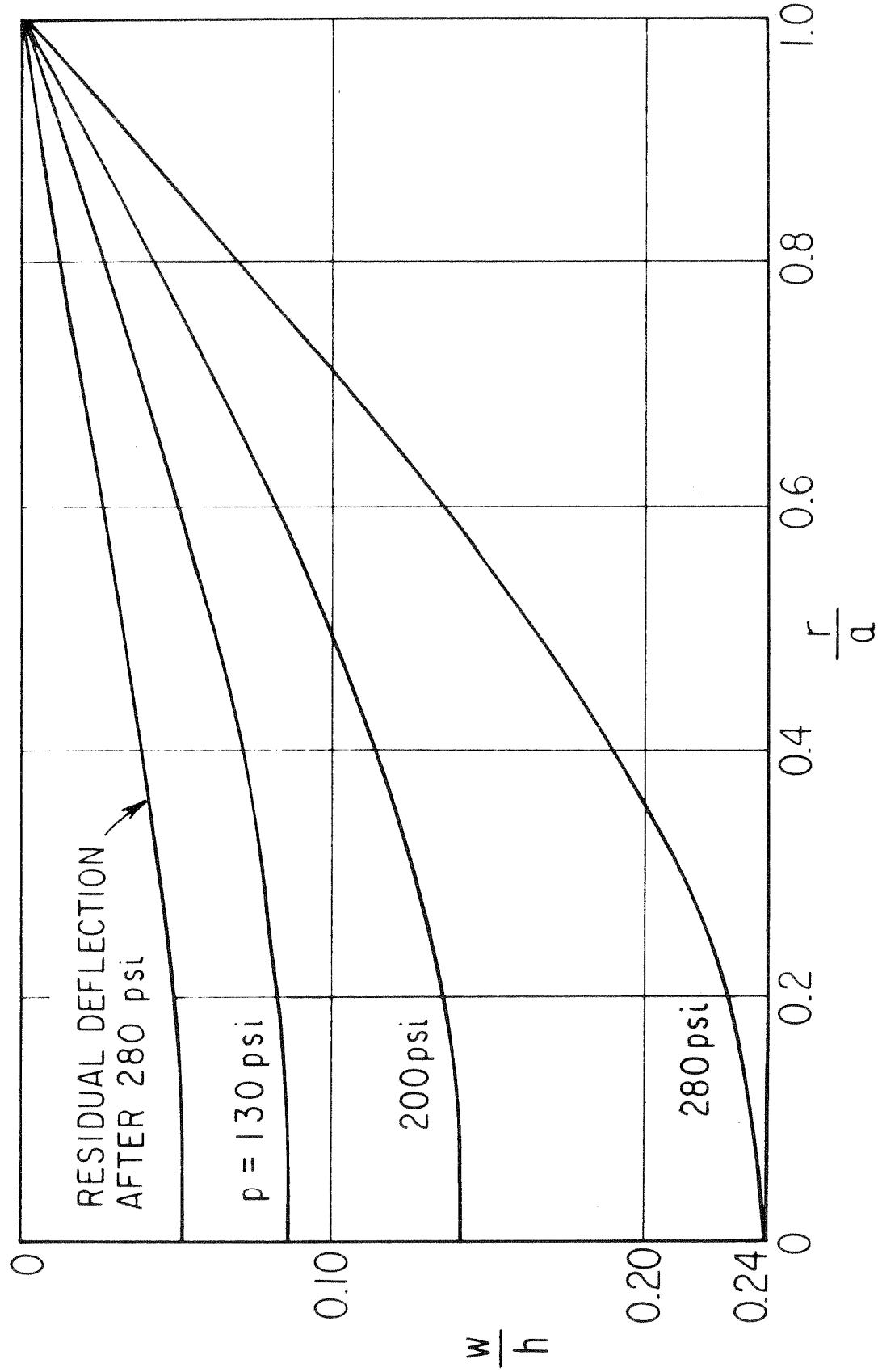

FIG. 31 DISTRIBUTIONS OF DEFLECTION

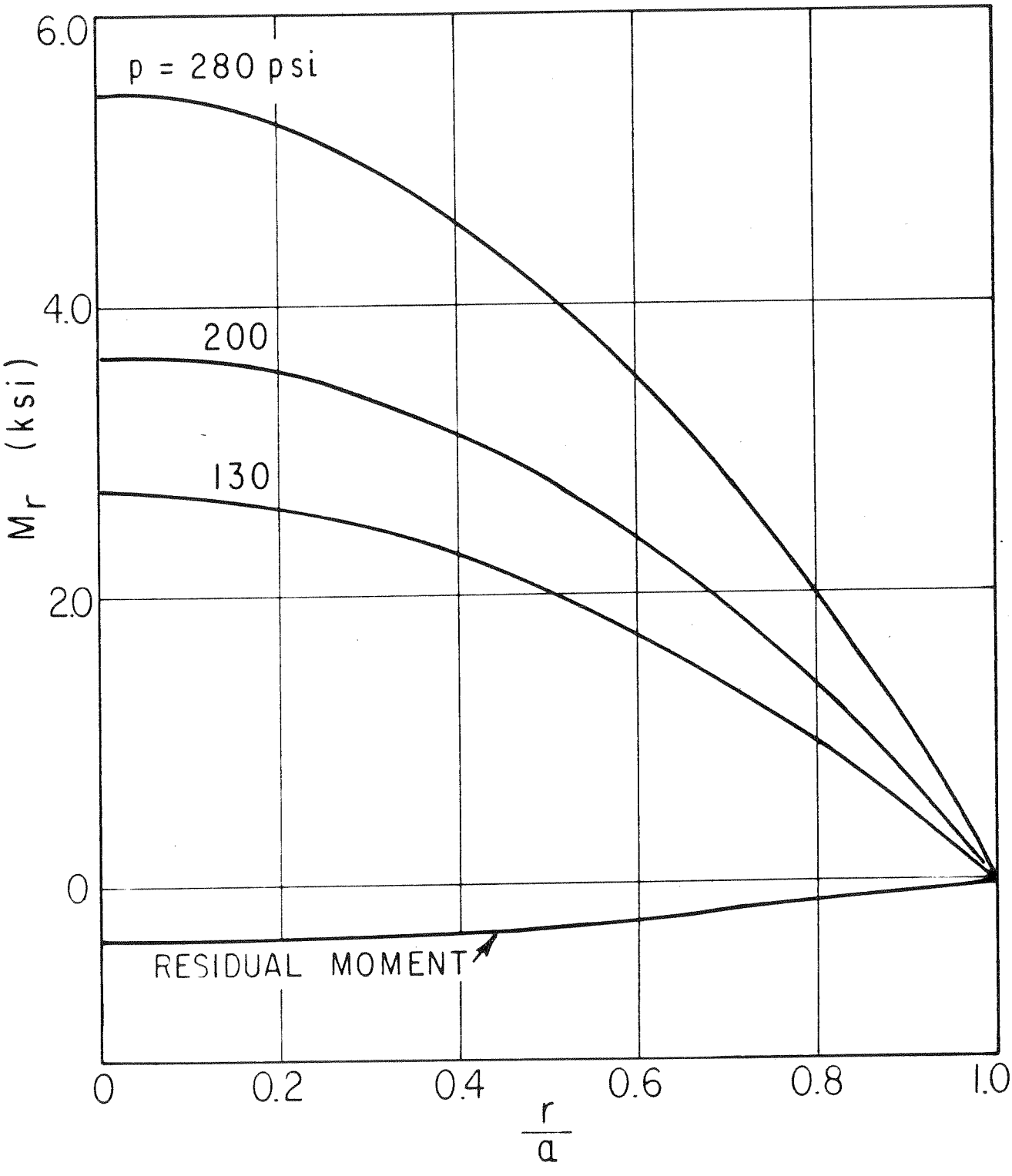

FIG. 32 DISTRIBUTIONS OF RADIAL MOMENT

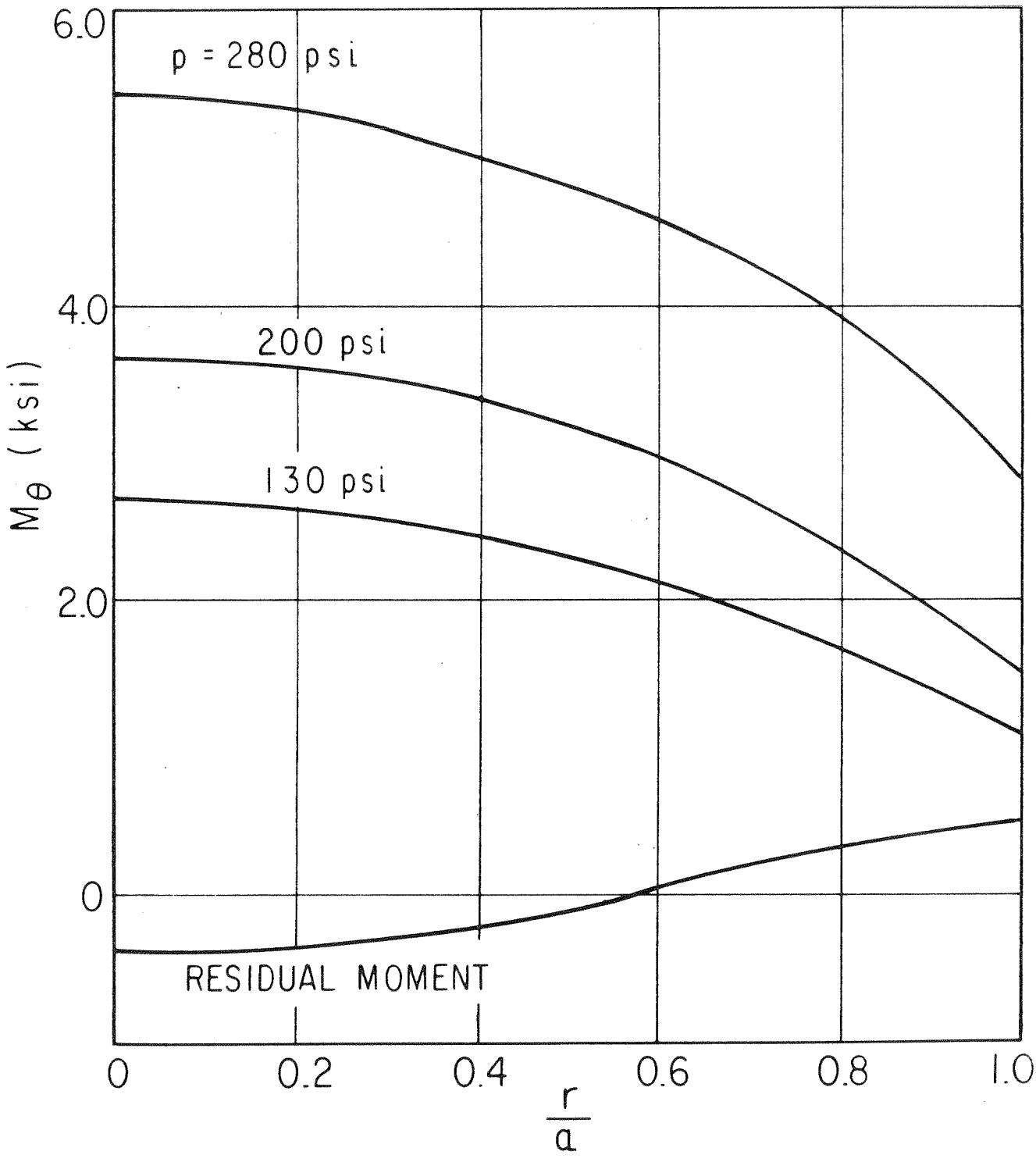

FIG. 33 DISTRIBUTIONS OF M_θ

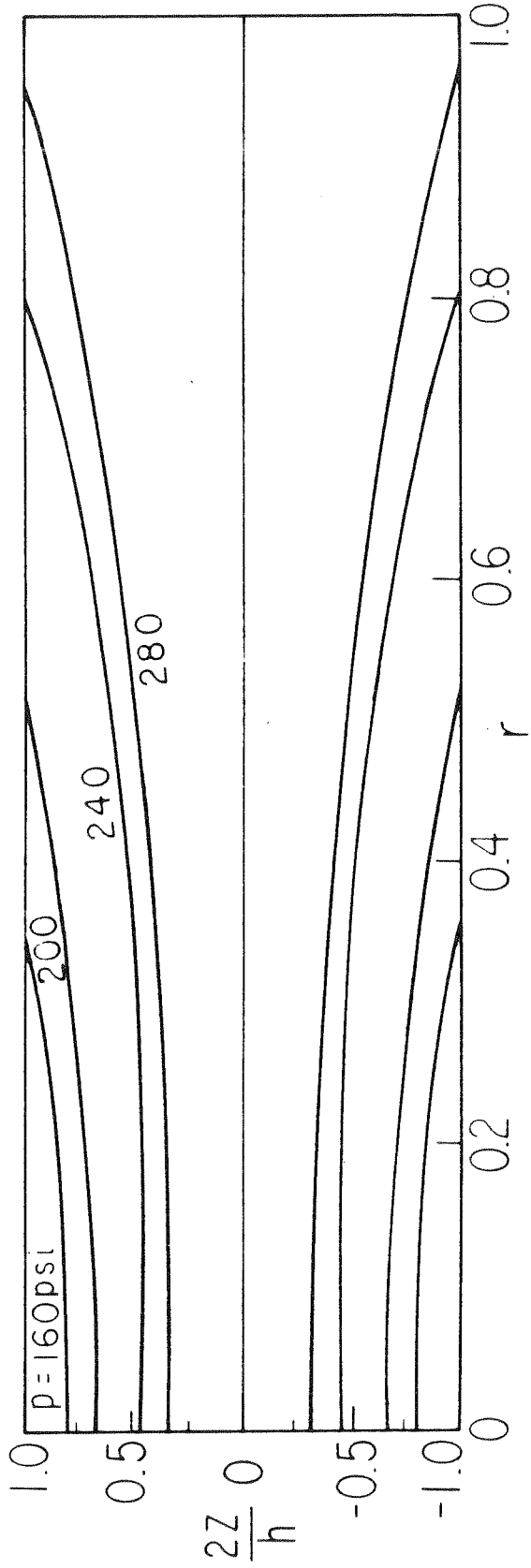

FIG. 34 ELASTIC PLASTIC BOUNDARIES

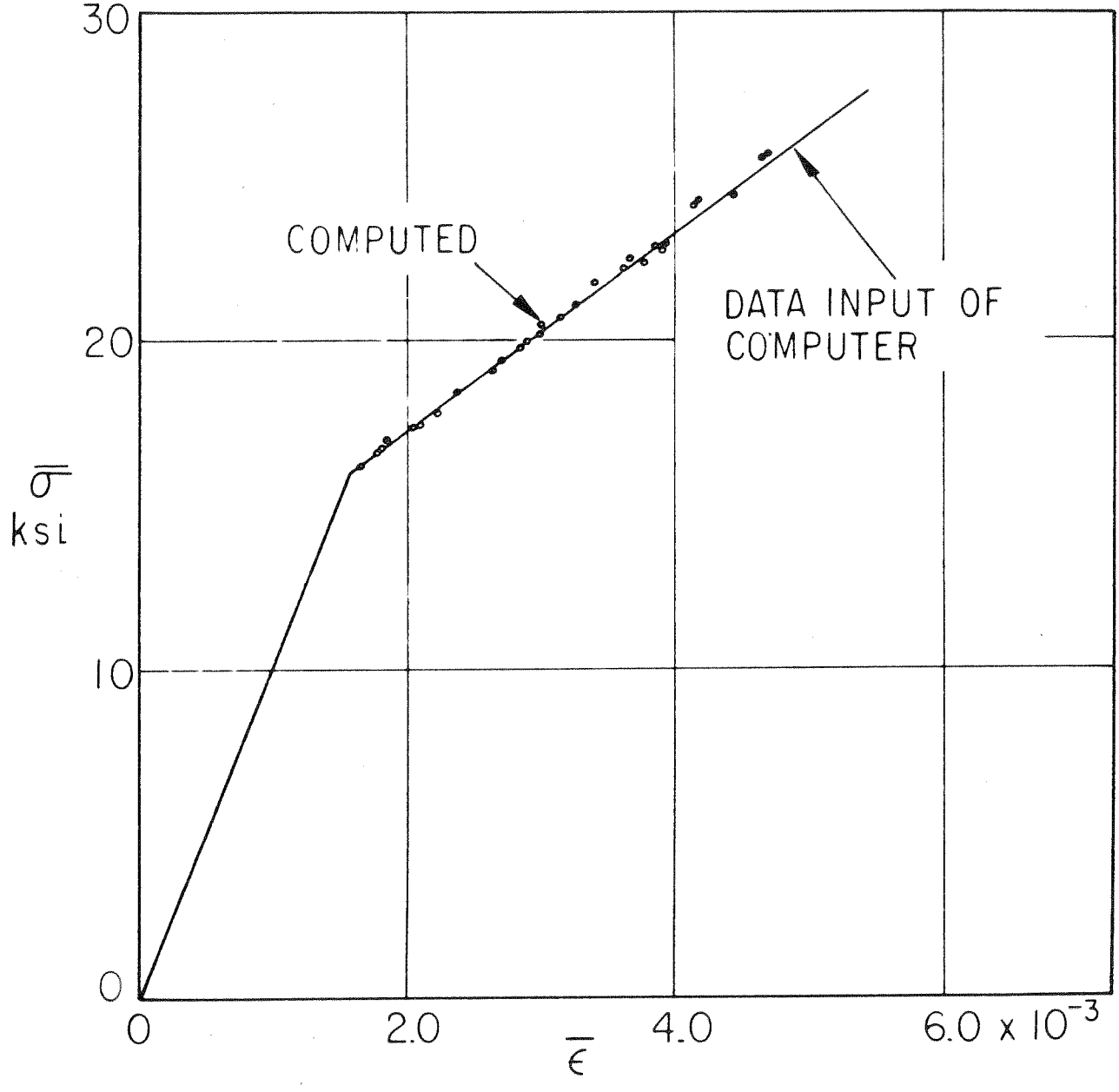

FIG. 35 COMPARISON OF INPUT AND COMPUTED STRESS-STRAIN DIAGRAMS

Example 7

A clamped plate of the same size and material property as in Example 6 is subjected to uniformly distributed load.

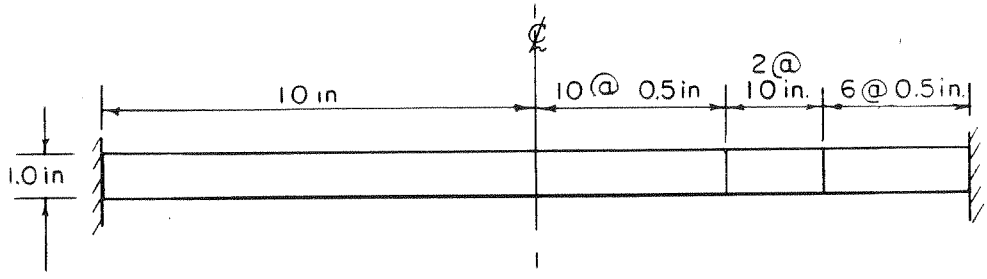

Fig. 36

There are 40 layers; and 18 elements which are distributed as shown in Fig. 36. Load increments of 25 and 20 psi are used.

Results are plotted in Figs. 37 to 40.

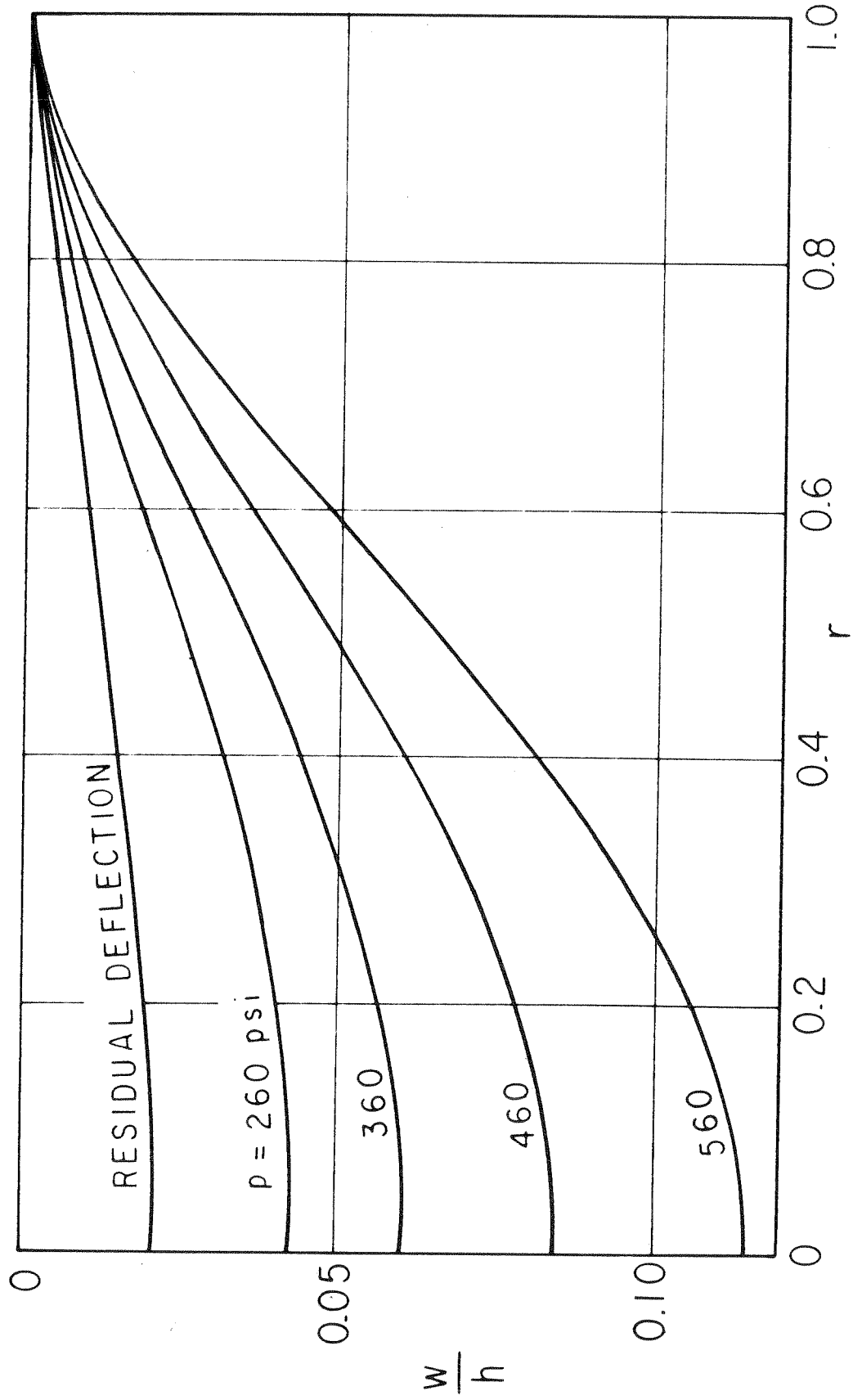

FIG. 37 DISTRIBUTIONS OF DEFLECTIONS

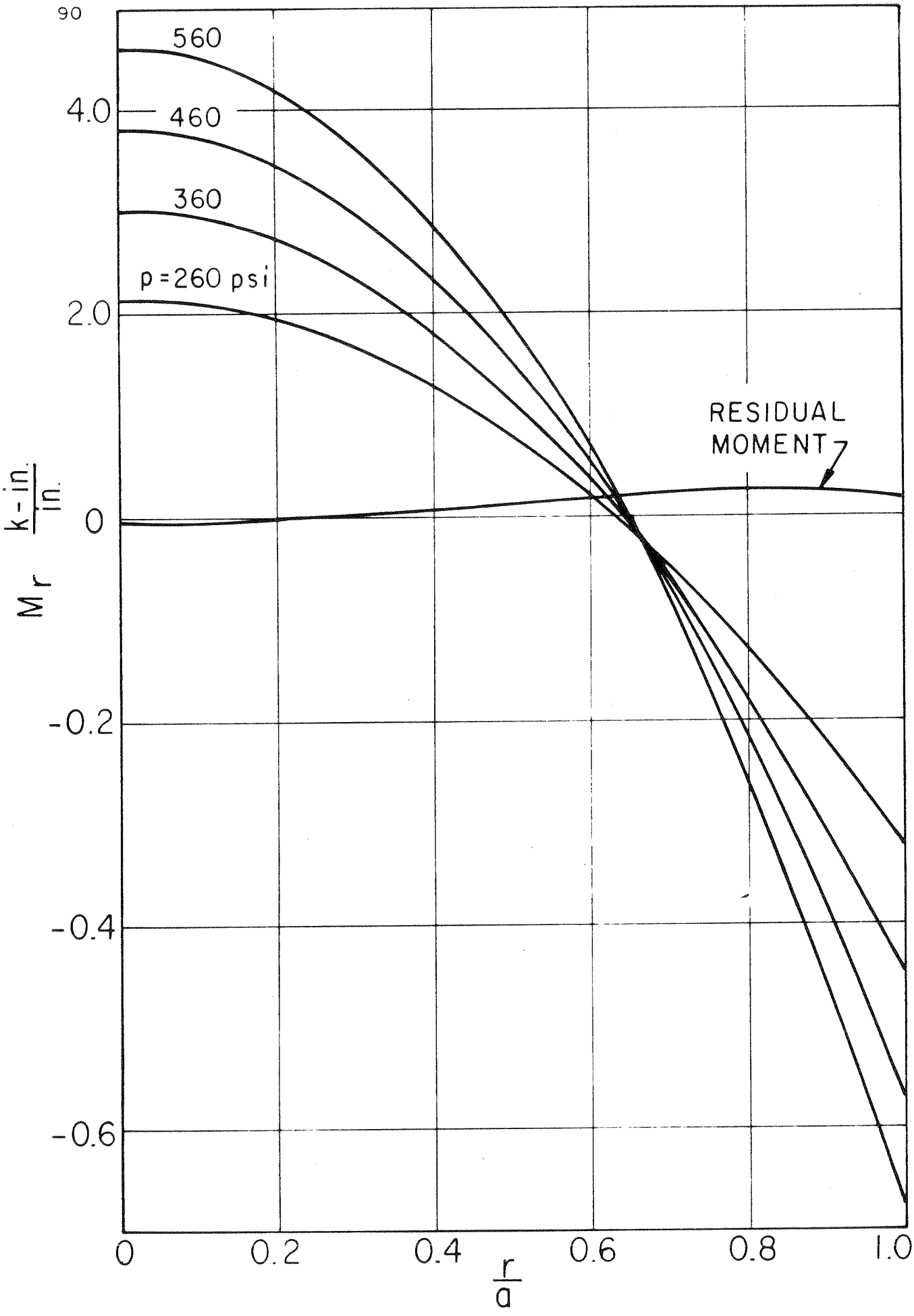

FIG. 38 DISTRIBUTIONS OF RADIAL MOMENT

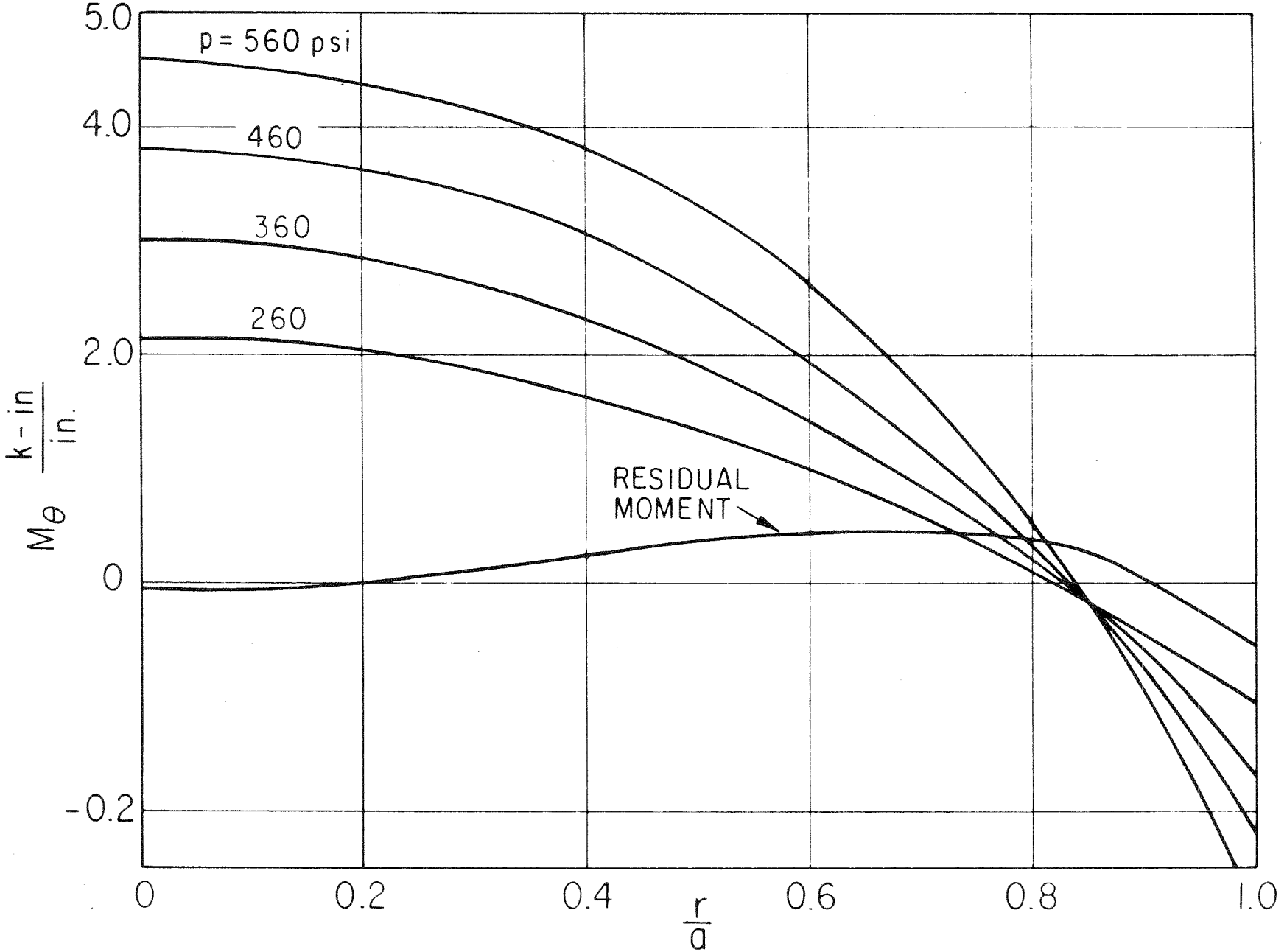

FIG. 39 DISTRIBUTIONS OF TANGENTIAL MOMENT

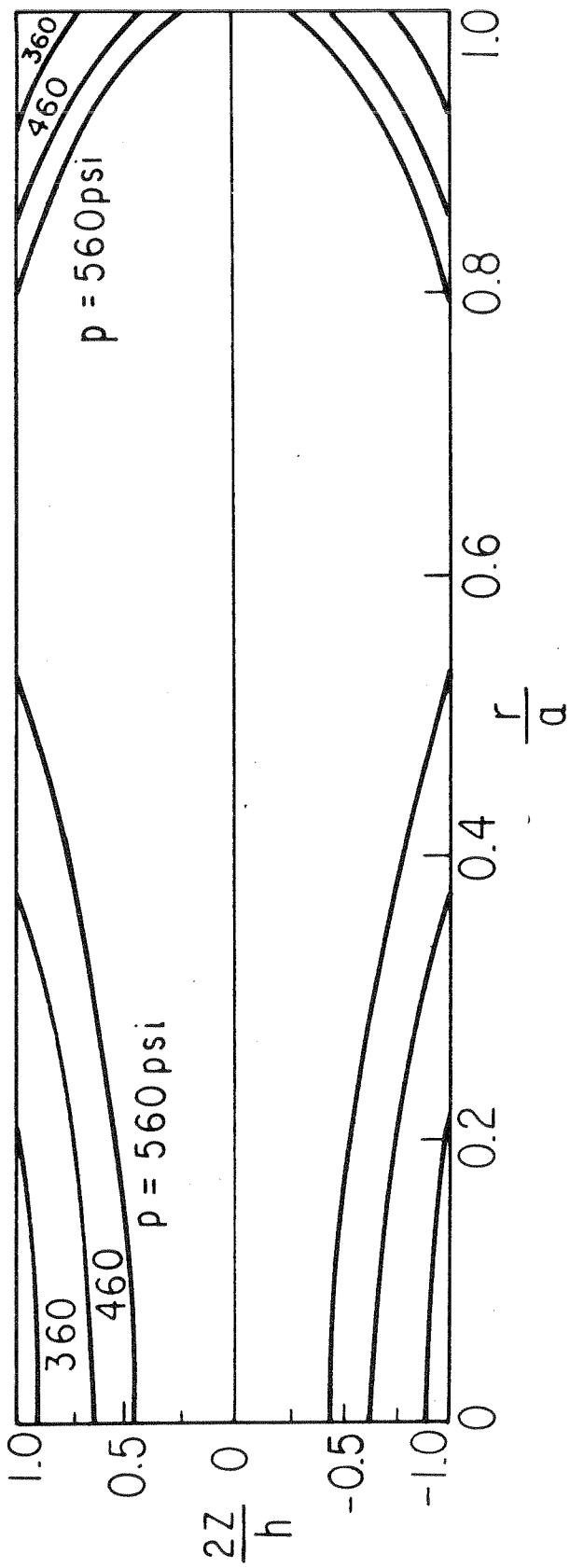

FIG.40 ELASTIC PLASTIC BOUNDARIES

Example 8

A simply supported plate exactly the same as that in Example 6 except with the uniaxial stress-strain diagram shown in Fig. 46 is subjected to uniformly distributed load.

The E_t-σ diagram of the stress-strain curve is shown in Fig. 41. The reason for using such a stress-strain curve is that it has an initial linear elastic part and also it is quite easy to modify the two other linear parts of the E_t-σ diagram to obtain different shapes of the stress strain diagram. The results are plotted in Figs. 42 to 46.

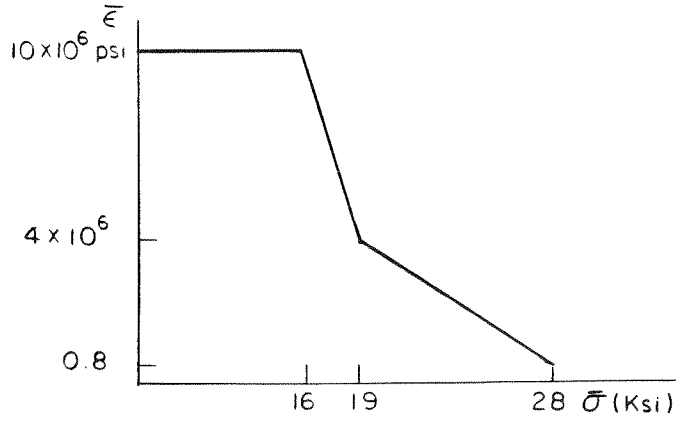

Fig. 41

Example 9

A clamped plate of same geometrical and material properties as that in Example 8 is subjected to uniformly distributed load.

Results are plotted in Fig. 47 to 50.

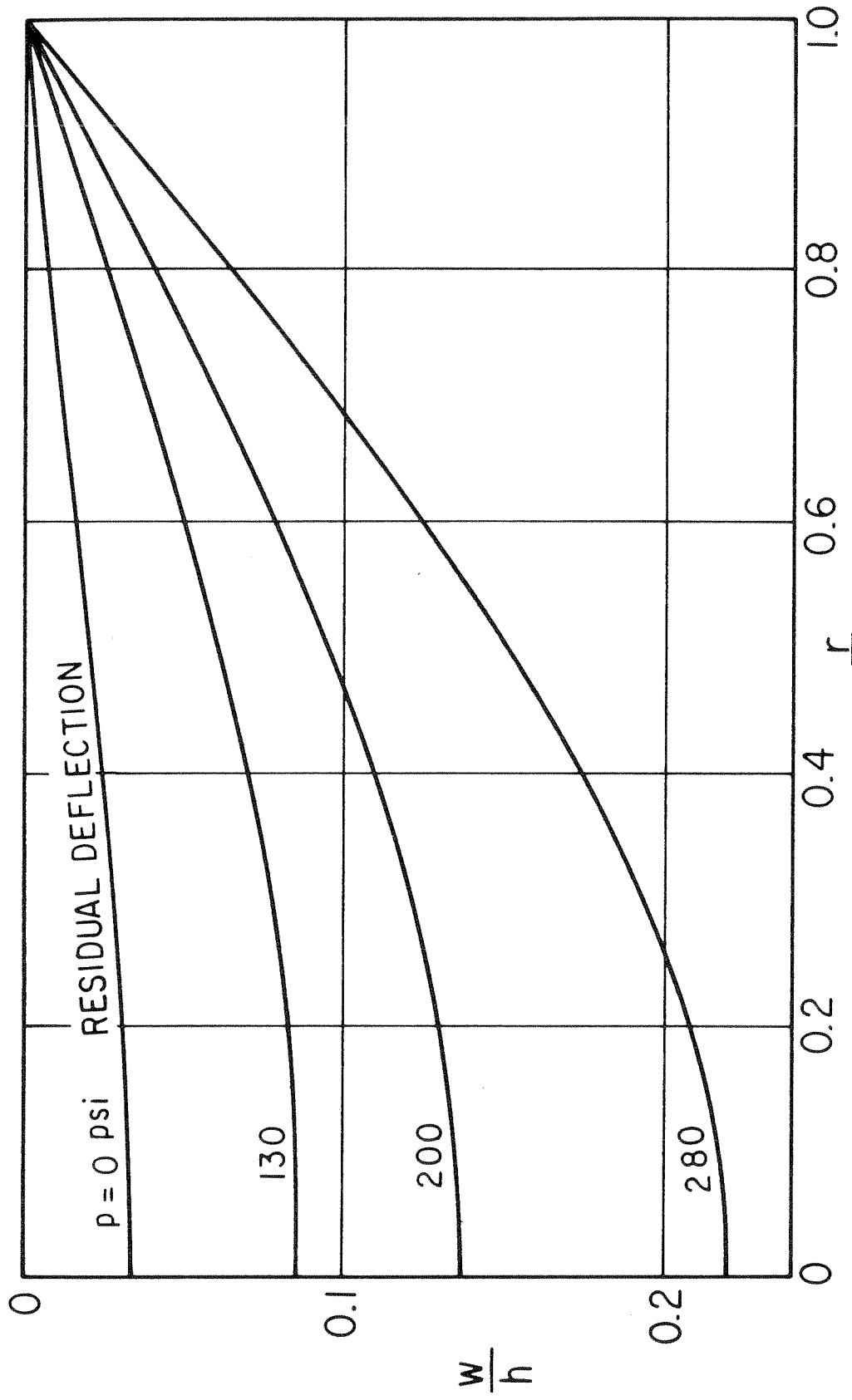

FIG. 42 DISTRIBUTIONS OF DEFLECTION

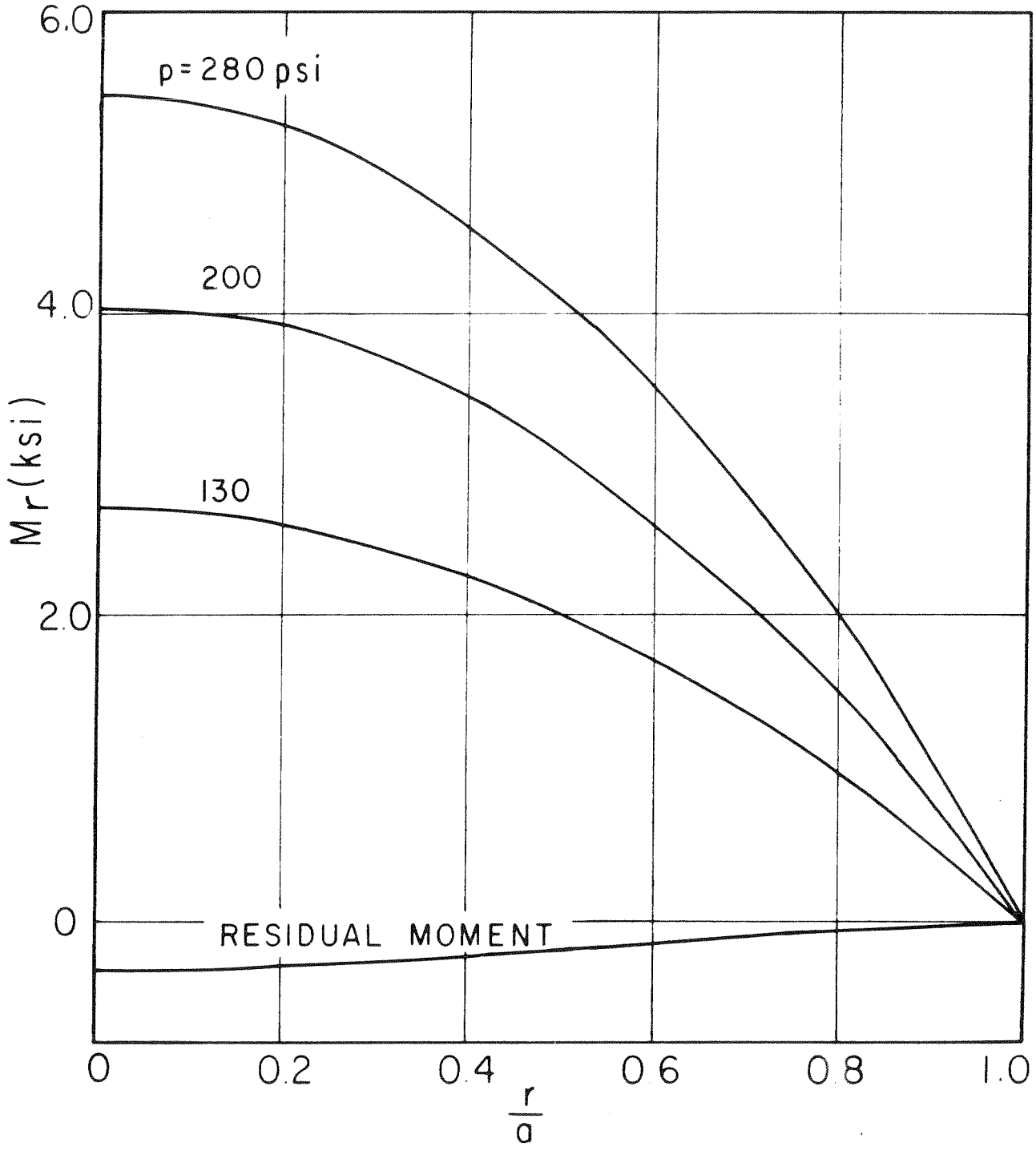

FIG. 43 DISTRIBUTIONS OF RADIAL MOMENT

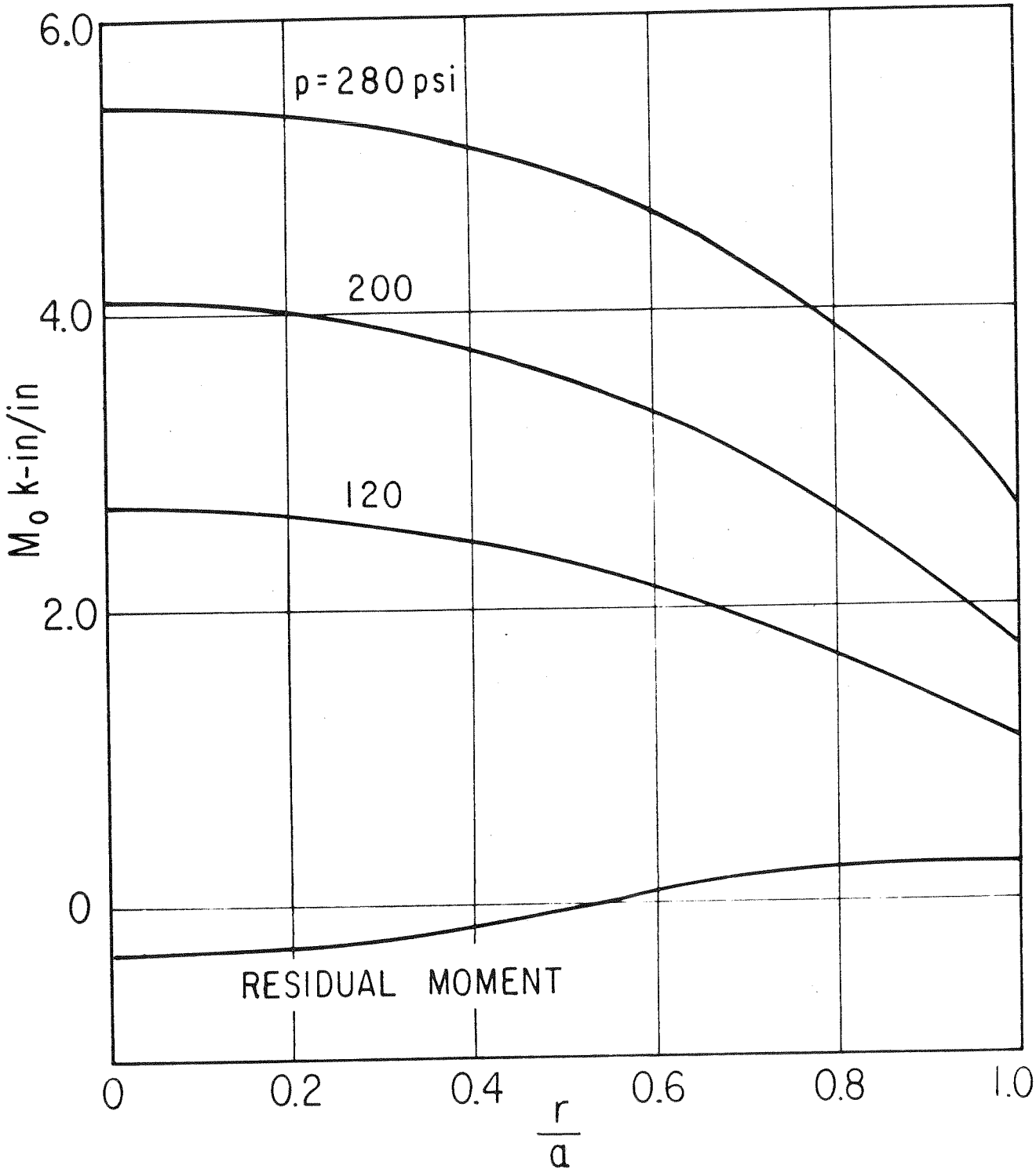

FIG. 44 DISTRIBUTIONS OF TANGENTIAL MOMENT

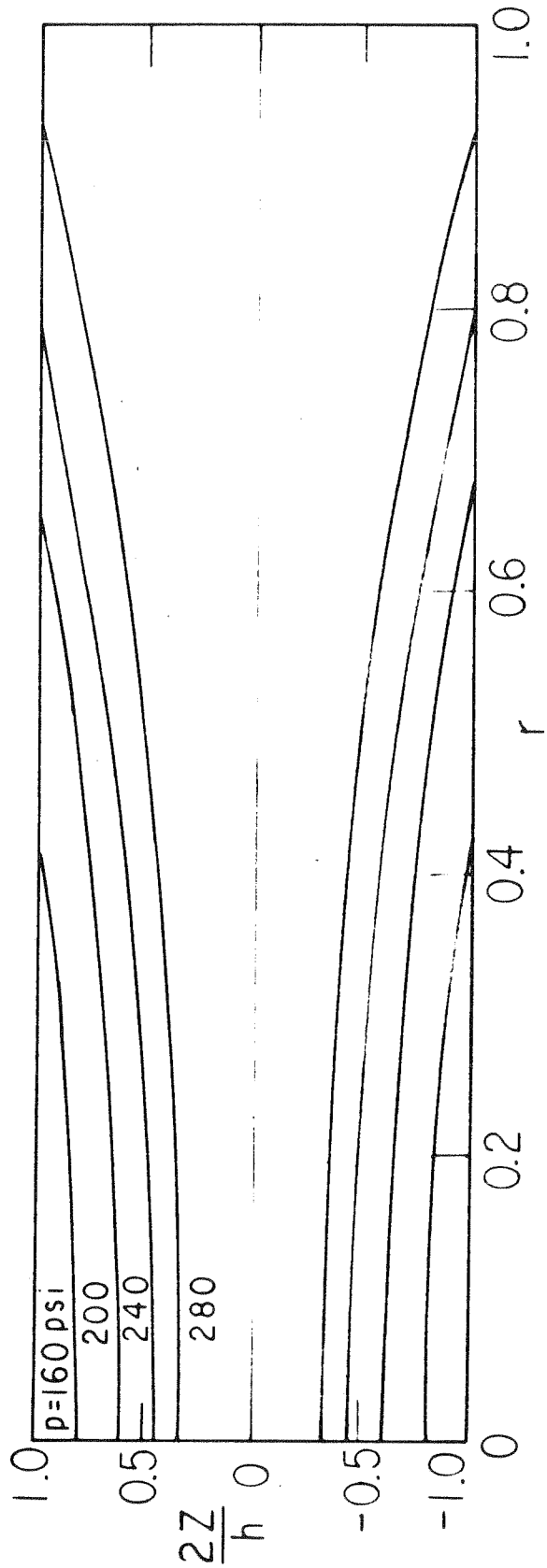

FIG. 45 ELASTIC PLASTIC BOUNDARIES

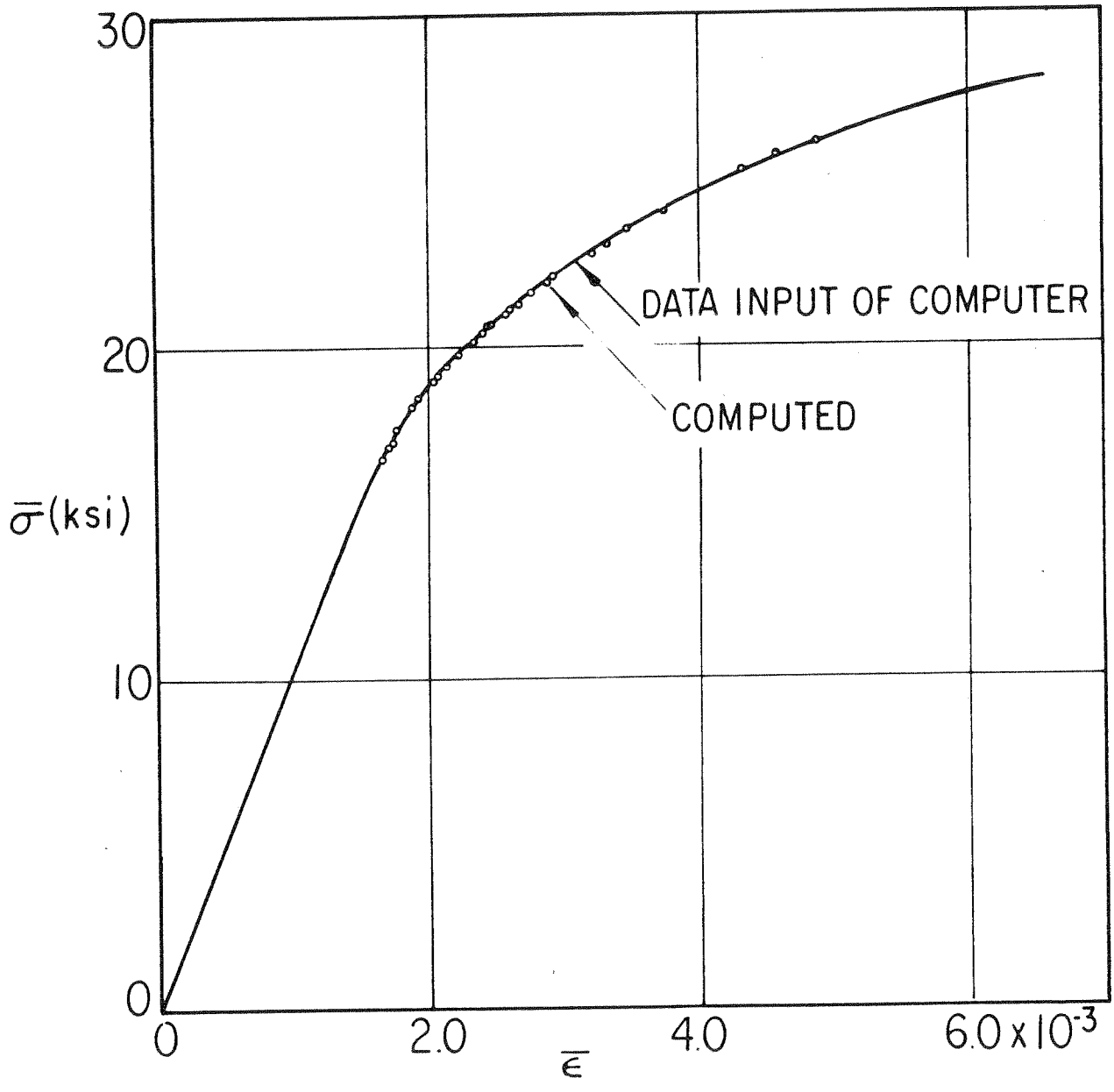

FIG.46 COMPARISON OF INPUT AND COMPUTED STRESS-STRAIN DIAGRAMS.

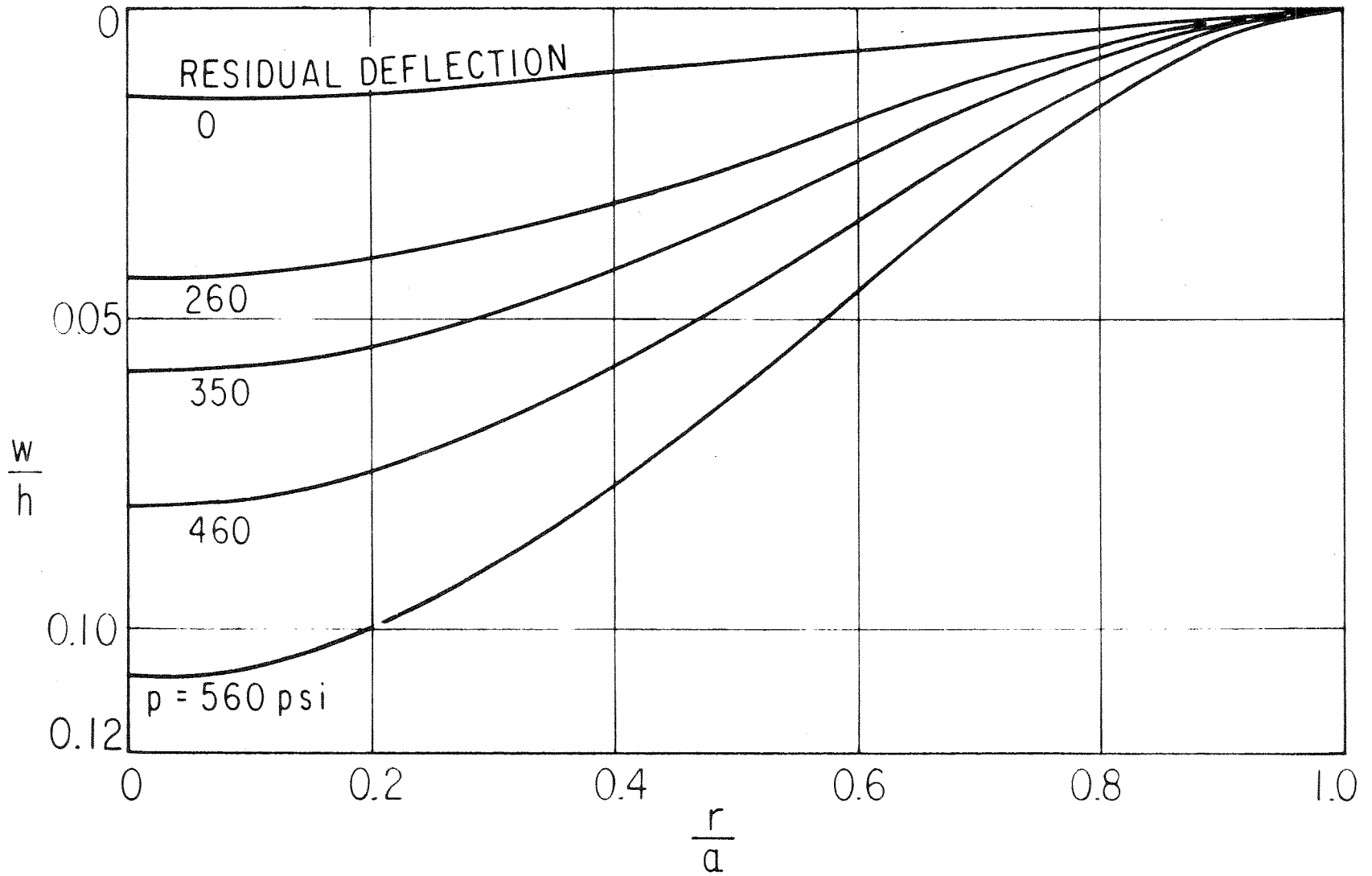

FIG 47 DISTRIBUTIONS OF DEFLECTION

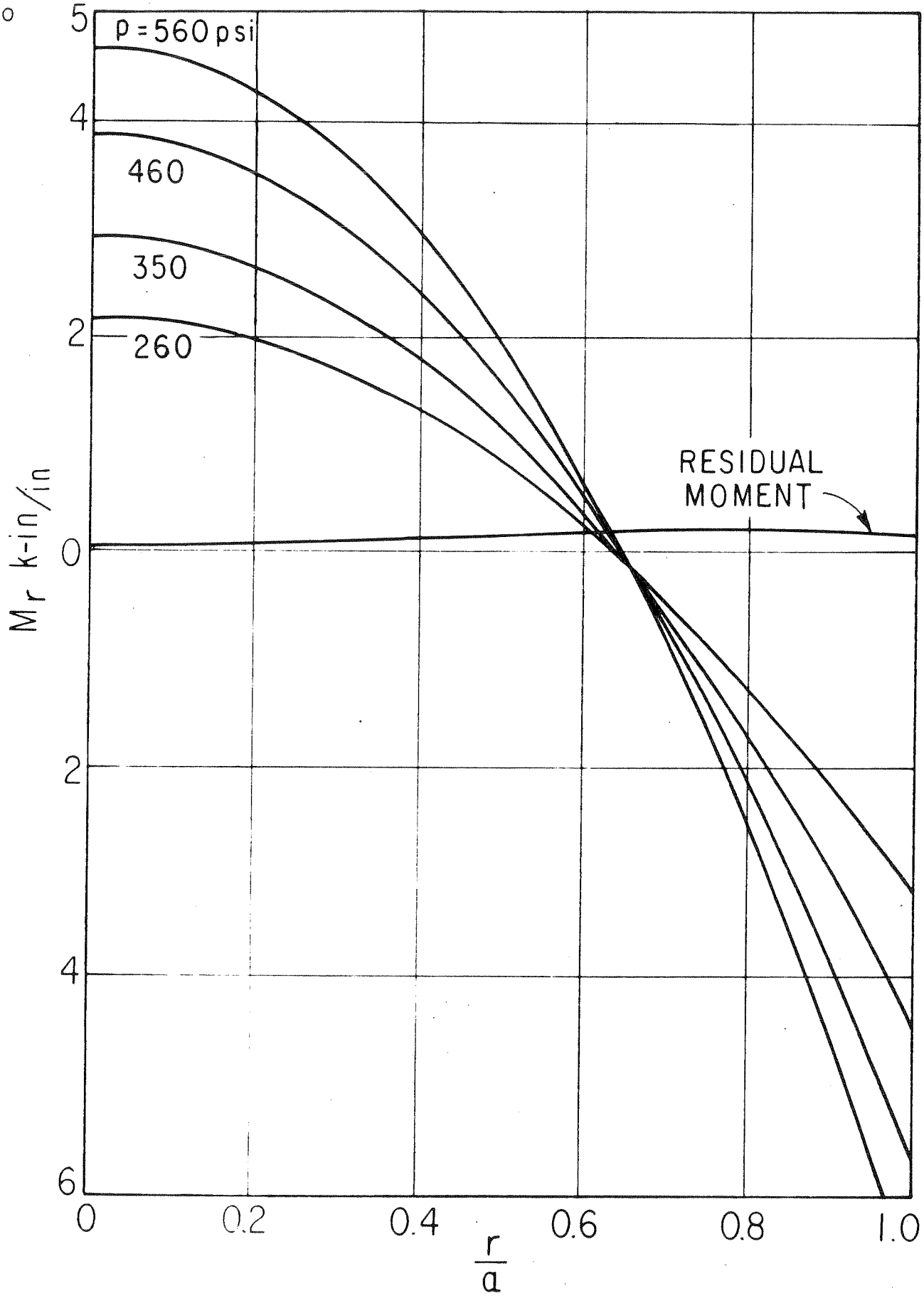

FIG 48 DISTRIBUTIONS OF RADIAL MOMENT

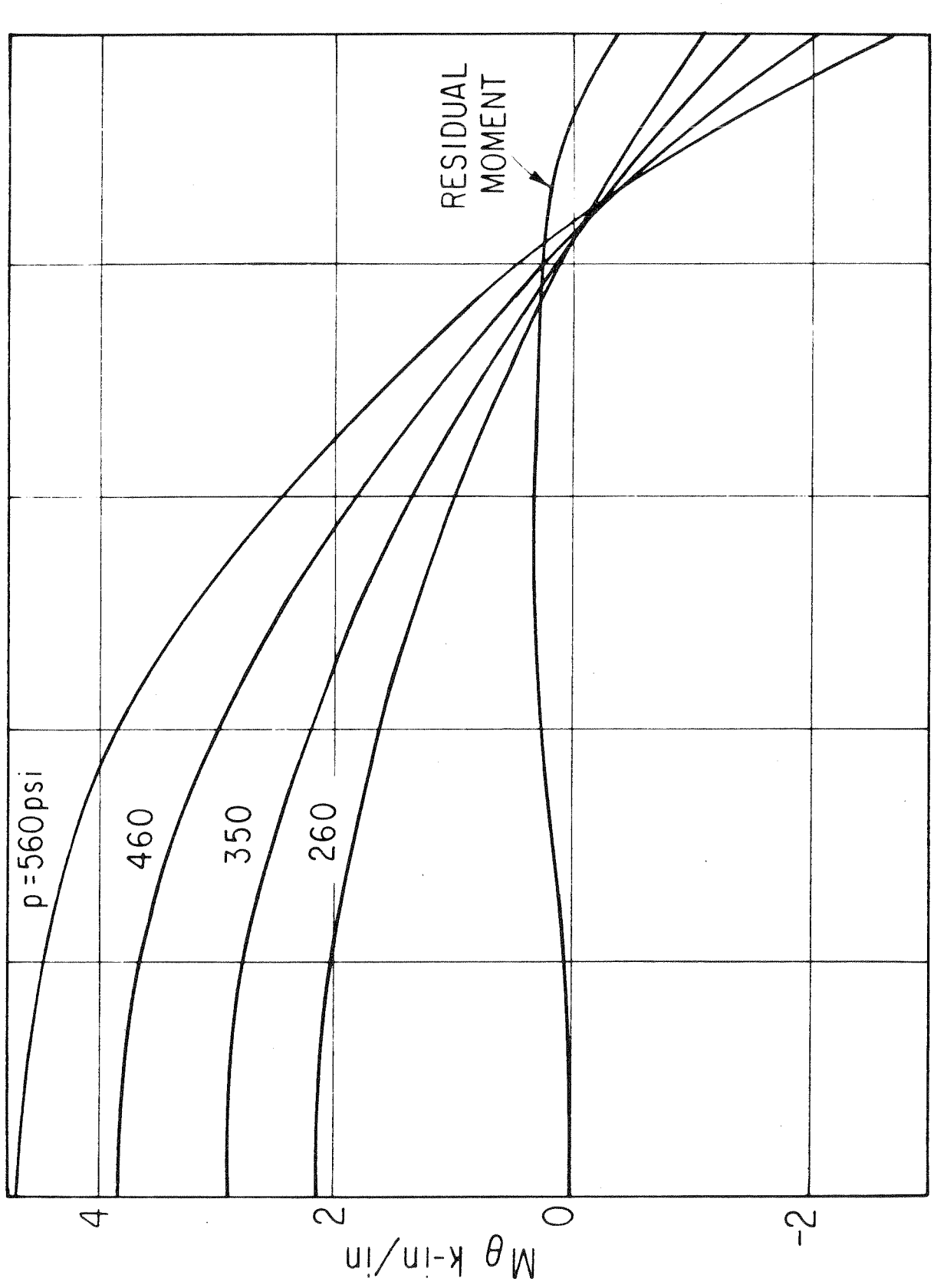

FIG 49 DISTRIBUTIONS OF TANGENTIAL MOMENT

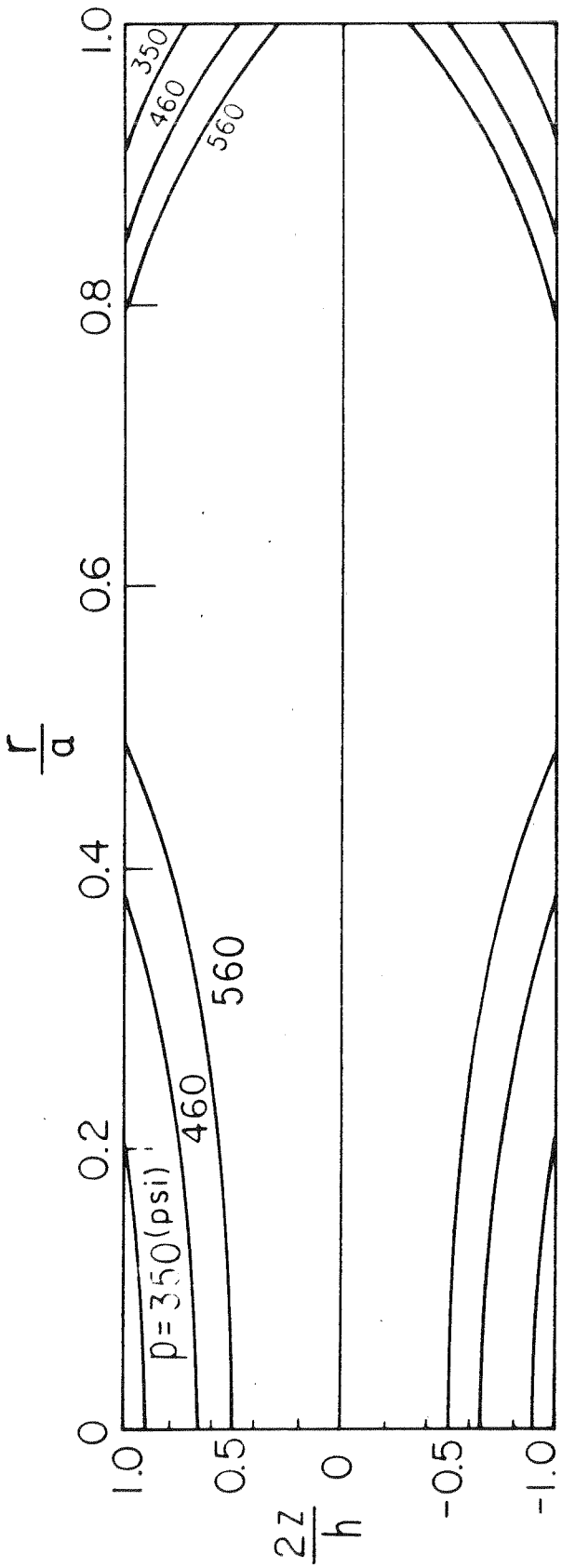

FIG. 50 ELASTIC PLASTIC BOUNDARIES

Example 10

The purpose of this example is to compare the results of the elastic-perfectly plastic plate solution of Example 1 with a solution for a plate with hardening material having uniaxial stress-strain diagram of Fig. 51. Such a diagram closely approximates that of elastic-perfectly plastic material.

The number of elements, layers and magnitude of load increments are the same as in Example 1.

Results are plotted in Fig. 52 to 55.

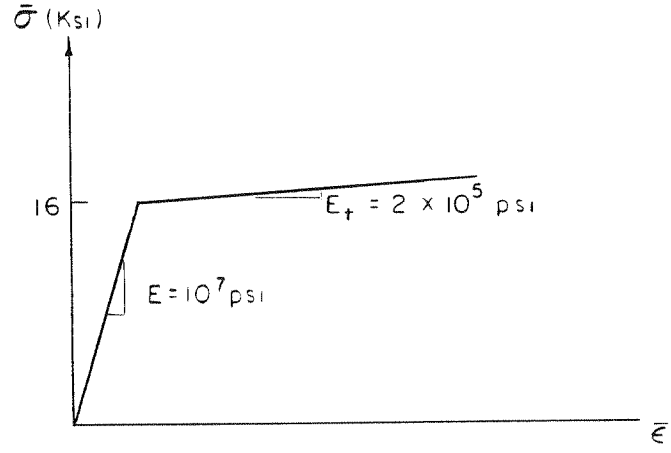

Fig. 51

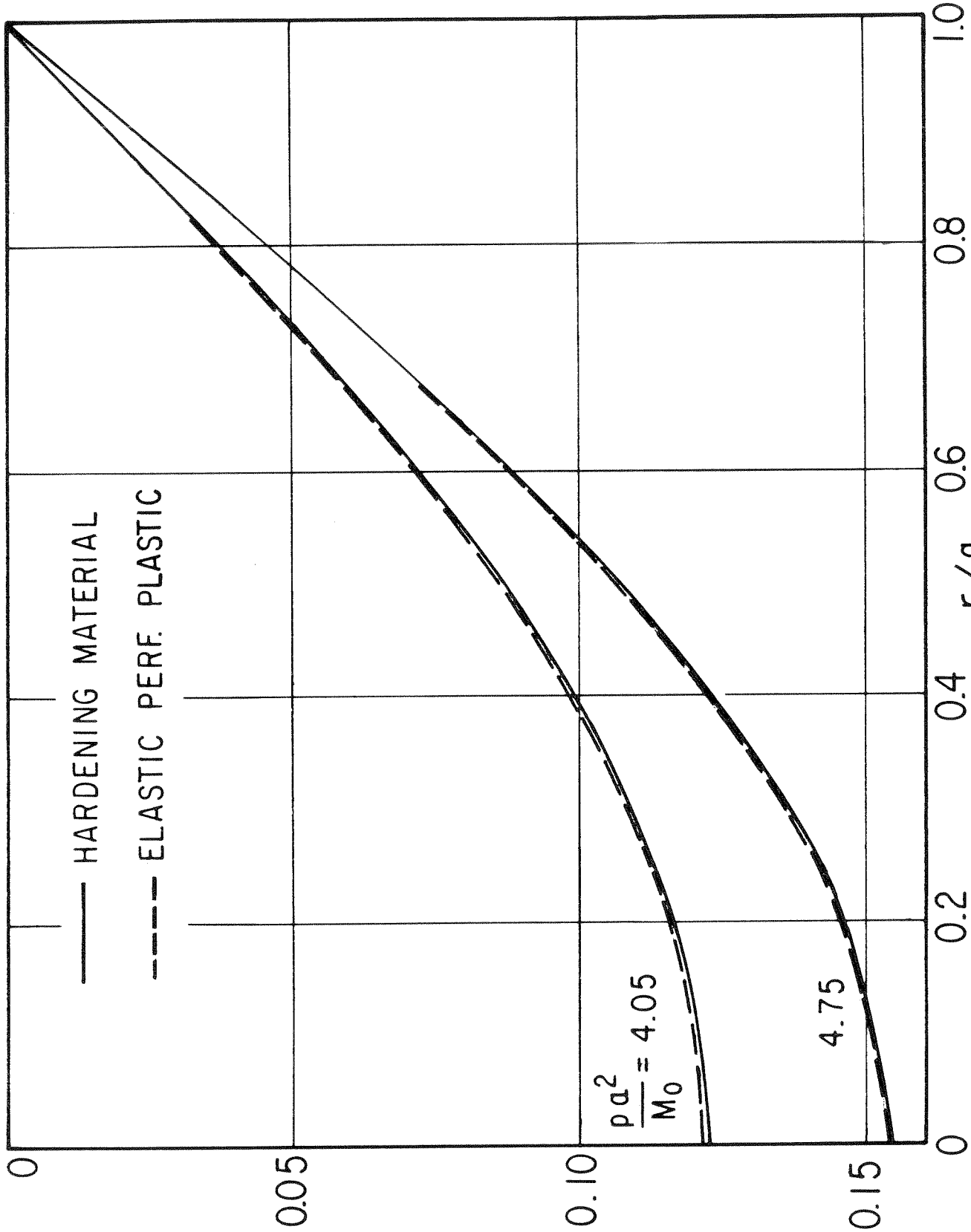

FIG. 52 DISTRIBUTIONS OF DEFLECTION

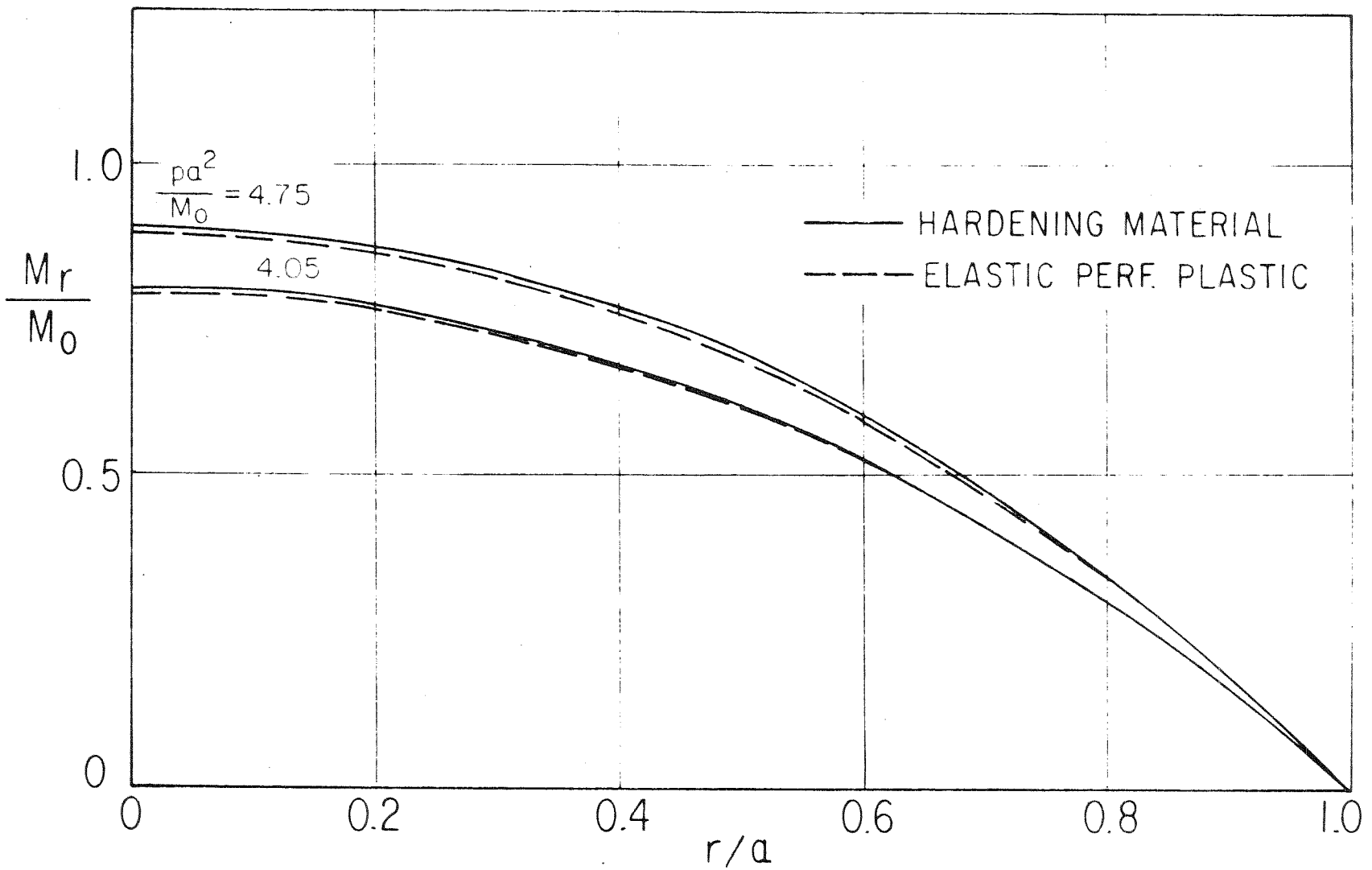

FIG 53 DISTRIBUTIONS OF RADIAL MOMENT

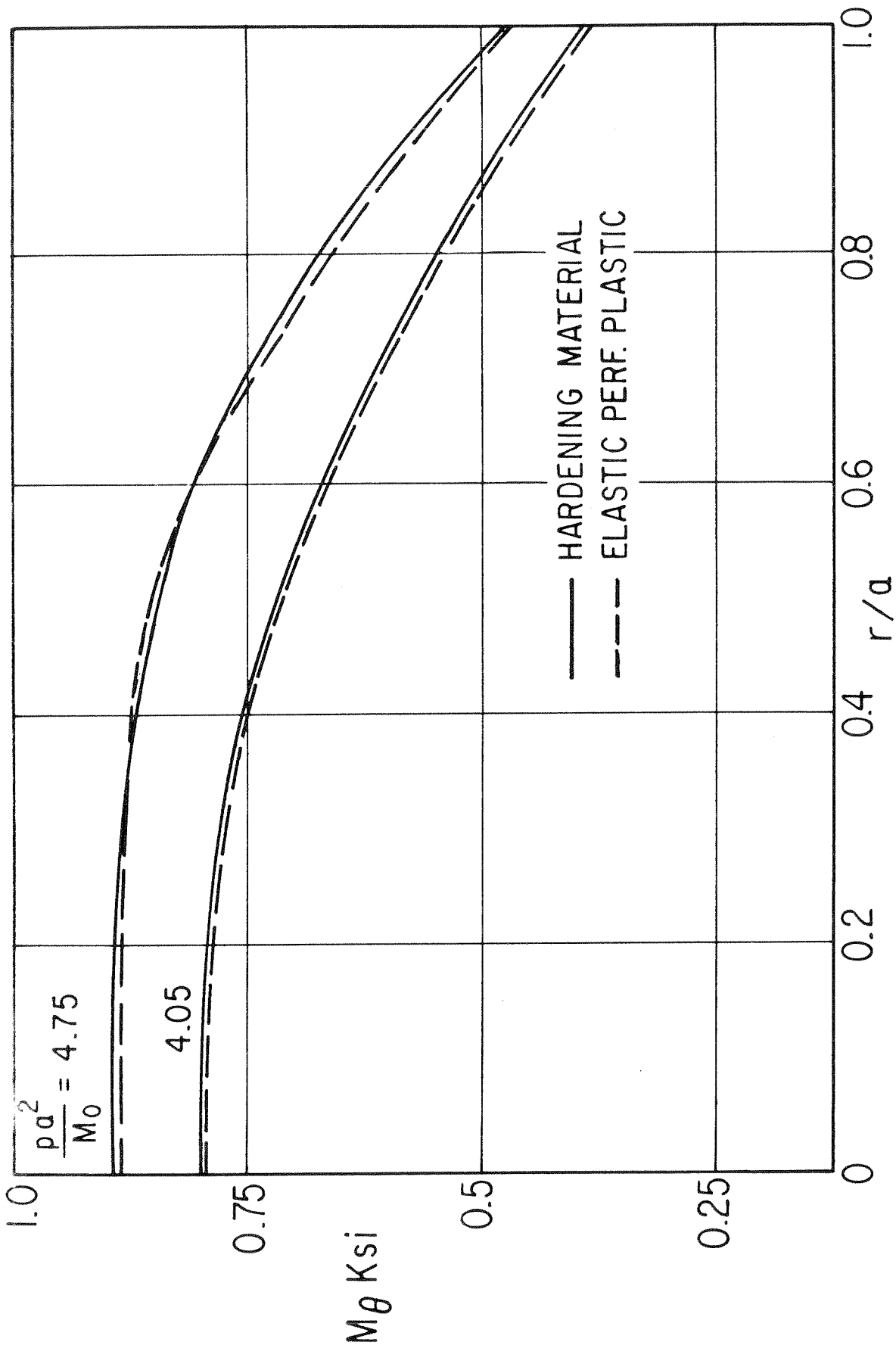

FIG. 54 DISTRIBUTIONS OF M_θ

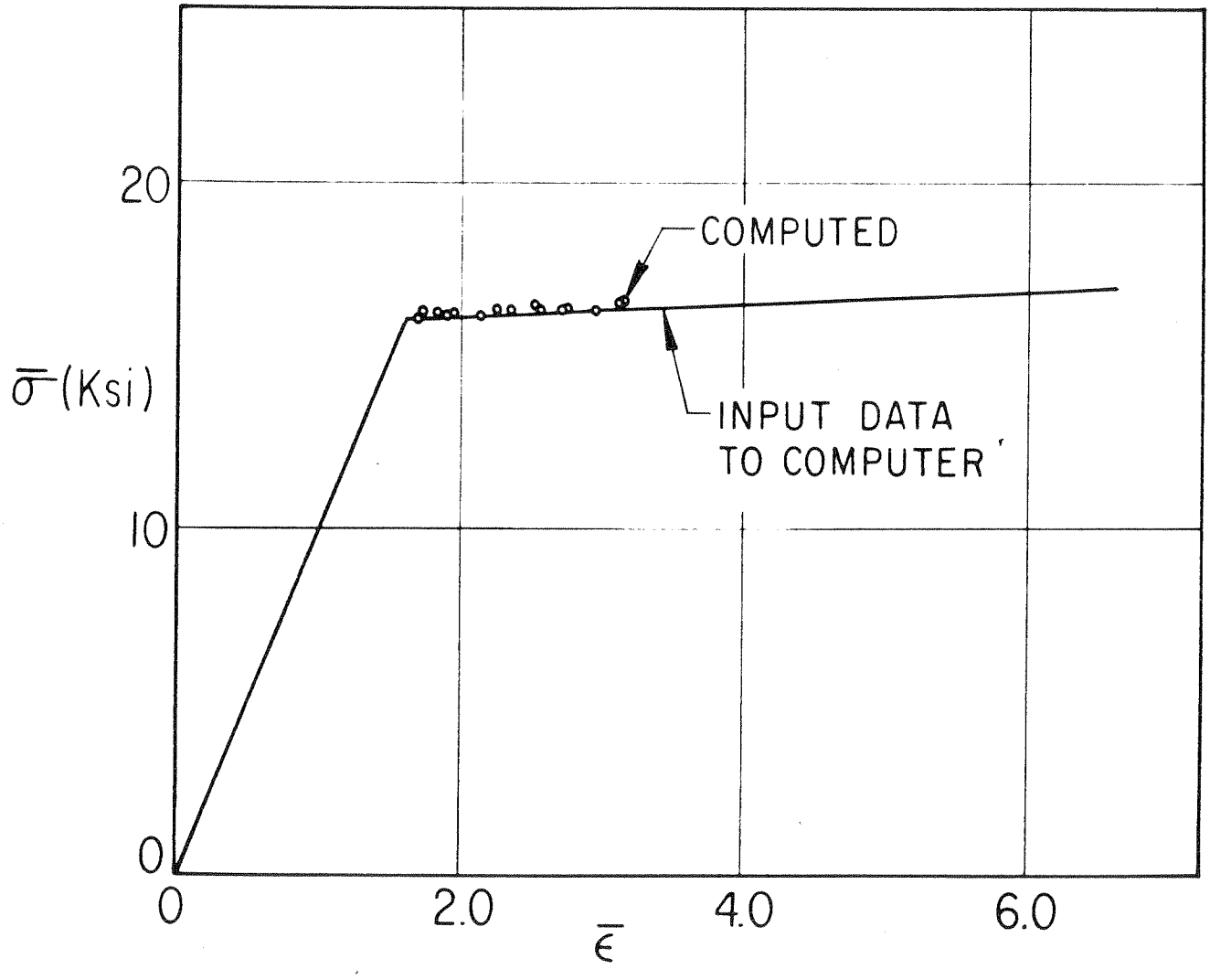

FIG 55 COMPARISON OF INPUT AND COMPUTED STRESS STRAIN DIAGRAMS

Example 11

The simply supported plate shown in Fig. 56 is subjected to uniformly distributed load.

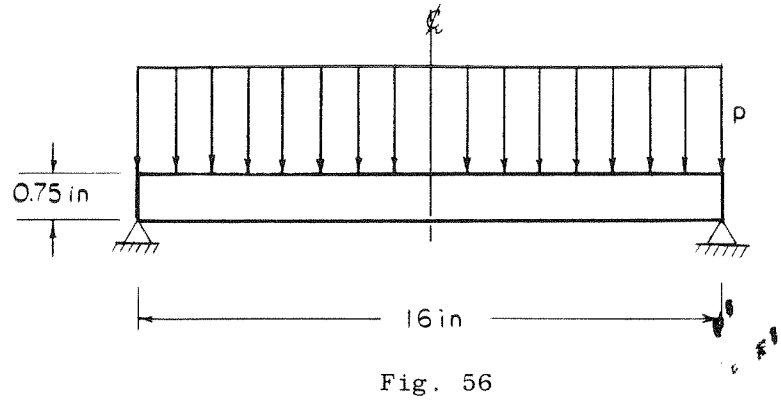

Fig. 56

The material properties are tabulated in Table 1 (from Ref. 48)

The plate is divided into 16 elements and 40 layers. Load increments of 40, 20, and 10 psi are used.

The results are compared with V. Lackman's solution in Fig. 57 and 58.

Table 1

stress (psi)	$E_t \times 10^{-6}$ (psi)
1	10.600
16,200	10.600
16,250	10.599
17,500	10.550
20,000	10.375
22,500	9.925
25,000	9.000
27,500	7.150
30,000	3.825
32,500	1.800

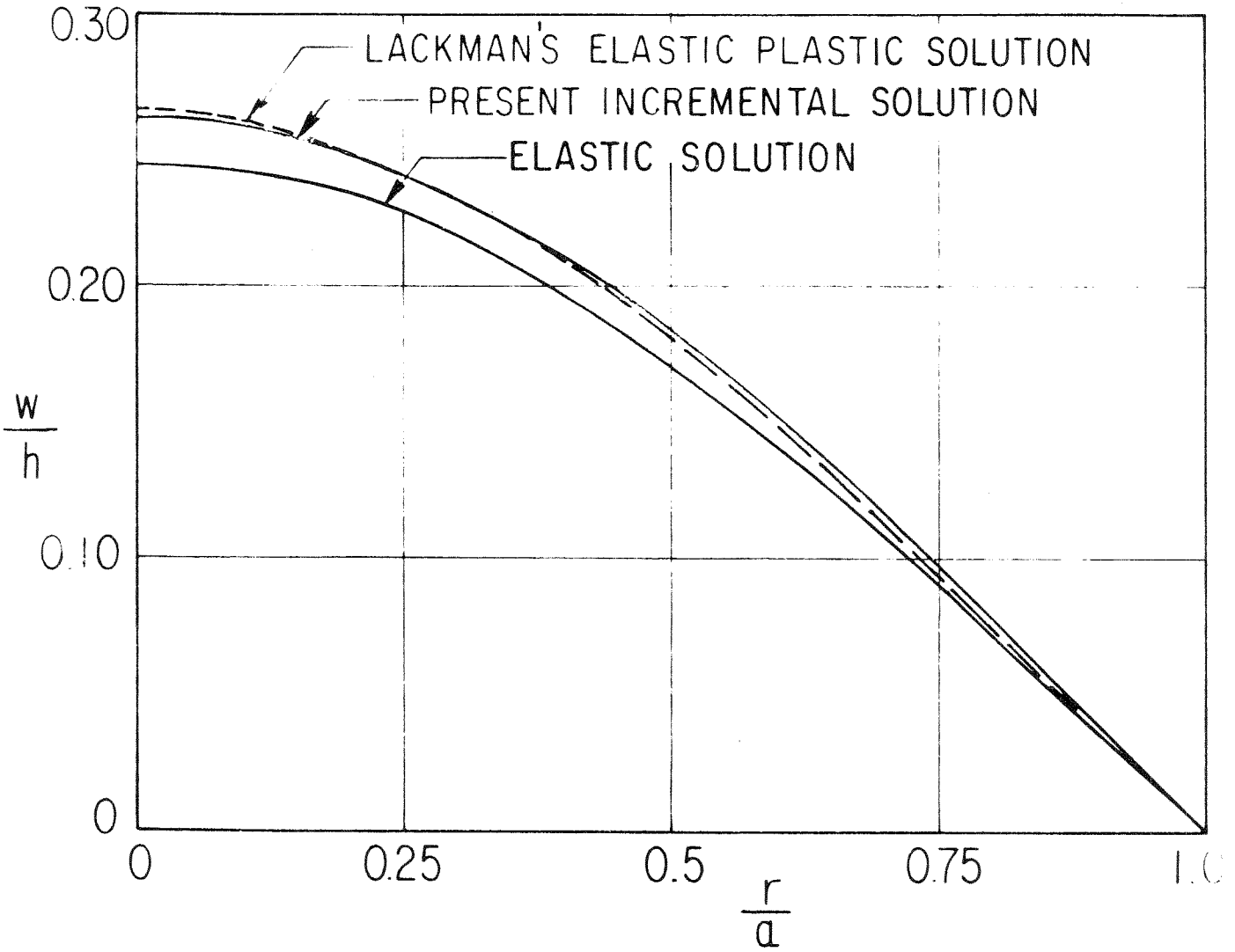

FIG 57 DEFLECTION OF CIRCULAR PLATE AT p = 300 psi

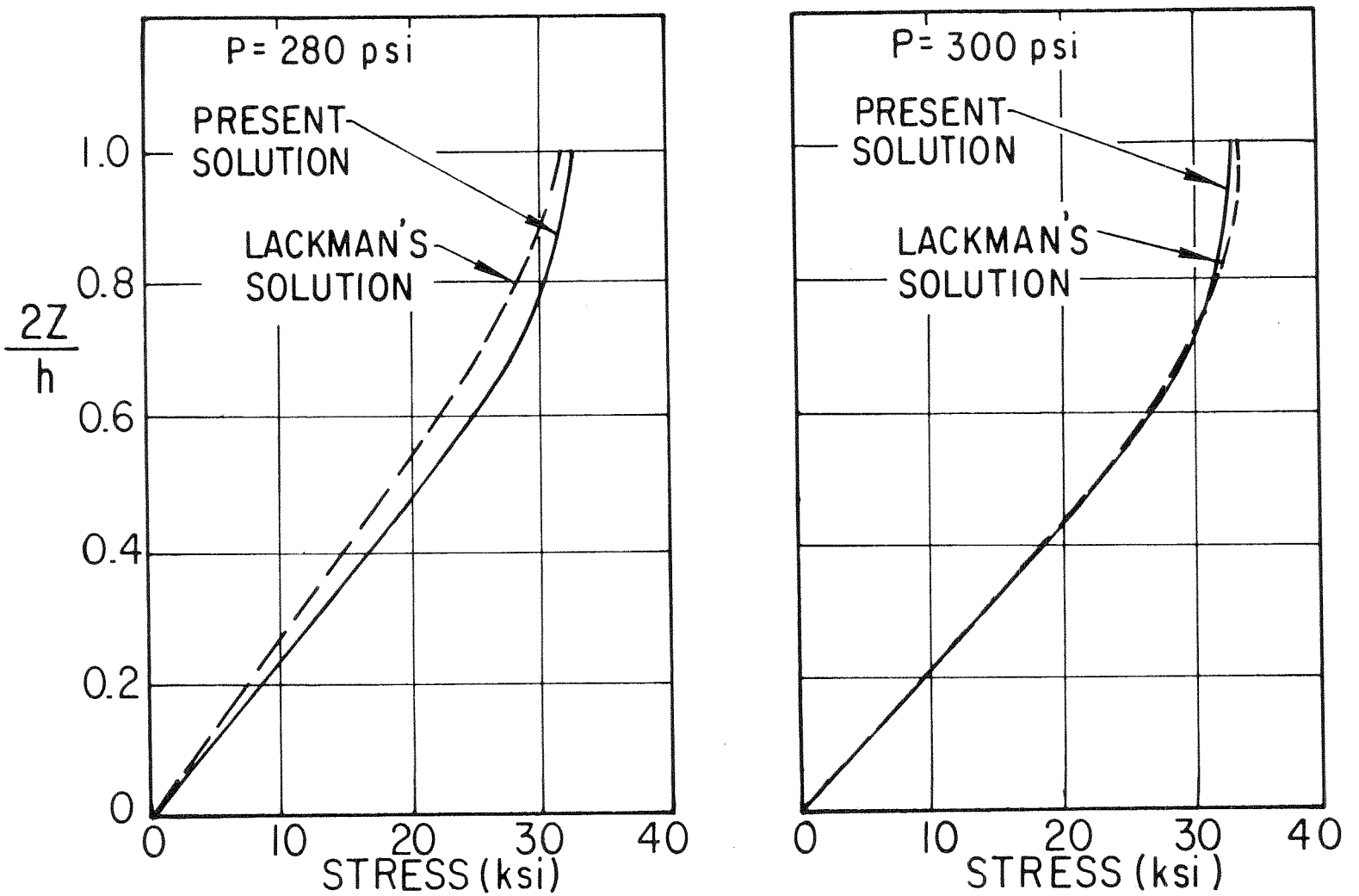

FIG 58 STRESS DISTRIBUTION τ_r, τ_θ AT r = 0

3-2. Description of Programs

Two computer programs have been prepared, in Fortran IV language, for the solution of clamped and simply-supported circular plates subject to axi-symmetric loading. One is for elastic-perfectly plastic material and the other for hardening material. The general procedure of solution is basically the same in both cases, although there are differences in details due to limitations in numerical accuracy of solution and inherent difference in material properties. A discussion on the computation problems and consideration of the variation of material property within each step of loading is given in the appendices E and F. The concise flow diagrams of the main program routines are presented in Appendix G. A brief description of the program follows.

(1-a) Elastic Perfectly Plastic Analysis of Circular Plates (EPPACP)

This routine is for matrix solution of elastic perfectly plastic circular plate. Presently a 30 element 60 layer plate can be handled but by decreasing the number of layers up to 35 elements or more can be used. Nodal ring loads in this routine are tributary.

(1-b) Formation of Average Material Property Functions (AMAFUN)

The functions of this subroutine is to form the average material property function within each step of loading.

(1-c) Formation of Initial Material Property Functions (IMAFUN)

In this subroutine the initial material properties for the next step of external load are calculated.

(2-a) Elastic Plastic Analysis of Circular Plates (EPACP)

This routine is for matrix solution of circular plates of hardening material. It is a double precision program. The number of elements and layers which is presently handled by this routine is 20 and 40, respectively. Other combinations of elements and layers can be used.

(2-b) Equivalent Nodal Ring Load (ENRIL)

This double precision subroutine is used to find the consistent nodal ring loads assuming linear variation of loads between the nodal rings. If it is desired to use the program for isolated concentrated ring loads, this subroutine should be deleted from (EPACP).

(2-c) Formation of Material Property Functions (MATFUN)

In this subroutine both the average material property functions in each step of load and the initial functions for the next increment of load are computed. This subroutine is in double precision.

IV. CONCLUSIONS

From the study of the examples in Chapter III as well as other observations, the following conclusions were reached on the calculated behavior of elastic-plastic circular plates.

The comparison of elastic and inelastic moments in Example 1 indicates some re-distribution of moments in the inelastic state. This can also be seen from the distribution of residual moments in all of the examples. The re-distribution patterns are in general similar for elastic-perfectly plastic and hardening material.

The stress paths in Fig. 14 indicate that the internal loading does not progress proportionally once the elastic limit is exceeded. Therefore, the deformation theory is not strictly applicable. However, results of Examples 3 and 4, which show the influence of different loading histories, indicate that this effect does not contribute significantly to the general behavior of the plate.

In Fig. 14 the small variation of the stress paths inside the yield surface justifies the application of a correction based on a radial approximation explained in Art. 2.4.1. It can also be observed that when the increments of external load are small, the distance between consecutive points of stress paths on the yield surface is small enough to justify the tangential approximation for neutral loading explained in Art. 2.4.1.

The comparison between the central deflections of the simply supported elastic-perfectly plastic plate as calculated in the present incremental

appraoch and the deformation solution due to V.V. Sokolovsky [2], Fig. 15, indicates the close agreement of the two solutions for loads not far above elastic limit. However, the incremental solution predicts greater deflections near collapse load.

The results in Examples 3 and 4 indicate that moments and deflections in the circular plate are affected very little by different loading histories for the two different sequences of loading. However, the inelastic zones are appreciably different near the boundary of the clamped plate.

From the results of Example 5 we conclude that as the magnitude of the load increments in calculations decreases, the deflections of the elastic-perfectly plastic plate increases. Figure 28 shows two groups of curves for the convergence of central moments. The full line was obtained by integrating the stress distribution across the depth of the plate. These moments, in general, satisfy the yield condition. The dashed line was determined by utilizing the stiffness matrix. The moments obtained in this manner satisfy equilibrium, but may not satisfy the yield conditions. However, as the magnitude of the load increments decreases they approach each other. These results establish bounds on the moments. It appears that the average of the two solutions is close to the correct one and can be taken as such. The fact that the variations in moment and deflection in Fig. 27 and 28 are almost linear can be used to advantage to predict the results when the size of load increments approaches zero. The dependence of the moments and deflections on the magnitude of load increments in hardening material varies with the hardening rate and is relatively less significant.

A comparison of the input data stress-strain diagrams, $\bar{\sigma}$, $\bar{\epsilon}$, for the hardening materials with the one computed from the calculated state of strain in the plate is presented in Figs. 35, 46, 55 for Examples 6, 8, 10. A good agreement between the two curves is evident which indicates good accuracy and convergence of the developed solution for the hardening material.

The results in Example 10 show that the solution for a hardening material with very low hardening rate (Fig. 55) agrees well with that for a corresponding elastic-perfectly plastic material. This is as could be expected intuitively. Part of the small differences is due to the different level of accuracies in the computer programs used for the two materials -- double precision for hardening material and single precision for elastic-perfectly plastic material.

The comparison of the solution for hardening material presented in Example 11 with the one published by V. Lackman [48] indicates that for the uniformly distributed load of 300 psi the deflections and stress distributions along the depth of the plate are practically the same.

The variation of stresses along the depth of plates indicates that the behavior of plates is not highly sensitive to the number of layers used in calculations within a reasonable range. For example, for hardening material of the type used in Example 11 results using 40 layers agreed well with those of 20.

Bibliography

A) Plate Bending Utilizing Deformation Theory of Plasticity

(1) Sokolovsky, V.V., "Elastic-Plastic Bending of Circular and Annular Plates," Prikl. Mat. Mech. Vol. 8, No. 2, 1944, pp. 141-166..

(2) Sokolovsky, V.V., "Theory of Plasticity," (in Russian) 1946, pp. 253-273 and German Edition, 1955, VEB, pp. 412-441.

(3) Grigoriev, A.S., "Bending of Circular and Annular Plates with Variable Thickness Beyond the Elastic Limit," (in Russian). Ingh. Shorn. Vol. 20, Moscow 1954, pp. 59-92.

(4) Dvorak, J., "Circular Ring Plate in Elastic-Plastic State," (in German) Proc. Sym. Non-Homo. in Elast. and Plast. (Warsaw) 1959, pp. 519-521. Pergamon Press.

(5) Ohashi Y. and Murakami, S., "On the Elastic Plastic Bending of a Clamped Circular Plate Under a Partial Circular Uniform Load," Bull. of JSME, Vol. 7, No. 27, Aug. 1964, pp. 491-498.

B) Limit Analysis

(6) Pell, W.H., and Prager, W., "Limit Design of Plates," Proc. 1st U.S. Nat. Cong. Appl. Mech., Chicago, Ill., 1951, pp. 547-550.

(7) Hopkins, H.G., and Prager, W., "The Load-Carrying Capacities of Circular Plates," Jour. of Mech. and Phys. Solids, Vol. 2, Oct. 1953, pp. 1-13.

(8) Drucker, D.C. and Hopkins, H.G., "Combined Concentrated and Distributed Load on Idealy-Plastic Circular Plates," Proc. 2nd U.S. Nat. Congr. Appl. Mech., Ann Arbor, Mich., 1954 pp. 517-520.

(9) Hopkins, H.G. and Wang, A.J., "Load Carrying Capacities for Circular Plates of Perfectly Plastic Materials with Arbitrary Yield Condition," Jour. Mech. and Phys. Solids, Vol. 3, No. 2, Jan. 1955, pp. 117-129.

(10) Prager, W., "Theory of Plastic Plates," (in French) Bull. Tech. Suisse Romande Vol. 81, No. 6, March 1955, pp. 85-90.

(11) Hu, L.W., "Design of Circular Plates Based on Plastic Limit Load," Jour. Eng. Mech. Div. ASCE, Vol. 86, Jan. 1960, pp. 91-115.

(12) Schumann, W., "On Limit Analysis of Plates," Quart. Appl. Math., Vol. 16, No. 1, April 1958, pp. 61-71.

(13) Zaid, M., "On the Carrying Capacity of Plates of Arbitrary Shapes and Variable Fixity Under a Concentrated Load," Jour. of Appl. Mech. Vol. 25, Dec. 1958, pp. 598-602.

(14) Chernina, V.S., "Approximate Carrying Capacity of an Annular Plate Under a Uniformly Distributed Pressure," (in Russian), Iz. Akad. Nank. SSSR, No. 7, 1958, pp. 33-39.

(15) Hodge, Jr., P.G., "Yield Point Load of an Annular Plate," Jour. Appl. Mech., Vol. 26, No. 3, Sept. 1959, pp. 454-455.

(16) Hopkins, H.G. and Prager, W., "Limits of Economy of Material in Plates," Jour. Appl. Mech. Vol. 22, No. 3, Sept. 1955, pp. 372-374.

(17) Freiberger, W. and Tekinalp, B., "Minimum Weight Design of Circular Plates," Jour. Mech. Phys. Solids, Vol. 4, No. 4, Aug. 1956, pp. 294-299.

(18) Onat, E.T., Schumann, W., and Shield, R.T., "Design of Circular Plates for Minimum Weight," Zeit Ang. Math und Phys. ZAMP Vol. 8, No. 6, Nov. 1957, pp. 485-499.

(19) Prager, W., and Shield, R.T., "Minimum Weight Design of Circular Plates Under Arbitrary Loading," Zeit. Ang. Math and Phys. ZAMP, Vol. 10, No. 4, July 1959, pp. 421-426.

(20) Shield, R.T., "Plate Design for Minimum Weight," Quart. Appl. Math. Vol. 18, No. 2, July 1960, pp. 131-144.

(21) Marcal, P.V. and W. Prager, "A Method of Optimal Plastic Design," Jour. de Mechaniqu, Vol. 3, No. 4, Dec. 1964, pp. 509-530.

(22) Sawczuk, A., "Some Problems of Load Carrying Capacities of Orthotropic and Non-homogeneous Plates," Proc. 9th Int. Congr. Appl. Mech. 1956, Vol. 8, pp. 93-99, Univ. of Brussels, 1957.

(23) Hu, L.W., "Modified Tresca's Yield Condition and Associated Flow Rules for Anistropic Materials and Applications," Jour. Franklin Inst. Vol. 265, No. 3, March 1958, pp. 187-204.

(24) Markowitz, J. and Hu, L.W., "Plastic Analysis of Orthotropic Circular Plates," ASCE Jour. Eng. Mech. Div. Vol. 90, Oct. 1964, pp. 251-292.

(25) Mura, T. and Kao, J.S., and Lee, S.L., "Limit Analysis of Circular Orthotropic Plates," ASCE Jour. Eng. Mech. Div., Oct. 1964, pp.

(26) Hodge, Jr., P.G., Sankaramarayanan, "Plastic Interaction Curve for Annular Plates in Tension and Bending," J. Mech. Phys. Solids, Vol. 8, No. 3, August 1960, pp. 153-163.

(27) Sawczuk, A., and Duczek, M., "A Note on the Interaction of Shear and Bending in Plastic Plates," Arch. Mech. Stas. Vol. 15, No. 3, 1963, pp. 411-426.

(28) Koopman, D.C.A. and Lance, R.H., "On Limit Programming and Plastic Limit Analysis," J. Mech. Phys. Solids, Vol. 13, No. 2, Apr. 1965, pp. 77-87.

(29) Hodge, Jr. P.G., Plastic Analysis of Structures, McGraw-Hill, N.Y., 1959.

(30) Hodge, Jr. P.G., Limit Analysis of Rotationally Symmetric Plates and Shells, Prentice-Hall, Int. Series, 1963, pp. 38-51.

(31) Sawczuk, A. and Jaeger, T., Grenztragfahigkeits-Theorie der Platten, Springer-Verlag 1963.

C) Rigid-Work Hardening Materials

(32) Boyce, W.E., "The Bending of a Work-Hardening Circular Plate by a Uniform Transverse Load," Quart. of Appl. Math. Vol. 14, Oct. 1956, pp. 277-288.

(33) Eason, G., "The Effect of Work-Hardening on the Behavior of Circular Plates Under Transverse Concentr Load," Proc. 9th Int. Congr. Appl. Mech. Vol. 8, 1956, pp. 103-111, Univ. of Brussels 1957.

(34) Prager, W., "A New Method of Analyzing Stresses and Strains in Work-Hardening Plastic Solids," Jour. Appl. Mech., Vol. 23, No. 4, Dec. 1956, pp. 493-496, also Brown Univ. Rept. A 11-123, 1955.

(35) Hodge, Jr. P.G., "Plastic Bending of an Annular Plate," Jour. of Math. and Phys., Vol. 36, 1957, pp. 130-137.

(36) Boyce, W.E., "A Note on Strain Hardening Circular Plates," Jour. Mech. and Phys. Solids, Vol. 7, No. 2, March 1959, pp. 114-125.

(37) Perrone, N. and Hodge, Jr. P.G., "Strain-Hardening Solutions to Plate Problems," Jour. Appl. Mech., Vol. 26, No. 2, Jun. 1959, pp. 277-284, Also, PiBAL Report No. 403, Polytechnic Inst. of Brooklyn, N.Y., 1957.

(38) Chintsun Hwang, "Incremental Stress-Strain Law Applied to Work-Hardening Plastic Materials," Jour. Appl. Mech. V. 26, No. 4, Dec. 1959, pp. 594-598.

(39) Chzhu-Khua, S., "Plastic Bending of a Freely Supported Circular Plate Under the Effect of Axisymmetric Loading," (in Russian) Izv. Akad. Nauk, SSSR, Mekh, i. Mashinostr. No. 6, Nov-Dec 1963, pp. 159-163.

D) Elastic-Plastic Analysis Utilizing Incremental Theory

(40) Haythornth waite, R.M., "The Deflection of Plates in Elastic-Plastic Range," Proc. 2nd U.S. Nat. Congr. of Appl. Mech. Ann Arbor, Michigan, 1954, pp. 521-526.

(41) Gaydon, F.A. and Nutall, H., "The Elastic-Plastic Bending of a Circular Plate by an All-Around Couple," Jour. Mech. Phys. of Solids, Vol. 5, No. 1, 1956, pp. 62-65

(42) Olszak, W. and Murzewski, Jr., "Elastic-Plastic Bending of Non-Homogeneous Orthotropic Circular Plate (I and II)," (in English) Arch. Mech. Sts. Vol. 9, No. 4, 1957, pp. 467-485 and Vol. 9, No. 5, 1957, pp. 605-630.

(43) Tekinalp, B., "Elastic-Plastic Bending of a Built-in Circular Plate under a Uniformly Distributed Load," Jr. Mech. Phys. Solids, Vol. 5, 1957, pp. 135-142.

(44) Olszak, W. and Murzewski, J., "Elastic-Plastic Bending of Non-Homogeneous Orthotropic Plates," (in English) Bull. Acad. Pol. Sci. TA4 P65, Vol. 6, No. 4, 1958, pp. 211-218.

(45) Olszak, W., "The General Case of Axi-Symmetric Bending of Elastic-Plastic Plates," (in English) Bull. Acad. Pol. Sci., Cl. IV, Vol. 6, No. 4, 1958, pp. Brotchie, J.R., "Elastic-Plastic Analysis of Transversely Loaded Plates," ASCE 86 No. EM5 (1960) p. 57-90.

(46) Eason, G., "The Elastic-Plastic Bending of Simply Supported Plate," Jr. Appl. Mech. Vol. 28, No. 3, Sept. 1961, pp. 395-401.

(47) French, F.W., "Elastic-Plastic Analysis of Centrally Clamped Annular Plates Under Uniform Loads," J. Franklin Inst. Vol. 277 No. 6, Jun. 1964, pp. 572-592.

(48) Lackman, L.M., "Circular Plates Loaded into the Plastic Region," J. ASCE, Eng. Mech. Div., Vol. 90 Dec. 1964, pp. 21-30.

E) Experiments on Circular Plates

(49) Cooper, R.M. and Shifrin, G.A., "An Experiment on Circular Plates in the Plastic Range," Proc. 2nd U.S. Nat. Congr. of Appl. Mech., Ann Arbor, Mich., 1954, pp. 527-534.

(50) Dyrbye, C. and Lange Hansen, P., "Studies on the Load Carrying Capacities of Steel Structures," Research Lab. of Bldg. Teck., Technical Univ. of Denmark, Bull. No. 3, 1954.

(51) Haythornthwaite, R.M., "The Deflection of Plates in Elastic-Plastic Range," Proc. 2nd U.S. Nat. Congr. Appl. Mech., Ann Arbor, Mich., 1954, pp. 521-526.

(52) Foulkes, J. and Onat, E.T., "Report of Static Tests of Circular Mild Steel Plates," Tech. Rep. 00R3172-3 Brown Univ., Providence, R.I., May 1955.

(53) Haythorthwaite, R.M. and Onat, E.T., "The Load Carrying Capacity of Initially Flat Circular Steel Plates Under Reversed Loading," Jr. Aero Sci., Vol. 22, No. 12, Dec. 1955, pp. 867-869.

(54) Lance, R.H. and Onat, E.T., "A Comparison of Experiments and Theory in the Plastic Bending of Circular Plates," Jour. Mech. & Phys. of Solids, Vol. 10, 1962, pp. 301-311.

F) Constitutive Laws of Plasticity

(55) Drucker, D.C., "Stress-Strain Relations in the Plastic Range - A Survey of Theory and Experiment," ONR Tech. Report, Contract N7-ONR-358, Brown Univ., Dec. 1950.

(56) Prager, W., "The Theory of Plasticity: A Survey of Recent Achievements," (James Clayton Lecture) Proc. Instn. Mech. Engro. Vol. 169, pp. 41-57, 1955.

(57) Drucker, D.C., "Stress-Strain Relations in the Plastic Range of Metals - Experiments and Basic Concepts," Rheology, Vol. 1, pp. 97-119, N.Y., 1956.

(58) Hodge, P.G., Jr., "The Mathematical Theory of Plasticity," In Elasticity and Plasticity (by J.N. Goodier and P.G. Hodge, Jr.), New York, 1958.

(59) Koiter, W.T., "General Theorems for Elastic-Plastic Solids," Progress in Solid Mechanics, Vol. 1 (Edited by I.N. Sneddon and R. Hill), Chap. 4, North-Holland, 1960.

(60) Naghdi, P.M., "Stress-Strain Relations in Plasticity and Thermoplasticity," "Plasticity" Proc. 2nd Symp. on Naval Struct. Mech., pp. 121-167, Pergamon Press, 1960.

(61) Olszak, W., Mroz, Z., and Perzyna, P., Recent Trends in the Development of The Theory of Plasticity, Pergamon Press, 1963.

(62) Green, A.E., and Naghdi, P.M., "A General Theory of an Elastic-Plastic Continuum," Report No. AM-64-16, Office of Naval Research, Contract Nonr-222(69), Project NR 064-436, Div. of Appl. Mech., Univ. of Calif., Berkeley, Sept. 1964.

Appendix A

Elements of $[B_s]$ matrix

$\wedge = 1$

$$\{\Delta S\} = [B_s] \{a\}$$

$$\begin{Bmatrix} \Delta Q_i \\ \Delta M_i \\ \Delta Q_j \\ \Delta M_j \end{Bmatrix} = \begin{bmatrix} B_{11} & B_{12} & B_{13} & B_{14} \\ B_{21} & B_{22} & B_{23} & B_{24} \\ B_{31} & B_{32} & B_{33} & B_{34} \\ B_{41} & B_{42} & B_{43} & B_{44} \end{bmatrix} \begin{Bmatrix} a_1 \\ a_2 \\ a_3 \\ a_4 \end{Bmatrix}$$

$$\Delta Q_i = 4\, a_4\, D_{11}\, r^{-1}$$

$$\Delta M_1 = -2\, a_2\, (D_{11} + D_{12}) - a_3\, (-D_{11} + D_{12})\, r^{-2}$$

$$-a_4\, [D_{11}\, (2\, \ell nr + 3) + D_{12}\, (2\, \ell nr + 1)]$$

$B_{11} = 0$ $\qquad$ $B_{12} = 0$

$B_{21} = 0$ $\qquad$ $B_{22} = -2\, (D_{11} + D_{12})$

$B_{31} = 0$ $\qquad$ $B_{32} = 0$

$B_{41} = 0$ $\qquad$ $B_{42} = +2\, (D_{11} + D_{12})$

$$B_{13} = 0 \qquad B_{14} = 4\, D_{11}\, r_i^{-1}$$

$$B_{23} = -\,(-D_{11} + D_{12})\, r_i^{-2} \qquad B_{24} = -\,D_{11}\,(2\,\ell nr_i + 3) - D_{12}(2\,\ell nr_i + 1)$$

$$B_{33} = 0 \qquad B_{34} = -\,4\, D_{11}\, r_j^{-1}$$

$$B_{43} = +\,(-\,D_{11} + D_{12})\, r_j^{-2} \qquad B_{44} = +\,D_{11}\,(2\,\ell nr_j + 3) + D_{12}\,(2\,\ell nr_j + 1)$$

Elements of $[B_v]$ Matrix

$\angle = 1$

$$\{\Delta v\} = [B_v]\ \{a\}$$

$$\begin{Bmatrix} \Delta w_i \\ \Delta w_i' \\ \Delta w_j \\ \Delta w_j' \end{Bmatrix} = \begin{bmatrix} B_{11} & B_{12} & B_{13} & B_{14} \\ B_{21} & B_{22} & B_{23} & B_{24} \\ B_{31} & B_{32} & B_{33} & B_{34} \\ B_{41} & B_{42} & B_{43} & B_{44} \end{bmatrix} \begin{Bmatrix} a_1 \\ a_2 \\ a_3 \\ a_4 \end{Bmatrix}$$

where:

$$B_{11} = 1 \qquad B_{12} = r_i^2 \qquad B_{13} = \ell nr_i \qquad B_{14} = r_i^2\, \ell nr_i$$

$$B_{21} = 0 \qquad B_{22} = 2r_i \qquad B_{23} = r_i^{-1} \qquad B_{24} = r_i\,(2\ell nr_i + 1)$$

$$B_{31} = 1 \qquad B_{32} = r_j^2 \qquad B_{33} = \ell nr_j \qquad B_{34} = r_j^2\, \ell nr_j$$

$$B_{41} = 0 \qquad B_{42} = 2r_j \qquad B_{43} = r_j^{-1} \qquad B_{44} = r_j(2\ell nr_j + 1)$$

$$\triangle w = a_1 + a_2 r^2 + a_3 \ell nr + a_4 r^2 \ell nr$$

$$\triangle w' = +2 a_2 r + a_3 r^{-1} + a_4 r (2 \ell nr+1)$$

$$\triangle w'' = 2 a_2 - a_3 r^{-2} + a_4 (2 \ell nr + 3)$$

Appendix B

Elements of $[B_v]$ Matrix

$\lambda \neq 0, \lambda \neq 1$

$$\{\Delta v\} = [B_v] \{a\}$$

$$\begin{Bmatrix} \Delta w_i \\ \Delta w'_i \\ \Delta w_j \\ \Delta w'_j \end{Bmatrix} = \begin{bmatrix} B_{11} & B_{12} & B_{13} & B_{14} \\ B_{21} & B_{22} & B_{23} & B_{24} \\ B_{31} & B_{32} & B_{33} & B_{34} \\ B_{41} & B_{42} & B_{43} & B_{44} \end{bmatrix} \begin{Bmatrix} a_1 \\ a_2 \\ a_3 \\ a_4 \end{Bmatrix}$$

where:

$$B_{11} = r_i^{1+\lambda} \qquad B_{12} = r_i^{1-\lambda} \qquad B_{13} = r_i^2 \qquad B_{14} = 1$$

$$B_{21} = (1+\lambda) r_i^{\lambda} \qquad B_{22} = (1-\lambda) r_i^{-\lambda} \qquad B_{23} = 2r_i \qquad B_{24} = 0$$

$$B_{31} = r_j^{1+\lambda} \qquad B_{32} = r_j^{1-\lambda} \qquad B_{33} = r_j^2 \qquad B_{34} = 1$$

$$B_{41} = (1+\lambda) r_j^{\lambda} \qquad B_{42} = (1-\lambda) r_j^{-\lambda} \qquad B_{43} = 2r_j \qquad B_{44} = 0$$

$$\Delta w = a_1 r^{1+\lambda} + a_2 r^{1-\lambda} + a_3 r^2 + a_4$$

$$\Delta w' = a_1(1+\lambda) r^{\lambda} + a_2(1-\lambda) r^{-\lambda} + 2 a_3 r$$

$$\Delta w'' = a_1 \lambda(1+\lambda) r^{\lambda-1} - a_2 \lambda (1-\lambda) r^{-(1+\lambda)} + 2a_3$$

Elements of $[B_s]$ Matrix

$\bigwedge \neq 0, \bigwedge \neq 1$

$$\{\Delta S\} = [B_s] \{a\}$$

$$\begin{Bmatrix} \Delta Q_i \\ \Delta M_i \\ \Delta Q_j \\ \Delta M_j \end{Bmatrix} = \begin{bmatrix} B_{11} & B_{12} & B_{13} & B_{14} \\ B_{21} & B_{22} & B_{23} & B_{24} \\ B_{31} & B_{32} & B_{33} & B_{34} \\ B_{41} & B_{42} & B_{43} & B_{44} \end{bmatrix} \begin{Bmatrix} a_1 \\ a_2 \\ a_3 \\ a_4 \end{Bmatrix}$$

where

$B_{11} = 0$

$B_{12} = 0$

$B_{21} = -(1+\lambda)(\lambda D_{11}+D_{12}) r_i^{\lambda-1}$

$B_{22} = -(1-\lambda)(-\lambda D_{11}+D_{12}) r_i^{-(1+\lambda)}$

$B_{31} = 0$

$B_{32} = 0$

$B_{41} = +(1+\lambda)(\lambda D_{11}+D_{12}) r_j^{\lambda-1}$

$B_{42} = +(1-\lambda)(-\lambda D_{11}+D_{12}) r_j^{-(1+\lambda)}$

$B_{13} = 2(D_{11}-D_{22}) r_i^{-1}$

$B_{14} = 0$

$B_{23} = -2(D_{11}+D_{12})$

$B_{24} = 0$

$B_{33} = -2(D_{11}-D_{22}) r_j^{-1}$

$B_{34} = 0$

$B_{43} = +2(D_{11}+D_{12})$

$B_{44} = 0$

$$\Delta M_1 = -a_1(1+\lambda)(\lambda D_{11}+D_{12})\ r^{\lambda-1} - a_2\ (1-\lambda)(-\lambda D_{11}+D_{12})\ r^{-(1+\lambda)}$$

$$-2a_3(D_{11}+D_{12})$$

$$\Delta Q_1 = 2a_3(D_{11}-D_{22})r^{-1}$$

Appendix C

Transformation of distributed load to normal ring forces.

See Article 2.10.

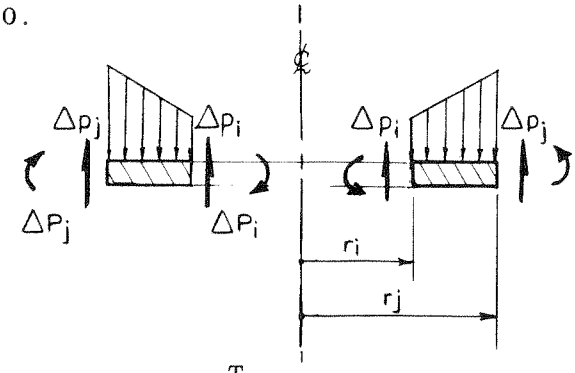

$$\begin{Bmatrix} r_i \Delta P_i \\ r_j \Delta P_j \end{Bmatrix} = \begin{bmatrix} B_v^{-1} \end{bmatrix}^T \begin{Bmatrix} \Delta p_i^* \end{Bmatrix}, \quad \Delta p_m^* = \int_{r_i}^{r_j} \Delta p(r) \Phi_m(r) r dr$$

Linear approximation $\Delta p(r) = \Delta p_i + \dfrac{\Delta p_j - \Delta p_i}{r_j - r_i} r$

Case I $\wedge = 1$

$$\Delta p_1^* = \int_{r_i}^{r_j} \Delta p(r)\, r dr = \frac{1}{2} \Delta p_i (r_j^2 - r_i^2) + \frac{1}{3} (\Delta p_j - \Delta p_i)(r_j^2 + r_j r_i + r_i^2)$$

$$\Delta p_2^* = \int_{r_i}^{r_j} \Delta p(r)\, r^3 dr = \frac{1}{4} \Delta p_i (r_j^4 - r_i^4) + \frac{1}{5} (\Delta p_j - \Delta p_i)(r_j^4 + r_j^3 r_i + r_j^2 r_i^2 + r_j r_i^3 + r_i^4)$$

$$\Delta p_3^* = \int_{r_i}^{r_j} \Delta p(r)\, \ell n r\, dr = \frac{1}{2} \Delta p_i (r_j^2 \ell n r_j - r_i^2 \ell n r_i - \frac{1}{2} r_j^2 + \frac{1}{2} r_i^2)$$

$$+ \frac{1}{3} (\Delta p_j - \Delta p_i) \left[(r_j^2 + r_j r_i + r_i^2)(\ell n r_j - \frac{1}{3}) + \ell n \frac{r_j}{r_i} \frac{r_i^3}{r_j - r_i} \right]$$

$$\Delta p_4^* = \int_{r_i}^{r_j} \Delta p(r)\ r^3 \ell nr\ dr = \frac{1}{4}\Delta p_i\ (r_j^4 \ell nr_j - r_i^4\ \ell nr_i - \frac{1}{4} r_j^4 + \frac{1}{4} r_i^4)$$

$$+ \frac{1}{5}\ (\Delta p_j - \Delta p_i) \left[(r_j^4 + r_j^3\ r_i + r_j^2 r_i^2 + r_j r_i^3 + r_i^4)\ (\ell nr_j - \frac{1}{3}) + \ell n \frac{r_j}{r_i} \frac{r_i^5}{r_j - r_i} \right]$$

Case II $\Lambda \neq 1, 0$

$$\Delta p_1^* = \int_{r_i}^{r_j} \Delta p(r)\ r^{1+\Lambda}\ rdr = \frac{\Delta p_i}{3+\Lambda}\ (r_j^{3+\Lambda} - r_i^{3+\Lambda}) + \frac{\Delta p_j - \Delta p_i}{4+\Lambda} \left[\frac{r_j^{4+\Lambda} - r_i^{4+\Lambda}}{r_j - r_i} \right]$$

$$\Delta p_2^* = \int_{r_i}^{r_j} \Delta p(r)\ r^{1-\Lambda}\ rdr = \frac{\Delta p_i}{3-\Lambda}\ (r_j^{3-\Lambda} - r_i^{3-\Lambda}) + \frac{\Delta p_j - \Delta p_i}{4-\Lambda} \left[\frac{r_j^{4-\Lambda} - r_i^{4-\Lambda}}{r_j - r_i} \right]$$

$$\Delta p_3^* = \int_{r_i}^{r_j} \Delta p(r)\ r^2\ rdr = \frac{1}{4}\Delta p_i\ (r_j^4 - r_i^4) + \frac{1}{5}\ (\Delta p_j - \Delta p_i)\ (r_j^4 + r_j^3\ r_i + r_j^2\ r_i^2 + r_j\ r_i^3 + r_i^4)$$

$$\Delta p_4^* = \int_{r_i}^{r_j} \Delta p(r)\ r\ dr = \frac{1}{2}\Delta p_i\ (r_j^2 - r_i^2) + \frac{1}{3}\ (\Delta p_j - \Delta p_i)\ (r_j^2 + r_j r_i + r_i^2)$$

For disc element

$r_i = 0$

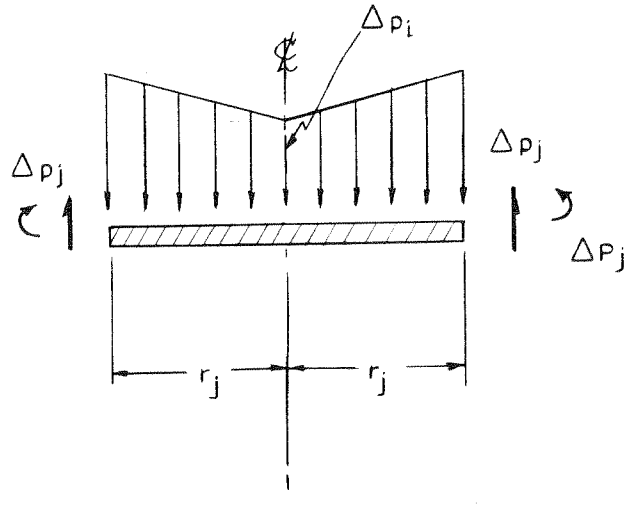

Case I $\Lambda = 1$

$$\Delta p(r) = \Delta p_i + \Delta p_j \frac{r}{r_j}$$

$$\Delta p_m^* = \int_0^{r_j} \Delta p(r) \; \phi_m(r) \; r dr, \qquad m = 1, 2.$$

$$\Delta p_1^* = \int_0^{r_j} \Delta p(r) \; r \; dr = \frac{1}{6} (\Delta p_i + 2 \Delta p_j) \; r_j^2$$

$$\Delta p_2^* = \int_0^{r_j} \Delta p(r) \; r^3 \; dr = \frac{1}{20} (\Delta p_i + 4 \Delta p_j) \; r_j^4$$

Appendix D

Expanded form of $[B] = [Bv]^{-1}$ matrix, case $\Lambda \neq 1, 0$

$$B(1,1) = 2(1-\Lambda)^{-1}\delta \quad [r_j^{-1-\Lambda} - r_i^{-1-\Lambda}]$$

$$B(1,2) = -(1-\Lambda)^{-1}\ \delta\ r_i^{-\Lambda}\ [\ (\frac{r_i}{r_j})^{1+\Lambda} - (\frac{r_j}{r_i})^{1-\Lambda} + 2\ (\frac{r_j}{r_i})^{1-\Lambda}\ \text{Beta}\ ]$$

$$B(1,3) = -B(1,1)$$

$$B(1,4) = -(1-\Lambda)^{-1}\ \delta\ r_j^{-\Lambda}\ [(\frac{r_j}{r_i})^{1+\Lambda} - (\frac{r_i}{r_j})^{1-\Lambda} - 2\ \text{Beta}\ ]$$

$$B(2,1) = 2(1+\Lambda)\ (1-\Lambda)^{-1}\ \delta\ r_i^{-1+\Lambda}\ \text{Beta}$$

$$B(2,2) = (1-\Lambda)^{-1}\ \delta\ r_i^{\Lambda}\ [\ (\frac{r_j}{r_i})^{1+\Lambda} - (\frac{r_i}{r_j})^{1-\Lambda} - 2\ \text{Beta}\ ]$$

$$B(2,3) = -\ B\ (2,1)$$

$$B(2,4) = (1-\Lambda)^{-1}\ \delta\ r_j^{-\Lambda}\ [\ (\frac{r_i}{r_j})^{1+\Lambda} - (\frac{r_j}{r_i})^{1-\Lambda} + 2\ (\frac{r_j}{r_i})^{1-\Lambda}\ \text{Beta}\ ]$$

$$B(3,1) = (1+\Lambda)\ (1-\Lambda)^{-1}\ \delta\ (r_i r_j)^{-1}\ [\ (\frac{r_j}{r_i})^{\Lambda} - (\frac{r_i}{r_j})^{\Lambda}\ ]$$

$$B(3,2) = (1-\Lambda)^{-1}\ \delta\ r_i^{-1}\ [\ (\frac{r_i}{r_j})^{1+\Lambda} - 1 + (1+\Lambda)\ \text{Beta}\ ]$$

$$B(3,3) = -B\ (3,1)$$

$$B(3,4) = (1-\Lambda)^{-1}\ \delta\ r_j^{-1}\ [\ (\frac{r_j}{r_i})^{1+\Lambda} - 1 - (1+\Lambda)\ (\frac{r_j}{r_i})^{1-\Lambda}\ \text{Beta}\ ]$$

$$B(4,1) = (1-\Lambda)^{-1}\ \delta\ \left\{(1-\Lambda)\ \left[\left(\frac{r_j}{r_i}\right)^{1+\Lambda} - 1\right]\ -\ (1+\Lambda)^2\ \left(\frac{r_j}{r_i}\right)^{1-\Lambda}\ \text{Beta}\right\}$$

$$B(4,2) = (1-\Lambda)^{-1}\ \delta\ r_i\ \left[-\left(\frac{r_j}{r_i}\right)^{1+\Lambda} + 1 + (1+\Lambda)\ \left(\frac{r_j}{r_i}\right)^{1-\Lambda}\ \text{Beta}\right]$$

$$B(4,3) = (1-\Lambda)^{-1}\ \delta\ \left\{(1-\Lambda)\ \left[\left(\frac{r_i}{r_j}\right)^{1+\Lambda} - 1\right]\ +\ (1+\Lambda)^2\ \text{Beta}\right\}$$

$$B(4,4) = -\ (1-\Lambda)^{-1}\ \delta\ r_j\ \left[\left(\frac{r_i}{r_j}\right)^{1+\Lambda} - 1 + (1+\Lambda)\ \text{Beta}\right]$$

Expanded form of [k] matrix, case $\Lambda \neq 1,0$

$$k(1,1) = 2\ (1+\Lambda)^2\ \delta\ D_{11}\ r_i^{-2}\ r_j^{-1}\ \left[\left(\frac{r_j}{r_i}\right)^{\Lambda} - \left(\frac{r_i}{r_j}\right)^{\Lambda}\right]$$

$$k(1,2) = 2\ (1+\Lambda)\ \delta\ D_{11}\ r_i^{-2}\ \left[\left(\frac{r_i}{r_j}\right)^{1+\Lambda} - 1 + (1+\Lambda)\ \text{Beta}\right]$$

$$k(1,3) = -k\ (1,1)$$

$$k(1,4) = 2\ (1+\Lambda)\ \delta\ D_{11}(r_i r_j)^{-1}\ \left[\left(\frac{r_j}{r_i}\right)^{1+\Lambda} - 1 - (1+\Lambda)\ \left(\frac{r_j}{r_i}\right)^{1-\Lambda}\ \text{Beta}\right]$$

$$k(2,1) = k(1,2)$$

$$k(2,2) = -\ (D_{11}+D_{12})\ r_i^{-1} + (1+\Lambda)\ \delta\ D_{11}\ r_i^{-1}\ \left\{\left(\frac{r_j}{r_i}\right)^{1+\Lambda} - \left(\frac{r_i}{r_j}\right)^{1+\Lambda} - (1+\Lambda)\ \left[\left(\frac{r_j}{r_i}\right)^{1-\Lambda} + 1\right]\ \text{Beta}\right\}$$

$$k(2,3) = -k\ (2,1)$$

$$k(2,4) = (1+\Lambda)\ \delta\ D_{11}\ r_i^{-2}\ r_j \left\{ \left[\left(\frac{r_i}{r_j}\right)^{1-\Lambda} + 1 \right] \left[\left(\frac{r_i}{r_j}\right)^{1+\Lambda} - 1 \right] + (1+\Lambda) \left[\left(\frac{r_i}{r_j}\right)^{1+\Lambda} + 1 \right] \text{Beta} \right\}$$

$$k(3,1) = \frac{r_i}{r_j}\ k(1,3)$$

$$k(3,2) = \frac{r_i}{r_j}\ k\ (2,3)$$

$$k(3,3) = -k\ (3,1)$$

$$k(3,4) = -\frac{r_i}{r_j}\ k\ (1,4)$$

$$k(4,1) = \frac{r_i}{r_j}\ k(1,4) = -k\ (3,4)$$

$$k(4,2) = \frac{r_i}{r_j}\ k\ (2,4)$$

$$k(4,3) = k(3,4) = -k\ (4,1)$$

$$k(4,4) = (D_{11}+D_{12})\ r_j^{-1} + (1+\Lambda)\ \delta\ D_{11}\ r_j^{-1} \left\{ \left(\frac{r_j}{r_i}\right)^{1+\Lambda} - \left(\frac{r_i}{r_j}\right)^{1+\Lambda} - (1+\Lambda) \left[\left(\frac{r_j}{r_i}\right)^{1-\Lambda} + 1 \right] \text{Beta} \right\}$$

where,

$$\delta^{-1} = \left(\frac{r_j}{r_i}\right)^{1+\Lambda} + \left(\frac{r_i}{r_j}\right)^{1+\Lambda} -2- (1+\Lambda)^2 \left(\ell n \frac{r_j}{r_i}\right)^2 \left[1 + \frac{2}{4!} (1-\Lambda)^2 \left(\ell n \frac{r_j}{r_i}\right)^2 \right.$$

$$\left. + \frac{2}{6!} (1-\Lambda)^4 \left(\ell n \frac{r_j}{r_i}\right)^4 + \frac{2}{8!} (1-\Lambda)^6 \left(\ell n \frac{r_j}{r_i}\right)^6 + \ldots\ldots \right]$$

$$\text{Beta} = \ell n \frac{r_j}{r_i} \left[1 - \frac{1}{2!} (1-\Lambda) \ell n \frac{r_j}{r_i} + \frac{1}{3!} (1-\Lambda)^2 \left(\ell n \frac{r_j}{r_i}\right)^2 \right.$$

$$\left. - \frac{1}{4!} (1-\Lambda)^3 \left(\ell n \frac{r_j}{r_i}\right)^3 + \frac{1}{5!} (1-\Lambda)^4 \left(\ell n \frac{r_j}{r_i}\right) \ldots\ldots \right]$$

Appendix E

Consideration of Numerical Errors

The numerical inaccuracies are due to two main causes both of which exist in matrix $[B_v]$, see Chapter II. It can be observed that the 1st and 3rd; and the 2nd and 4th rows of this matrix respectively are of the same form. For a ringe element whose inside and outside radii are of nearly the same magnitude, the matrix becomes ill conditioned for inversion. The other and more important cause of inaccuracy is due to parameter Λ as it approaches unity $\Lambda \neq 1$. Then some of the terms in the inversion of the $[B_v]$ matrix take the form of $(\frac{0}{0})$ which lead to computational errors.

In general, these two causes of numerical errors do not occur in the same element. A graph showing the plot of $|1-\Lambda|$ vs. r_i/r_j for the elements, and the probable zone of computational error is shown in Fig. 60. This is a result of many tests on simply supported and clamped plates using the single precision computer program.

Two measures have been taken to prevent these errors: In the program for the elastic-perfectly plastic material, the elements of $[B_v]^{-1}$ and $[k]$ have been expanded in series form as presented in Appendix D . In calculations enough terms of this expansion have been taken to assure accuracy of results. This eliminates the inaccuracy due to Λ but not due to r_i/r_j as it approaches unity. The method used to minimize computational errors for hardening material consisted of using double precision in the computer program. The results have been checked by testing whether $[B_v]\,[B_v]^{-1} = [I]$. This procedure yielded satisfactory results.

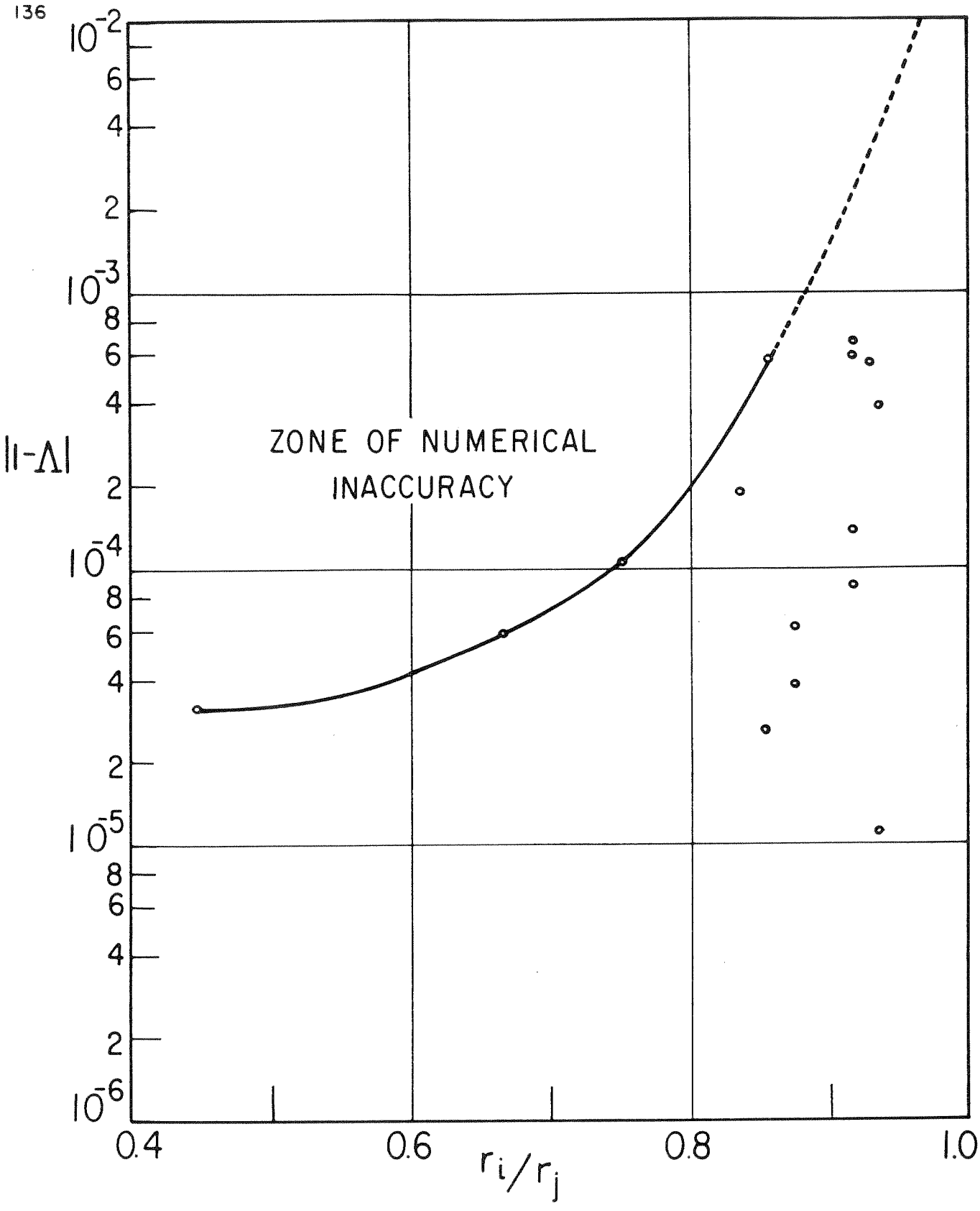
10^{-2}
6
4
2
10^{-3}
8
6
4
2
10^{-4}
8
6
4
2
10^{-5}
8
6
4
2
10^{-6}
|1-Λ|
ZONE OF NUMERICAL
INACCURACY
0.4
0.6
0.8
1.0
r_i/r_j

FIG. 60

Appendix F

Consideration of Variation of Material Properties Function Within A Step of External Load

Considering the plate load and the state of stress as the independent and dependent variables respectively, we can write

$$\underset{\sim}{d\tau} = \underset{\sim}{F(\tau)} \; \underset{\sim}{dp} \tag{1}$$

where F(t) represents a function that transforms the external loads into internal stresses and is expressed as a function of the state of stress. Equation (1) is solved numerically by replacing $\underset{\sim}{dp}$ and $\underset{\sim}{d\tau}$ by finite increments $\underset{\sim}{\Delta p}$ and $\underset{\sim}{\Delta\tau}$

$$\underset{\sim}{\Delta\tau} \doteq \underset{\sim}{F(\tau)} \; \underset{\sim}{\Delta p} \tag{2}$$

To solve Equation (2) with reasonable accuracy, Euler's modified method* is used where the order of error is $0(\Delta p)^3$.

Figure (59) is the flow diagram of the substeps taken in the computer program to complete the (k+1)-th step of calculation represented by Equation (2) for the hardening material. The procedure is basically the same for the elastic perfectly plastic material. The notations are the same as in Chapter II.

Whenever unloading from a plastic state takes place in a layer the new elastic properties are utilized and this modification is not used.

*Levy, H., and Baggott, E.A., "Numerical Solutions of Differential Equations," pp. 92-96, Dover 1950.

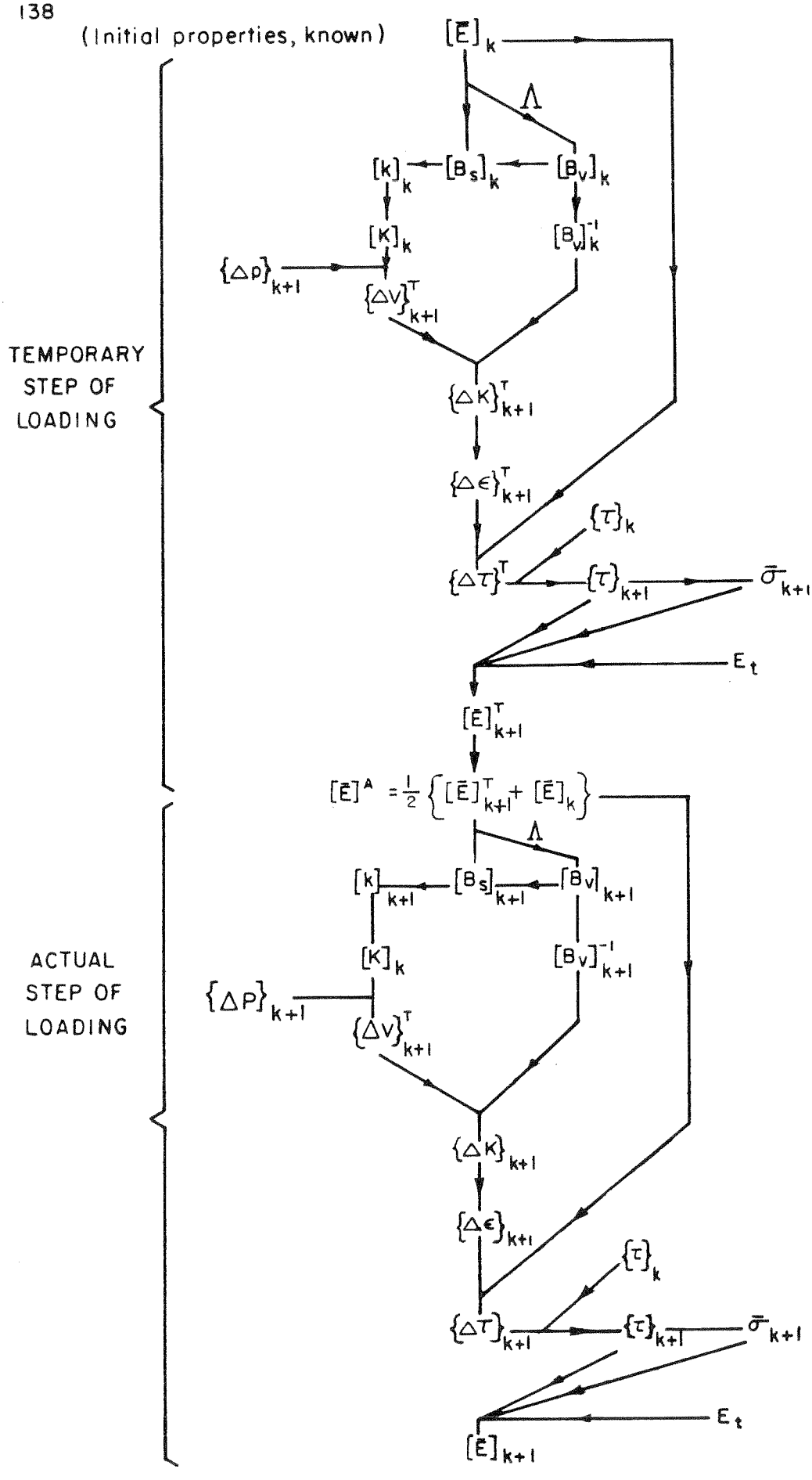
(Initial properties, known)
$[\bar{E}]_k$
Λ
$[k]_k$
$[B_s]_k$
$[B_v]_k$
$[K]_k$
$[B_v]^{-1}_k$
$\{\Delta p\}_{k+1}$
$\{\Delta v\}^T_{k+1}$
$\{\Delta K\}^T_{k+1}$
$\{\Delta \epsilon\}^T_{k+1}$
$\{\tau\}_k$
$\{\Delta \tau\}^T$
$\{\tau\}_{k+1}$
$\bar{\sigma}_{k+1}$
E_t
$[\bar{E}]^T_{k+1}$
TEMPORARY STEP OF LOADING
$[\bar{E}]^A = \frac{1}{2}\left\{[\bar{E}]^T_{k+1} + [\bar{E}]_k\right\}$
$[k]_{k+1}$
$[B_s]_{k+1}$
$[B_v]_{k+1}$
$[K]_k$
$[B_v]^{-1}_{k+1}$
$\{\Delta P\}_{k+1}$
$\{\Delta v\}^T_{k+1}$
$\{\Delta K\}_{k+1}$
$\{\Delta \epsilon\}_{k+1}$
$\{\tau\}_k$
$\{\Delta \tau\}_{k+1}$
$\{\tau\}_{k+1}$
$\bar{\sigma}_{k+1}$
E_t
$[\bar{E}]_{k+1}$
ACTUAL STEP OF LOADING

FIG. 59

Appendix G

CONCISE FLOW CHARTS OF COMPUTER PROGRAMS

ELASTIC- PLASTIC ANALYSIS OF A CIRCULAR PLATE WITH AXIS-SYMMETRIC LOADING

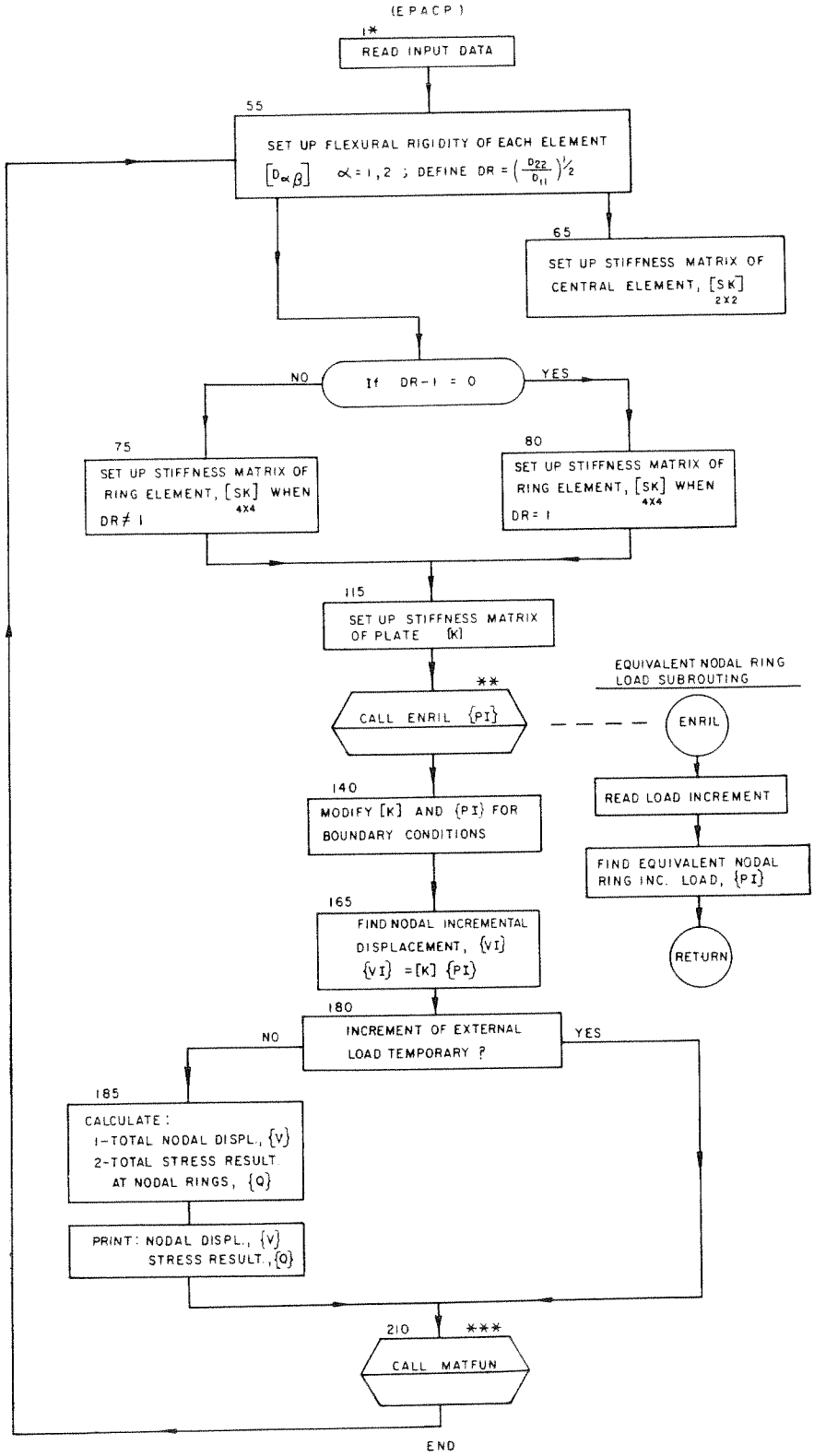

* THE NUMBERS REFER TO FORTRAN NUMBERS STATEMENTS IN THE PROGRAM.

** IN EPPACP, THE LOAD DISTRIBUTION ON NODAL RINGS IS TRIBUTARY HENCE ENRIL IS NOT USED

*** IN EPPACAP THERE ARE TWO SUBROUTINES FOR CONSTRUCTION OF MATERIAL PROPERTY FUNCTIONS, AMAFUN AND IMAFUN WHENEVER THE INCREMENT OF EXTERNAL LOADING IS TEMPORARY AMAFUN IS USED AND IF NOT IMAFUN.

SUBROUTINE FOR THE FORMATION OF MATERIAL PROPERTY FUNCTIONS

(FOR HARDENING MATERIALS)

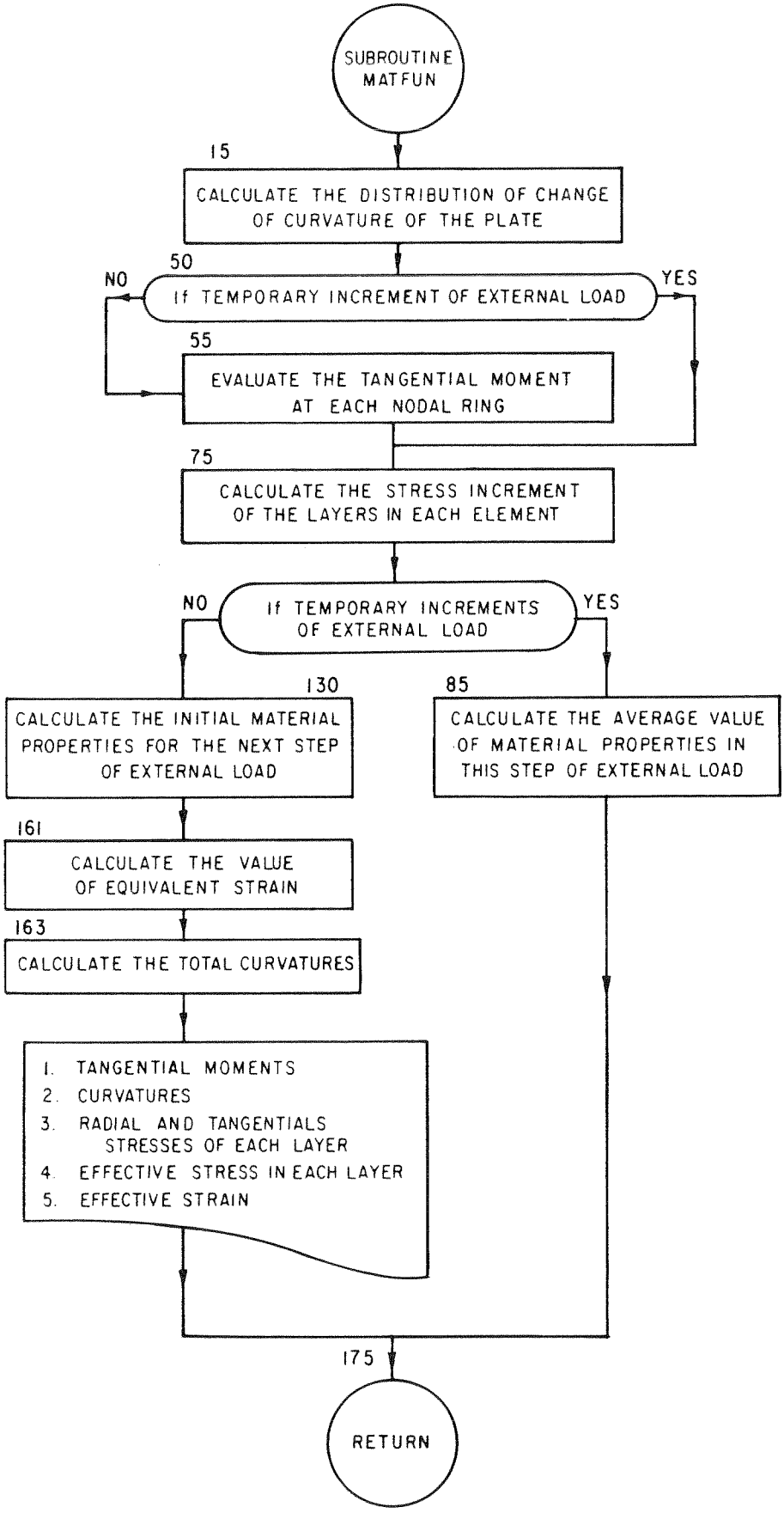

SUBROUTINE FOR THE CALCULATION OF AVERAGE MATERIAL PROPERTY FUNCTIONS
(FOR ELASTIC-PERFECTLY PLASTIC MATERIAL)

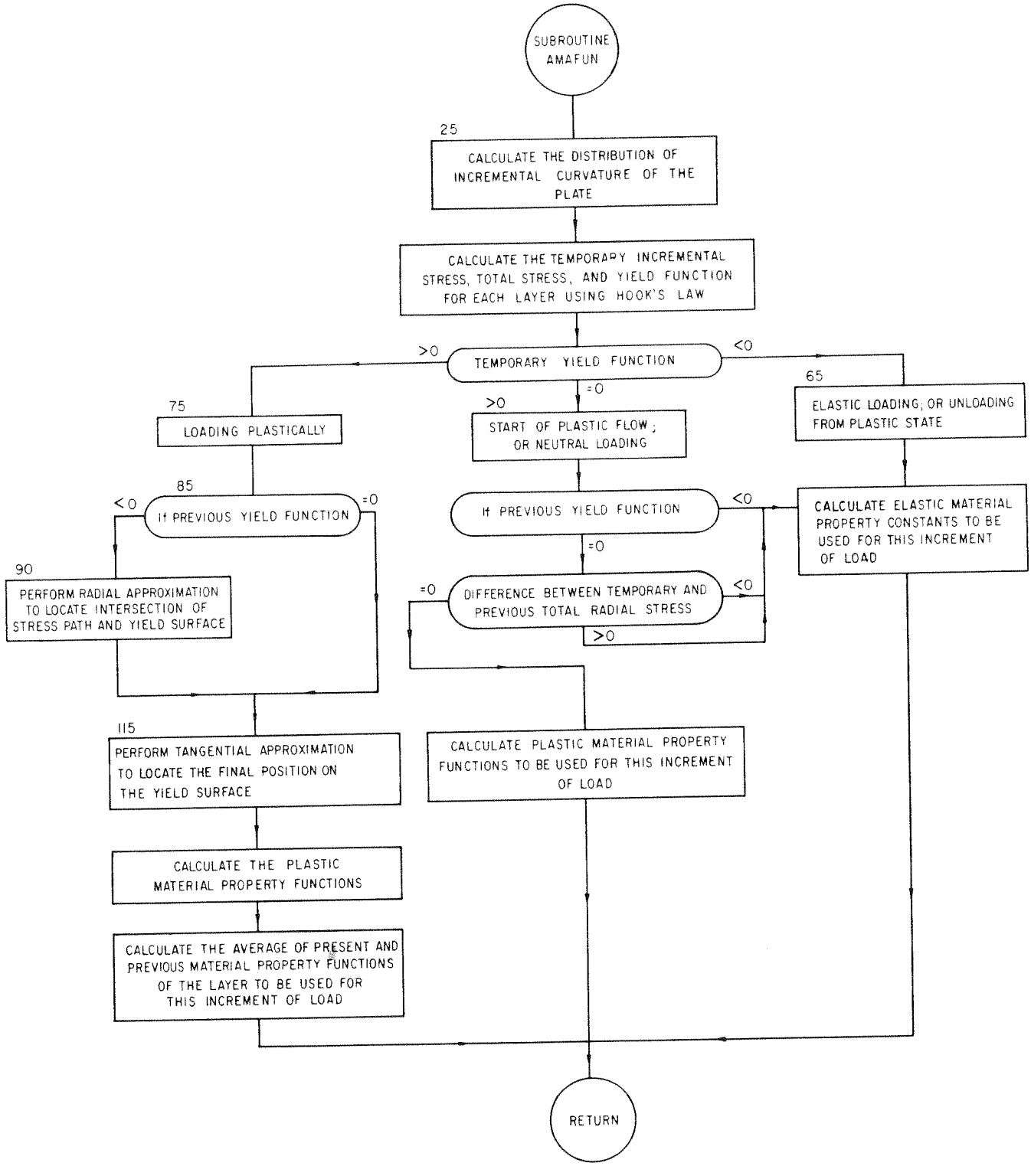

SUBROUTINE FOR THE CALCULATION OF INITIAL MATERIAL PROPERTY FUNCTIONS OF THE NEXT INCREMENT OF LOAD (FOR ELASTIC PERFECTLY PLASTIC MATERIAL)

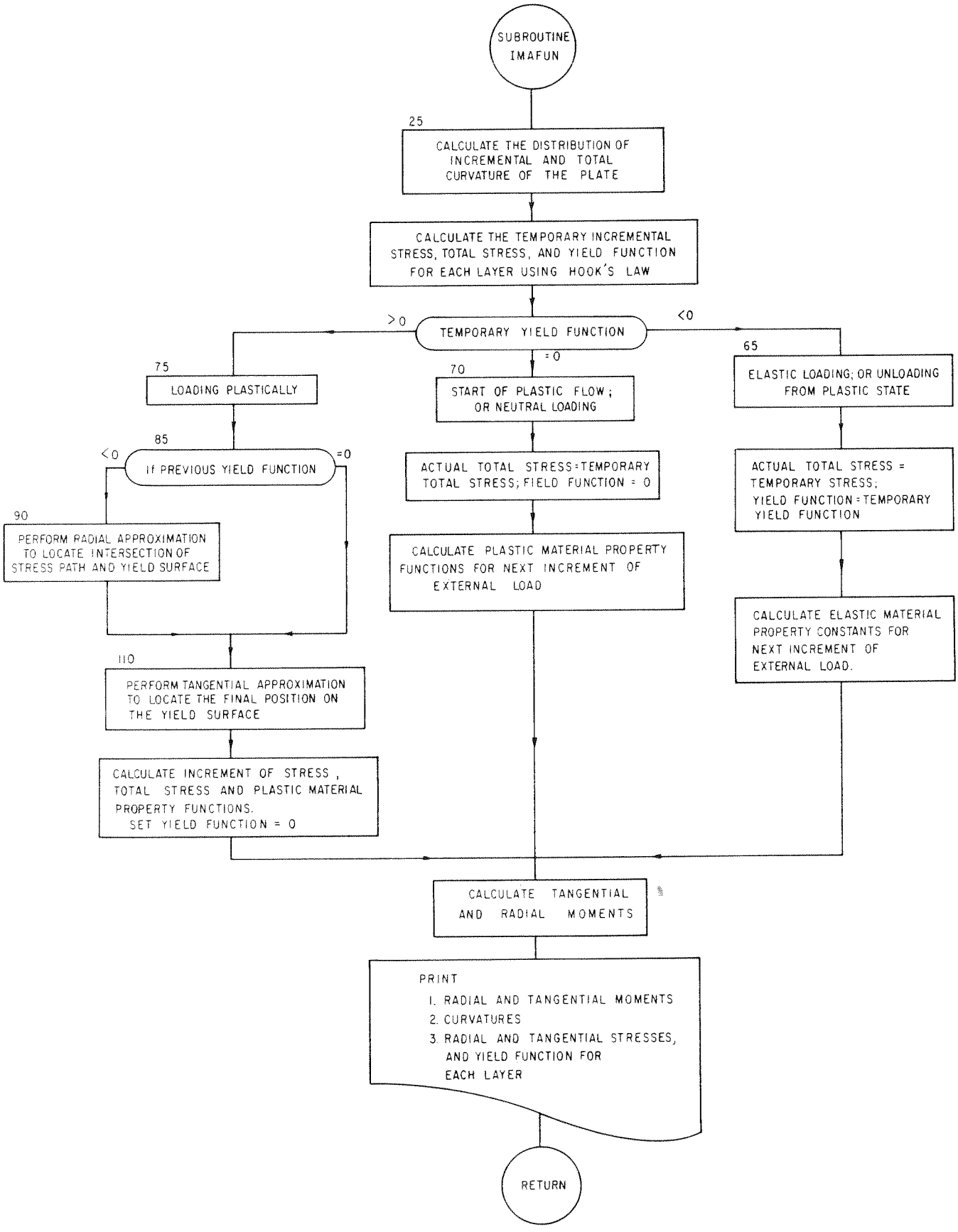

Nomenclature

a_i	constants of integration, see (2.81) to (2.83)
c	as defined in (2.46)
$C_{ijk\ell}$	elastic moduli
e_{ij}	deviatoric strain tensor
E	Young's modulus
E_t	tangent modulus in uniaxial test
$E_{ijk\ell}$	elastic-plastic modulus
f	yield function or loading function
g	a function as defined in (2.40)
G	non-negative function defined in (2.10)
h	plate thickness
h_k	the distance of k-th layer from the reference plane
H	function of equivalent plastic strain defined in (2.50)
J_2, J_3	second and third invariants of deviatoric stress tensor
k	yield stress in simple shear
K_r, K_θ	radial and tangential curvatures
M_r, M_θ	radial and tangential moments per unit length
N	number of elements
p(r)	transverse load per unit area
Q	radial transverse shear per unit length
r,θ,z	coordinate axes of plate, z is measured positive downward from the reference plane

s_{ij}	deviatoric stress tensor
$S_{ijk\ell}$	elastic-plastic compliance
w	vertical displacement of the middle plane, measured positive downward
W_p	total plastic work per unit volume
α_{ij}	a tensor representing the total translation of the center of initial yield surface, see (2.45)
β	defined in (2.69)
δ	defined in Appendix (D)
Δ	as a prefix desiginates finite increment
δ_{ij}	Kronecker delta
$d\bar{\epsilon}^p$	equivalent plastic strain increment defined in (2.42)
ϵ_r, ϵ_θ	radial and tangential strains, respectively
ϵ_{ij}	strain tensor
η	parameter defined in (2.47)
κ	work hardening parameter
λ	Lamé constant
$\Lambda = \sqrt{\frac{D_{22}}{D_{11}}}$	square root of the ratio of tangential to radial flexural rigidity of plate
μ	shear modulus
μ_t	tangent modulus in simple shear
ν	Poisson's ratio
ξ	defined in (2.69)
σ_y	yield stress in uniaxial tension
$\bar{\sigma}$	effective stress defined in (2.51)

τ_{ij} stress tensor

ϕ non-negative function defined in (2.9)

ω slope

Vectors and Matrices

$\{\ \}$ column vector

$[\ ]$ square matrix

$\underset{4x1}{\{a\}}$ arbitrary constants, see (2.81) to (2.83)

$\underset{4x4}{[B_s]}$ as defined in (2.90)

$\underset{4x4}{[B_v]}$ displacements transformation matrix, defined in (2.93)

$\underset{2x2}{[D]}$ flexured rigidity of plate, defined in (2.72)

$[E]$ elastic-plastic moduli

$\underset{2x2}{[E^{(k)}]}$ elastic-plastic moduli associated with k-th layer

$\underset{4x4}{[k]}$ element stiffness matrix

$\{p^*\}$ generalized nodal ring load, see (2.120)

$\underset{2Nx1}{\{r\}}$ displacements and rotations at nodal rings

$\underset{2Nx1}{\{R\}}$ nodal ring forces per unit length of plate

$\underset{4x1}{\{S\}}$ nodal ring forces per unit length for an element

$[S]_{9x9}$	elastic-plastic compliance
$\{v\}_{4x1}$	nodal ring displacement for an element see (2.94)
$\{d\epsilon\}$	strain increment vector (2.24)
$\{d\tau\}$	stress increment vector (2.24)

Subscripts

$\alpha,\beta,\gamma,\delta$	range 1, 2
i,j,k,ℓ	range 1, 2, 3